Cellular Seismology Analysis of the Western United States: Comparing and Contrasting the San Andreas Transform Zone, the Cascadia Subduction Zone, and the Western Intraplate Hinterland Region

Author: Eric Alan Fisher

Boston College Electronic Thesis or Dissertation, 2017

CELLULAR SEISMOLOGY ANALYSIS OF THE WESTERN UNITED STATES:

COMPARING AND CONTRASTING THE SAN ANDREAS TRANSFORM ZONE, THE CASCADIA SUBDUCTION ZONE, AND THE WESTERN INTRAPLATE HINTERLAND REGION

ERIC ALAN FISHER

A thesis

submitted to the Faculty of

the department of Earth and Environmental Science

in partial fulfillment

of the requirements for the degree of

Master of Science

Boston College
Morrissey College of Arts and Sciences
Graduate School

May 2017

Cellular Seismology Analysis of the Western United States:

Comparing and Contrasting the San Andreas Transform Zone, the Cascadia Subduction Zone, and the Western Intraplate Hinterland Region

Eric A. Fisher
Advisor: Dr. Alan Kafka, Ph. D.

Abstract

The western United States (WUS) is an area of high seismic activity. The Juan de Fuca, Pacific, and North American plates all meet in this area, resulting in zones of subduction and strike-slip faulting, as well as other styles of faulting, all of which make it prone to frequent, as well as large magnitude earthquakes. In this study the WUS encompasses the area between 30° to 52°N and 110° to 131°W. The diverse seismicity and tectonics of the area makes the study of seismo-tectonic processes in the WUS important not only in terms of basic geoscience, but also in terms of earthquake hazards. Understanding earthquake processes in this region is critical because of the potential for devastating earthquakes to occur along the Pacific-Juan de Fuca-North American plate boundary system. Large WUS earthquakes do not, however, only occur along these plate boundaries. They can also happen in intraplate environments within the WUS.

The WUS includes three distinct tectonic regions for which this study compares and contrasts characteristics of seismic activity: the Cascadia subduction region, the San Andreas strike-slip region, and a continental extension/intraplate region to the east of

the major plate boundaries referred to here as the “Western Intraplate Hinterland Region”. To help make these comparisons, the method of “Cellular Seismology” (CS; Kafka, 2002, 2007), is used here to investigate similarities and differences in the extent to which past earthquakes delineate zones where future earthquakes are likely to occur in the WUS and its various tectonic sub-regions. The results of this study show that while there seems to be a “signal” of CS predictability being dependent on tectonic region, that signal is subtle in most cases, meaning that there is not a significant difference in the level of CS predictability between the regions stated here. This means we can apply CS predictability studies widely across different regions, however, it also counterintuitively suggests that tectonic understanding of a region does not necessarily elucidate how well past seismicity predicts spatial patterns of earthquakes in a region.

Table of Contents

Preface

Acknowledgments

I would first like to thank Dr. Alan Kafka for his guidance, support, and trust. I came into graduate school without any idea of what I was going to research, and he made the process and experience incredibly easy and rewarding. My work would not have been possible without his help.

I would also like to thank Dr. Seth Kruckenberg and Dr. Ethan Baxter for their support throughout my research. They kept me on my toes, and asked the questions that I would have never thought of on my own.

I would like to thank Hannah Chambless for providing the tools necessary to start my work, and showing me the ins and outs of the programs I used to complete my studies.

I would like to thank all of the other graduate students for their support during the last two years. I am sure after hearing me give my presentation six-plus times over two years that you likely know just as much about my research as I do.

Lastly I would like to thank my family for their support. Writing was never, and still isn't, my strong suit. Proofreading my thesis proposal was probably a little rough for you, but thank you for all the feedback.

Preface

List of Abbreviations

Abbreviation	Meaning
BFZ	Blanco fracture zone
CAS	Cascades sub-region
CS	Cellular Seismology
CSZ	Cascadia Subduction Zone
ESA	Entire San Andreas sub-region
ESRP	East Snake River Plain
EXP	Explorer Plate
FMR	Full margin rupture
GR	Gorda Ridge
JDF	Juan de Fuca
MFZ	Mendocino fracture zone
NA	North American
NJDF	Northern Juan de Fuca
NSA	Northern San Andreas
NWSRP	Northeast Snake River Plain
PMR	Partial margin rupture
RELM	Regional Earthquake Likelihood Models
SAB	San Andreas Bend
SAC	San Andreas Central
SAF	San Andreas Fault
SAN	San Andreas North
SAS	San Andreas South
SCEC	Southern California Earthquake Center
SEA	Seattle sub-region
SJDF	Southern Juan de Fuca
SSA	Southern San Andreas
UCERF	Uniform California Earthquake Rupture Forecast
WAS	Wasatch Fault Zone
WHR	Western Intraplate Hinterland Region
WLB	Walker Lane Belt
WUS	Western United States
YS	Yellowstone

Table of abbreviations used within the text and their meanings. Several abbreviations listed in the captions of figures 3 and 17 are left off of this list as they pertain only to those individual figures and do not appear in the bulk of the text.

INTRODUCTION

Devastating earthquakes are a somewhat common occurrence along the western tectonic margin of the United States. Over historical times several earthquakes such as the 1868 Hayward Fault earthquake (between magnitude 6.8 and 7.0), the 1857 Fort Tejon earthquake (magnitude 7.9), and the 1906 San Francisco earthquake (magnitude 7.8) have shown that earthquakes along the San Andreas Fault zone (SAF) can be highly destructive. But, what about the Cascadia subduction zone (CSZ), or the continental extension/intraplate region that includes the area within Rectangle 3 in Figure 1, and is referred to here as the Western Intraplate Hinterland Region (WHR).

The Cascadia margin has not ruptured in recent times, but there is evidence from elastic deformation, paleosol studies, and tsunami records (Gutscher et al., 2001) that suggest a full-margin rupture (FMR) occurred there in the year 1700. If such a FMR were to occur today, it could produce an earthquake with a magnitude as high as 9.2 which would devastate large parts of the Pacific Northwest. The CSZ is part of a greater region, called the Cascadia region, which runs from 40°-52°N and 119°-131°W (Figure 1), and includes coastal areas of northern California, Oregon, Washington, and southern British Columbia. The Cascadia region also includes all of the Juan de Fuca plate.

In contrast, deformation in the Western Intraplate Hinterland Region consists of a combination of continental extension and intraplate processes such as volcanism and high heat flow (Lerner and Lerner, 2003; Parsons, 2006). The WHR is a region of high heat flow, and as such, the density of the lithosphere is lower causing isostatic uplift in

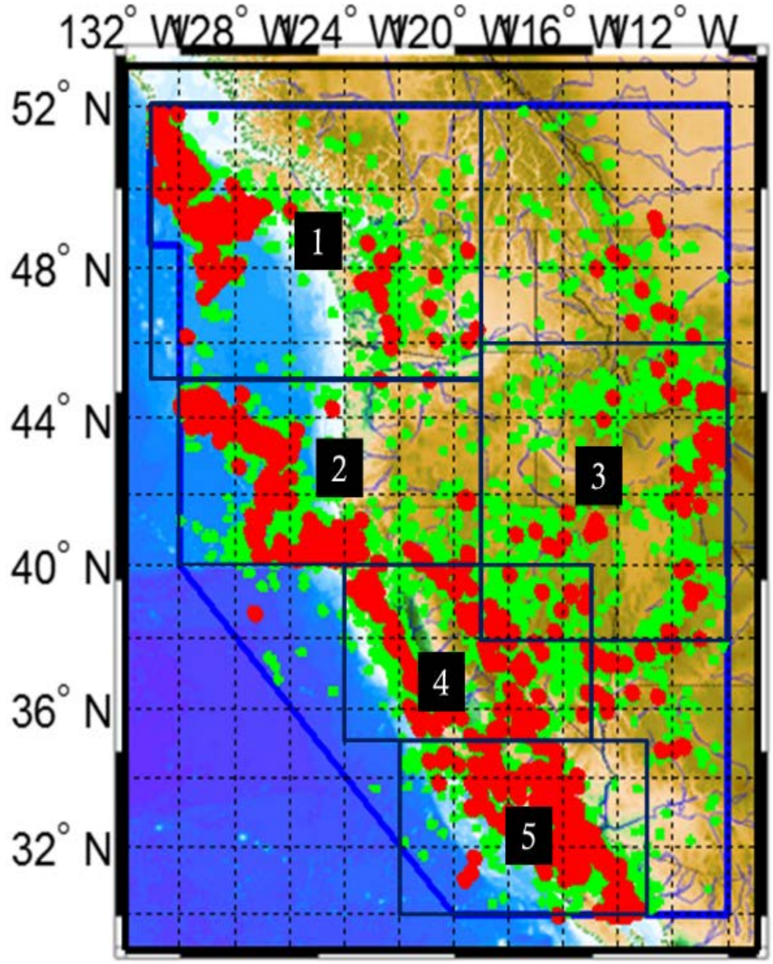

Figure 1: Western United States area of study. Blue polygon outlines the total area analyzed in this study. Green dots and red dots represent Pre-Cat and Post-Cat earthquakes respectively. Areas outlined in black with numbers inside them represent the five larger sub-regions analyzed in this study. 1: Northern Juan de Fuca, 2: Southern Juan de Fuca, 3: Western intraplate hinterland region, 4: Northern San Andreas, and 5: Southern San Andreas.

the region (Lerner and Lerner, 2003). We might therefore not expect major earthquakes to occur in this area, but the WHR has produced some moderate sized earthquake in historic times, even as high as an M7.3 earthquake near Borah Peak, ID which occurred in 1983 (Parsons, 2006).

Since the WUS is capable of producing such large earthquakes it is important that we attempt to understand where and when they might happen in the future. To that end, the spatial and temporal association between past and more recent earthquakes (e.g., Holliday et al., 2006, 2007; Kafka, 2002, 2007; Kafka and Ebel, 2011; Kafka and Levin, 2000; Kafka and Walcott, 1998; Rundle et al., 2007; Tiampo et al., 2002), along with geodesy (e.g., Bennett et al., 2003; Hammond and Thatcher, 2004; Williams et al., 2005), geology (e.g., Field and Milner, 2008; Field, 2015), and other possible precursors, have all been investigated to help determine where and when future earthquakes might happen. These studies form the basis of earthquake forecasting.

Earthquake "prediction", in contrast to "forecasting", deals in more specific terms, such as saying an earthquake of a specific magnitude will occur at a specific location, in a specific year or narrow range of years.

After the Parkfield earthquake of 1966 scientists realized that there was a pattern to the occurrence of magnitude 6 events in the Parkfield area, which led to an earthquake prediction: the Parkfield, CA earthquake prediction experiment of 1985. This prediction hypothesized that the segment of the SAF near Parkfield ruptures, producing magnitude ~6 earthquakes, on close to a 22 year cycle (Bakun and Lindh, 1985; Roeloffs and Langbein, 2014). Bakun and Lindh (1985) hypothesized that another magnitude 6 earthquake would occur around the year 1988, ± 5 years. By 1993 no earthquake of magnitude 6 had occurred in the Parkfield area, proving the hypothesis wrong. The actual "predicted" earthquake did not occur until 2004, 11 years later than the end of the prediction window, and many seismologists considered the attempt at a prediction to be a failure. This is just one of many examples illustrating that accurate prediction of earthquakes is not yet possible.

Accurate earthquake forecasting, on the other hand, is more likely to be possible. This thesis attempts to shed light upon one aspect of earthquake forecasting: the extent to which past earthquakes delineate zones where future earthquakes are likely to occur. Focusing on the association between past and more recent earthquakes in the western United States (WUS), this study investigates the extent to which that association might help delineate zones where future earthquakes are likely to occur. This spatial aspect of forecasting is investigated here for the Cascadia, SAF, and WHR regions of the western United States using “Cellular Seismology” (CS; Kafka 2002, 2007). CS is used to investigate which broad tectonic region, and also which smaller sub-regions of the WUS show a higher correlation between locations of past and more recent seismicity.

From Kafka (2012, akafka.wordpress.com):

> “CS is an *intentionally* simple method of systematically investigating the relationship between locations of past and future earthquakes in a given region. The name “Cellular Seismology” was chosen because it is analogous to a cellular phone system, with past earthquakes acting analogously to a cell phone tower. The cell tower is associated with a circular zone, extending some radius away from the tower, within which cell phones can receive a signal from the tower. Analogously, we envision that some circular zone surrounding the epicenter of a past earthquake is a zone that

presumably has the necessary geophysical characteristics to generate future earthquakes."

CS measures the extent to which past locations of earthquakes delineate zones where future earthquakes are likely to occur which, for simplicity, is referred to below as the level of "CS predictability."

The level of CS predictability is the percentage of earthquakes in a catalog of recent earthquakes (referred to below as the "Post-Cat") that fall within the regions close to the epicenters of past earthquakes ("Pre-Cat"). If there are 100 Post-Cat earthquakes and 95 of them fall within the bounds of the Pre-Cat radius, then we say there is a 95% "hit rate."

Here, I use CS to determine which region and sub-regions show the highest and lowest levels of CS predictability. Parsing out which area shows the highest level of CS predictability, especially for higher magnitude earthquakes, is important to seismic hazard analyses, and to the public in general. It is important because, if a large earthquake (e.g. M7+) were to be more likely to occur in a certain area, and this study shows that there is a high level of CS predictability for that area, then the CS results need to be considered as an important input into the seismic hazard mapping of that area.

CS has been shown to be a useful tool for forecasting locations of future earthquakes in southern California (Kafka and Ebel, 2007, 2011) as well as the Caribbean

(Cinella and Kafka, 2012), and the northeast United States (Kafka and Walcott, 1998; Kafka and Ebel, 2011), among other regions (e.g., Kafka, 2007; Kafka et al., 2014). Other spatial forecast methods such as Pattern Informatics (Rundle et al., 2002, 2007) have also been proven useful. The CS method uses spatial changes in seismicity to forecast where future earthquakes are likely to occur. The pattern informatics method uses not only spatial, but also temporal changes in the seismicity of a region for earthquake forecasting. However, when comparing the results of the pattern informatics method of Rundle et al. (2002, 2007) to the results of the CS method of Kafka and Ebel (2011), there is no evidence that the inclusion of the temporal changes produces significantly better forecasting results than the use of only the spatial patterns (i.e., CS).

Because the spatial changes (i.e., CS) generate nearly the same results as the spatial-temporal combination (Rundle et al., 2002, 2007), the CS method is just as valid a tool for earthquake forecasting, and as such, is used in this study to forecast future earthquakes in the western United States. Including CS analysis results in the Regional Earthquake Likelihood Models (RELM) by the Southern California Earthquake Center (SCEC) could help to further identify areas in California that are at risk of a major earthquake. The results in this study could also be used in hazard analyses for other areas in the WUS that are at risk of a major earthquake in the immediate future.

In previous CS studies there has been work done on plate boundary and intraplate regions, and there has been a publication (Kafka and Ebel, 2011) summarizing differences among a few of these areas in the United States. Previous studies, however, have not looked into the Cascadia subduction zone or the WHR. Furthermore, the comparison between a subduction zone, mid-ocean ridge segments, transform boundaries, and broad areas of extension has not been combined into one study as it is done here. The results of this study are, therefore, important for understanding how the seismicity in each of these areas can be forecasted, and how the ability of forecasting in each of the regions compares to one another.

Knowing how “predictable” the WUS is in terms of seismicity plays a big role in hazard analysis and mitigation. Having an idea of how big earthquakes in a specific area have been in historic times, how often those earthquakes occur, where they occur, and the effects large earthquakes can have on a region are all very important, and they are all things that scientists and the general public alike wish to know. This study gives some insight about those questions for the western United States.

Three fundamental questions regarding CS forecasts are investigated in this study: 1) what is the level of CS predictability for M3.5+ earthquakes in each of the regions and sub-regions?, 2) what is the level of CS predictability for higher magnitude earthquakes (such as, M5+) in each of the regions and sub-regions?, and 3) how does the type of plate boundary affect the level of CS predictability?

HYPOTHESES UNDERLYING THIS STUDY

The purpose of this study is to investigate how CS predictability varies for different tectonic regions of the western United States (Cascadia, SAF, or WHR, and associated sub-regions) Determining which of the sub-regions analyzed in this study has the highest level of CS predictability is also very important. A higher level of CS predictability is an important component of the knowledge base that might eventually lead to a successful earthquake forecast.

I hypothesize that the Cascadia region will show the greatest level of CS predictability. The number of plate boundaries, including ridges, transforms, and the Cascadia subduction zone (CSZ) in the Cascadia region (Figure 1), is the basis for this hypothesis. The basic idea behind this hypothesis is that future earthquakes would most likely occur along pre-existing, active faults, and given the abundance of such faults in the Cascadia region, past seismicity should occur along those faults, which would result in the past seismicity delineating zones where future earthquakes are likely to occur. Most of the seismicity in the Cascadia region is focused along its plate boundaries, and according to previous CS studies (Cinella and Kafka, 2012; Kafka, 2002, 2007; Kafka and Ebel, 2011; Kafka and Levin, 2000; Kafka and Walcott, 1998) recent earthquakes should have a tendency to occur near the same areas where previous earthquakes have occurred, leading to the hypothesized higher level of CS predictability.

I also hypothesize that the SAF will be the region with the second highest level of CS predictability, after the Cascadia Region, because of the more diffuse network of faults, and thus the more scattered pattern of earthquakes, in this region. Since the fault network in this region has many small branch faults spread over a large area (Figure 2), the seismicity is not as spatially focused on simple plate boundary faults as it is in the Cascadia region. Thus, I hypothesize that seismicity in the SAF region might migrate among those faults over time, making past seismicity not as good a predictor of future earthquake locations.

Thirdly, I hypothesized that the WHR would show the lowest level of CS predictability of the regions in this study due to its continental extension/intraplate setting. This region has a network of faults through it but does not include any major plate boundaries. Rather, it has a broad area of extensional faults, and therefore tends to have seismicity that is not as spatially focused as seismicity along plate boundaries despite having a number of clearly defined faults. This last hypothesis is consistent with the findings of Kafka et al. (2014), where it was shown that levels of CS predictability for the central and eastern United States, an intraplate region, were, on average, lower than the level of CS predictability for southern California, a plate boundary area. The WHR is an area of active extension, and is thus not wholly similar to the intraplate setting of the eastern US, but compared to the Cascadia or the SAF regions, the WHR, for the purpose of this study, is considered to be in the "intraplate region" category of Kafka et al. (2014).

Finally, I hypothesize that for the smaller sub-regions of this study, the SAF as whole or one of the smaller sub-regions along the SAF should show the highest level of

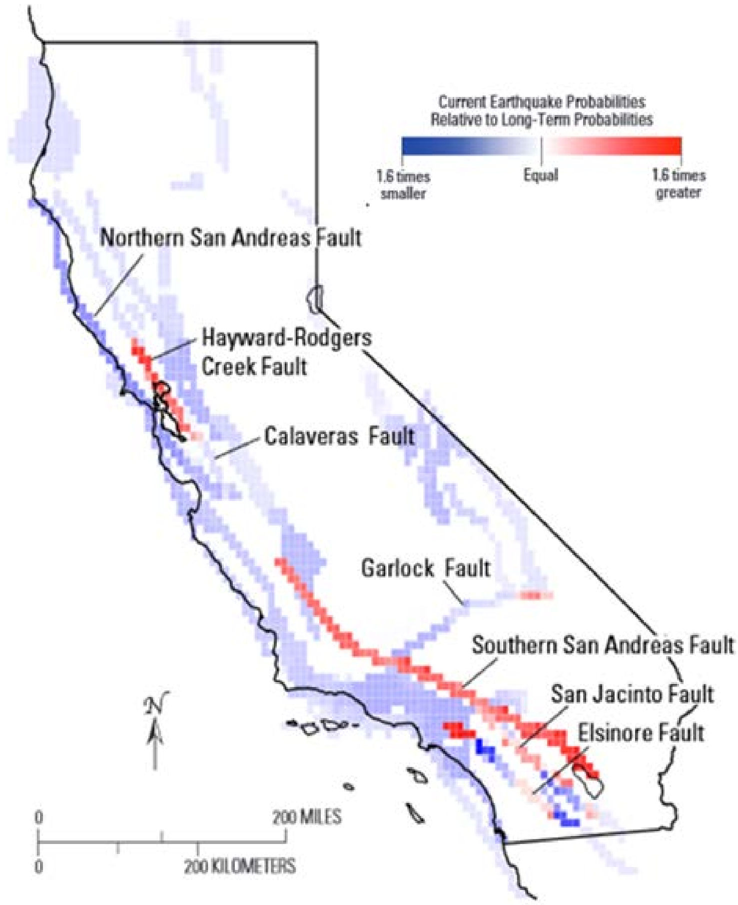

Figure 2: Current earthquake probabilities relative to long-term probabilities for the San Andreas Fault and its major branch faults. From Field and Milner (2008).

CS predictability. I hypothesize this based on the fact that the earthquakes that occur in the San Andreas transform region and its sub-regions are spatially focused, rather precisely, along the SAF or its branch faults. Because the SAF is a transform fault it is essentially vertical, and because of that the seismicity along the fault has a tendency to persistently occur in essentially the same locations when looking at the map from a birds-eye view. Since the seismicity is very spatially focused along the SAF, I expect/hypothesize that one of the SAF sub-regions will have the highest level of CS predictability.

BACKGROUND

Tectonic History, Past and Present, of the Western United States

In the past, the Farallon plate was a lone tectonic plate subducting underneath almost the entire stretch of western North America. The Farallon plate was an oceanic plate, like the Pacific and Juan de Fuca plates of today, which subducted underneath the continental margin of western North America (Atwater, 1970). Over time, portions of the subducting Farallon plate became completely subducted underneath NA. Around 30 Ma there is complete subduction of the first microplate, a segment of the larger Farallon plate, separated by fracture zones (Figure 3. From Atwater, 1970). After that, the boundary became one of strike-slip motion between the Pacific plate (PP) and NA. This was the beginning of the current San Andreas Fault zone. Since the onset of strike-slip motion there has been north-south lengthening of the transform boundary (Atwater, 1970) as the subduction of the oceanic plates continues.

Only small remnants of the ancient Farallon plate remain, comprising three microplates: the Gorda, Juan de Fuca (JDF), and Explorer plates, from south to north respectively (Figure 4). The Juan de Fuca plate, an oceanic plate, is subducting underneath the North American Plate (NA) in a N26.3°E direction (Plate Motion, 2015). The Gorda and Explorer plates have similar directions of subduction under the North American plate. Subduction in this region has changed over time as described above (Figure 3), and the tectonic and volcanic settings changed with it. Volcanoes of the past became inactive as the subduction of the oceanic plate beneath them ceased. These

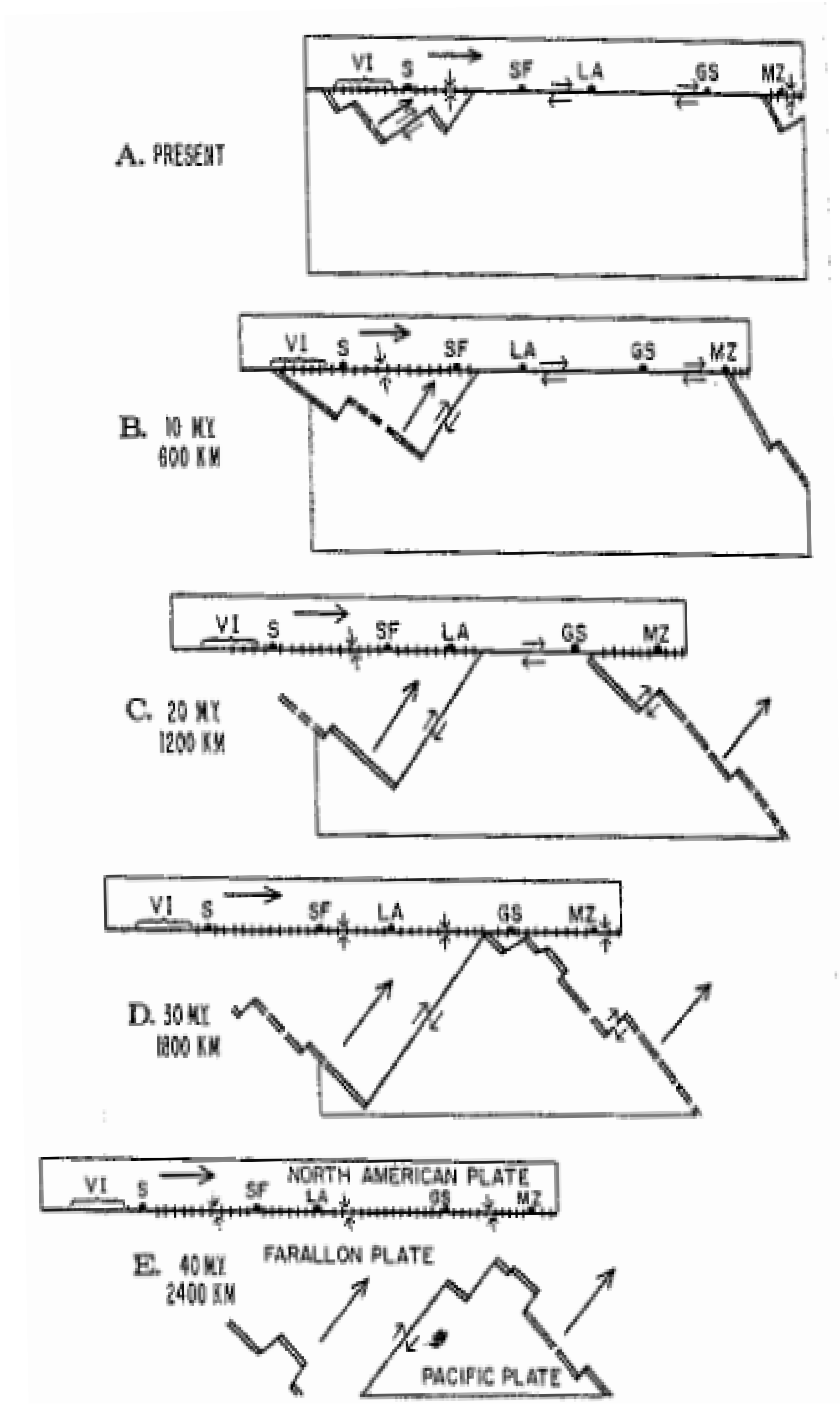

Figure 3: Model of Farallon-Pacific-North American Plate interaction from Atwater 1970. Assumes Pacific-North American Plate motion of 6 cm/yr. and that the Pacific plate is fixed. Initials represent cities: Vancouver Island (VI), Seattle (S), San Francisco (SF)), Los Angeles (LA), Guaymas (GS), and Mazatlan (MZ). Captions give times in millions of years before present.

Figure 4: Cascadia subduction zone showing the locations of the Explorer, Juan de Fuca, and Gorda plates along the subduction zone. Courtesy of Oregon.gov.

plates are currently subducting underneath NA in a region extending from the southern triple junction located off the coast of Cape Mendocino, California, to a point just north of Vancouver Island, British Columbia. The Gorda and Explorer plates are a bit smaller than the Juan de Fuca and their associated mid-ocean ridges are closer to the continental margin of North America (Figure 4). Thus, they have younger, hotter, thinner crust subducting underneath the continental margin. This increased buoyancy leads to a weaker slab pull force, and may lead to decoupling of the slab (Nicholson et al., 1994) which is evident between the Explorer and Juan de Fuca slabs. This difference in age of the subducting slab also leads to differences in other characteristics of the subduction zone, such as seismicity and volcanism.

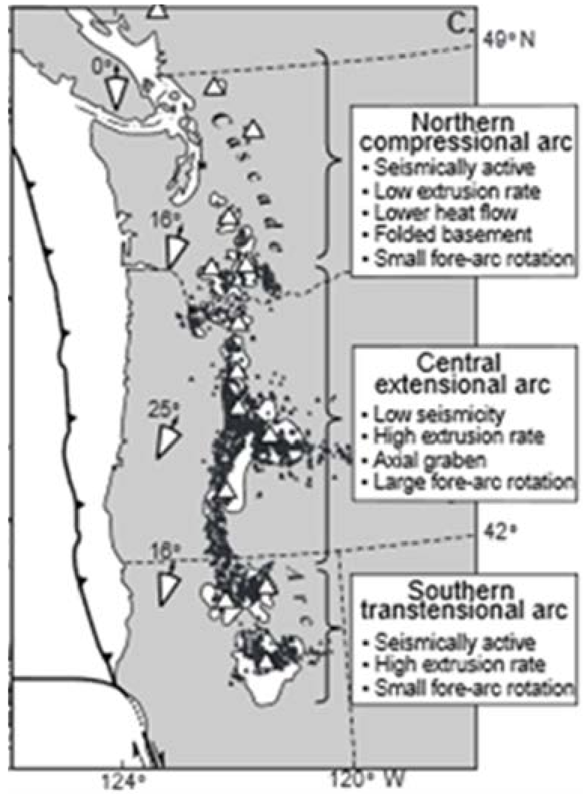

Figure 5: Cascadia fore-arc earthquakes, volcanoes, and fore-arc rotation. Sections highlighting seismicity, rotations, and extrusion rates. From Wells et al. (1998).

Relative to a fixed North American plate, the motion of plates G, JDF, and E are all northeast. The Gorda plate is moving the slowest of the three in this direction, moving at a rate of less than 3 cm/yr directed N26.4°E (UNAVCO, Plate Motion Calculator, 2015). The JDF plate is moving at around 3.6 cm/yr towards N26.3°E (UNAVCO, Plate Motion Calculator, 2015). The Explorer microplate is moving at the fastest rate of the three, about 4.3 cm/yr at N23.5°E (UNAVCO, Plate Motion Calculator, 2015). Wells et al. (1998) found similar directions of motion for these plates (Figure 5).

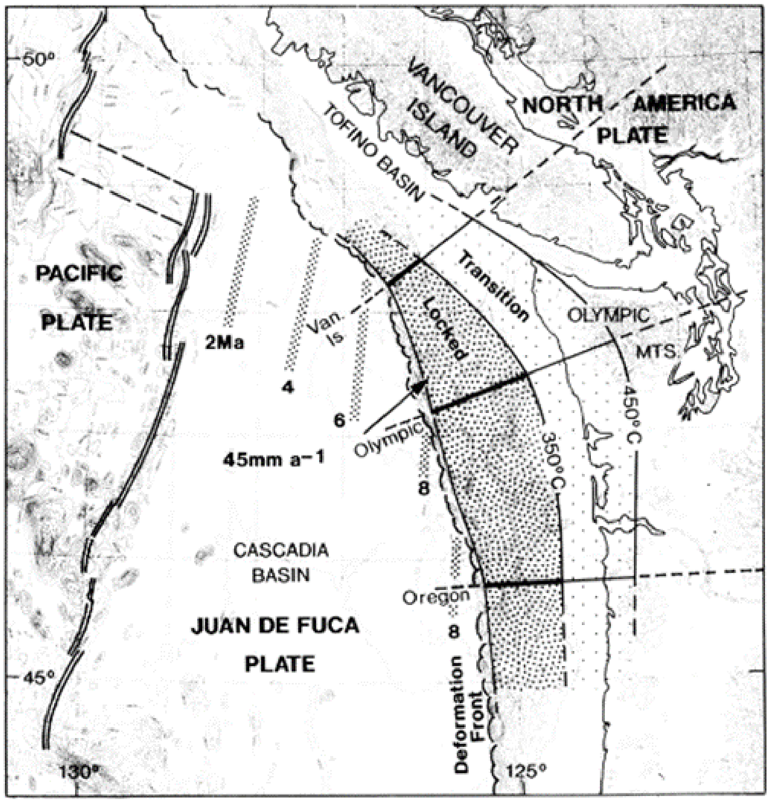

Figure 6: The Cascadia margin showing the extent of the locked and stable sliding zone, from Hyndman and Wang (1993).

The absolute plate motion of the JDF is actually in the southeast direction as opposed to its northeast relative motion. Pacific-NA motion is approximately 50 mm/yr (DeMets, 1989; Plate Motion, 2015).

The Cascadia Subduction Region

The Cascadia region is located in the Pacific Northwest and includes the coastal areas of northern California, Oregon, and Washington, and extends further north into British Columbia to just north of Vancouver Island (Figure 1, Region 1 and Region 2). The CSZ is part of the Pacific “Ring of Fire” and is an area of high seismic and volcanic activity. In this region the North American, Pacific, Explorer, Juan de Fuca, and Gorda plates interact in several ways. Relative to North America, the Explorer, Juan de Fuca and Gorda plates all move towards the northeast as described above. The Pacific plate moves to the northwest relative to all the other plates, but also has a slightly convergent interaction at the southern edge of the Gorda plate; the Mendocino fracture zone.

The Cascadia Region includes convergent, divergent and transcurrent motion. The Cascadia subduction zone runs north-to-south along the edge of the North American continental margin. The Juan de Fuca, Gorda, and Explorer mid-ocean ridge segments represent the divergent plate boundaries present within the region. The Sovanco, Blanco, and Mendocino fracture zones are areas of transcurrent motion present within the cascade region.

Deformation and Faulting in the Cascade Region

Tectonic "block" movement on land also has some effects on the seismic and volcanic activity of the Pacific Northwest (McCaffrey and Goldfinger, 1995; Wells et al., 1998; Wesnousky, 2005; Williams et al., 2005). Westward convergence of the Sierra Nevada-Great Valley block leads to accumulated strain at the southern end of the CSZ, which ultimately leads to earthquakes in the area. The Cascadia subduction zone is an area that is not highly seismically active. Much of the CSZ is currently locked or experiences aseismic creep (Gutscher et al., 2001; Hyndman and Wang, 1993; Hyndman and Wang, 1995; Wallace, 1970; Wang, 2000; Williams et al., 2005) and may be overdue for a major earthquake (Priest et al., 2014; Schulz, 2015), and will thus be the focus of many seismic studies and concerns in the near future.

The deformation front along the subduction margin is located completely offshore (Figure 6. Hyndman and Wang, 1993). This deformation front is the beginning of the subduction zone, and is locked along the entire length of the margin, with the exception of a small portion off the coast of Washington (Hyndman, 2013) down-dip, for about 20-40 km (Calvert, 2006; Hyndman, 2013). The fully locked portion of the subduction zone, and where the rupture can initiate, is limited to this depth by a temperature of 350°-450°c corresponding to changes from brittle to ductile behavior (Hyndman and Wang, 1995, Hyndman, 2013). Strain accumulates in the locked portion of the subduction zone for hundreds of years, and is suddenly released in an earthquake. Large earthquakes of this nature are called partial or full-margin ruptures (Schulz, 2015), depending on the length of the margin that undergoes the slip event, for which magnitude is directly correlated (Wallace, 1970). Schulz (2015), taking from the work of Goldfinger et al. (2003), describes partial margin ruptures as events reaching up to M8.6 and where as much as 50-70% of the margin ruptures, and full-margin ruptures as any event surpassing M8.6 where the entire margin ruptures.

North to south, along the length of the margin we see a change in the angle of the subduction (Romanyuk, 1998). In the south, off the coast of California and Oregon, the dip angle of the subducting slab is significantly steeper than the angle off the coast

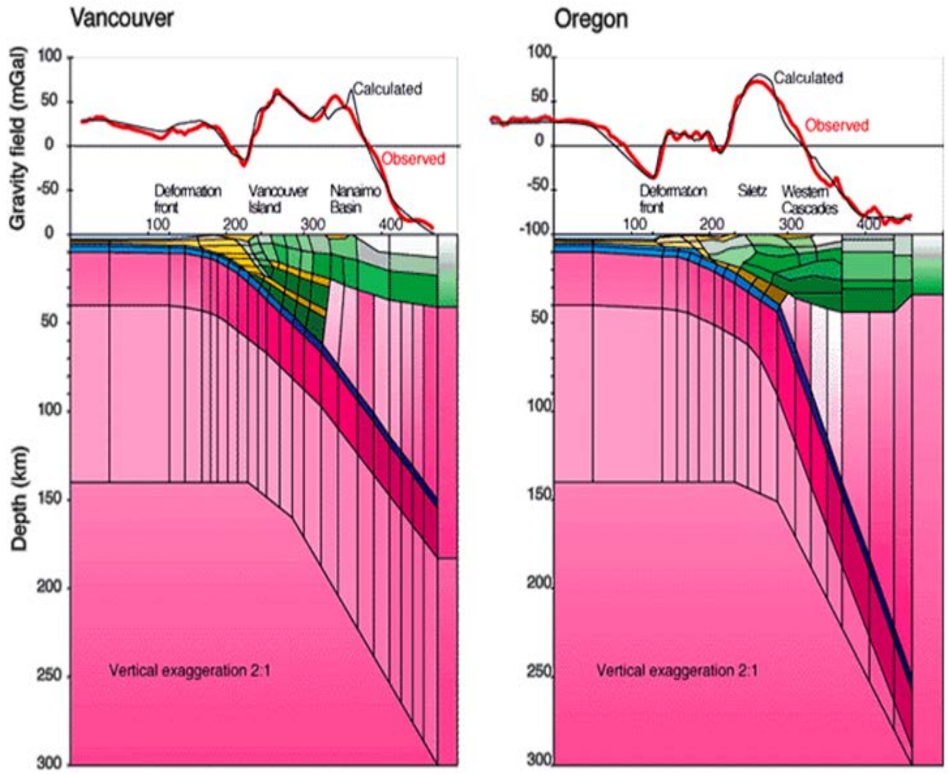

Figure 7: Density profiles of the subducting slab underneath Vancouver Island and Oregon. Difference in subduction angle is inferred to be the result of different density of the underlying mantle. Courtesy of the U.S. Geological Survey..

of Vancouver Island (Figure 7; U.S Geological Survey). This change in subduction angle supports the idea that the subduction zone is segmented (Romanyuk, 1998).

The difference in the subduction angle could be due to a number of things, but two main ideas (Romanyuk, 1998) are: 1) since the subducting slab beneath Oregon is slightly older than the slab beneath Vancouver Island, that the slab is colder and denser, and thus sinks more easily, and 2) the mantle wedge beneath Vancouver Island is denser and heavier than the mantle wedge beneath Oregon leading to a difference in buoyancy (Romanyuk, 1998). A combination of the two is also possible.

The change in subduction angle has effects on the distribution of earthquakes and volcanism. The difference in subduction would lead to a different geometry of the

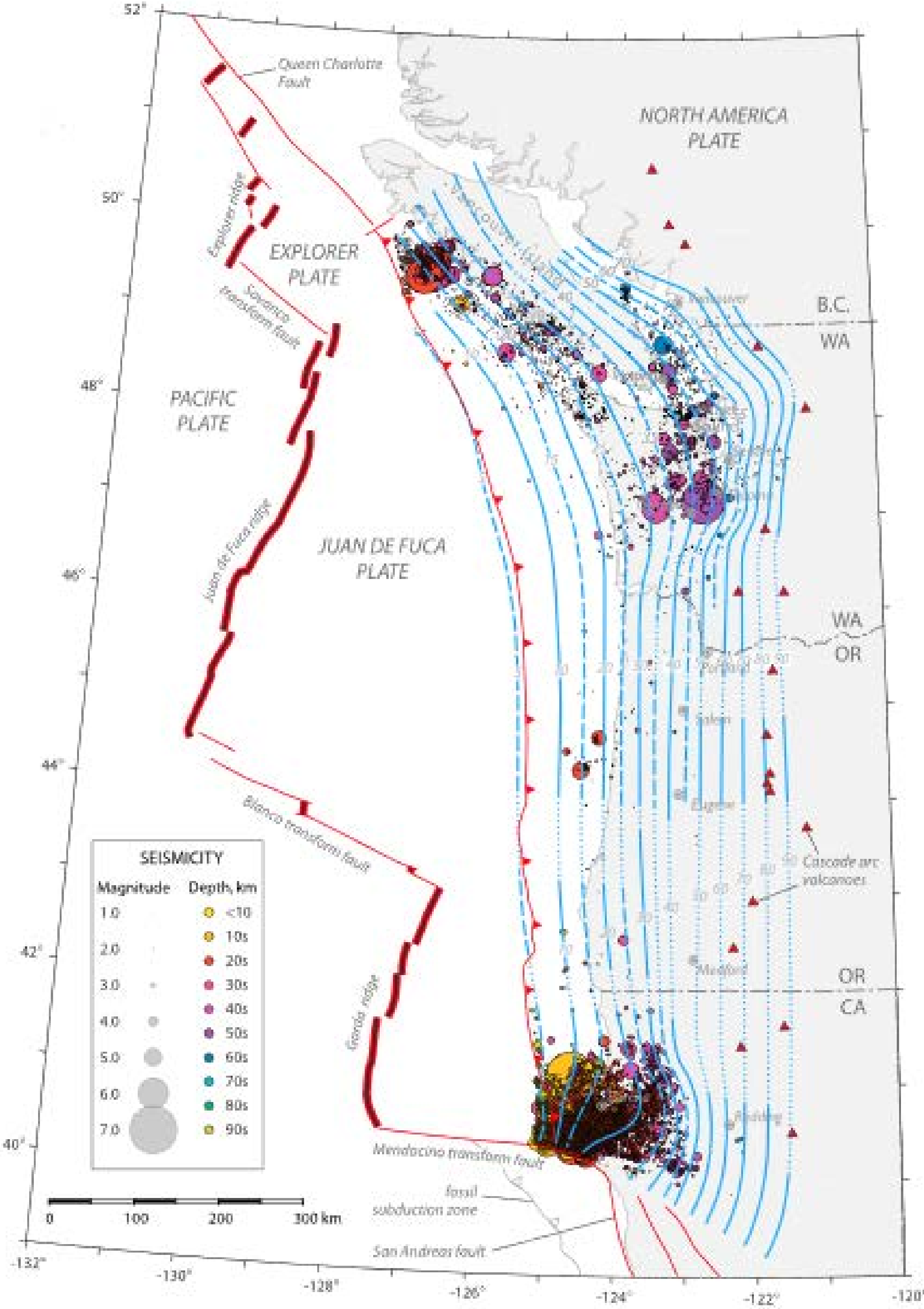

Figure 8: Contour map of the Cascadia subduction zone showing the location of Wadati-Benioff seismicity in the subducting slab. From McCrory et al. 2012.

Wadati-Benioff zone along the down-going slab, shallower dip leading to a shallower Wadati-Benioff zone and vice versa. There doesn't seem to be a correlation between the different angles of subduction and earthquake magnitude along the CSZ (Figure 8; McCrory et al., 2012), but rather there is a correlation between seismicity and internal slab deformation, specifically near the Nootka fracture zone, along a kink south of the Puget Sound, and near Cape Mendocino, which agrees with findings from Chen and Wu (2015).

Seismicity in the Cascade Region

At the southern end of the CSZ, the subduction zone meets the San Andreas Fault zone and is also affected by WHR extension. Williams (2005) states that besides elastic strain accumulation, westward convergence of the Sierra Nevada-Great Valley block and impingement of the SAF from the south, help account for the accumulated strain. The strain accumulation from all three of these factors is quite aggressive, and therefore results in an area of high seismic activity.

According to Chen and Wu (2015), “Seismicity mainly occurs beneath the strait of Georgia-Puget sound, the northern Cascade Range and northwestern California, and sparsely in the central part of the subduction zone.” There are a few other areas where earthquakes tend to occur in the Cascadia region. The first is along the mid-ocean ridge and its associated transform faults (Figure 9). This is the reason for the high seismicity in the northern Cascadia region. Second is the Explorer plate area where mid-ocean ridges, transforms and fracture zones, and the subduction zone are all spatially concentrated. The other area of seismicity, the locked portion of the subduction zone, produces the deadliest but less frequent margin ruptures, such as the January 26, 1700 earthquake of estimated magnitude 9 (Steele, 2013).

The subducting slab of Cascadia is not spatially uniform when it comes to seismicity. The part of the slab subducting beneath the Puget Sound and further north shows a great deal of seismicity, while the slab subducting underneath Oregon shows very little seismicity (Figure 8) and doesn't have a prominent Wadati-Benioff zone (Piana Agostinetti, 2014). At the very southern tip of the Cascadia region we have the Mendocino triple junction, where again, we have a lot of seismic activity (Figure 8).

The high seismicity in the northern Cascades, primarily around and off the coast of VI is attributed to the abundance, and close proximity of, the plate boundaries in that area.

The earthquakes in the Puget Sound area are mostly intra-slab earthquakes, and are abundant likely due to slab buckling or warping (Chen and Wu, 2015). Larger

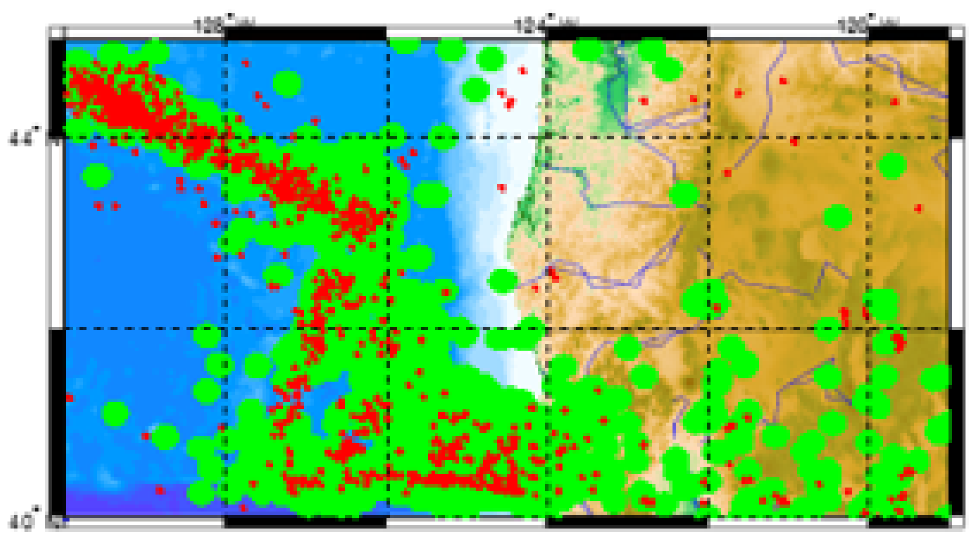

Figure 9: CS analysis of the Southern Cascadia (SJDF) sub-region for M3.5+ seismic events for the 1999-2000 date cutoff. Shows the absence of seismic events off the coast of, and beneath, Oregon.

earthquakes around the Puget Sound are located up-dip of the slab dehydration zone, indicating seismicity in this area may be controlled by hydration state (Chen and Wu, 2015).

The slab subducting underneath NA off of the Oregon coast shows very little seismicity in historic times (Figure 9, brown area). While there is a great deal of seismic activity along the Gorda ridge, there is very little along the margin and beneath the surface of NA in Oregon.

The most catastrophic, highest magnitude earthquakes that occur along the CSZ are margin rupture events like that of January 26, 1700. These margin ruptures, which are associated with “Episodic Tremor and Slip” events, have a higher magnitude than the other earthquakes of Cascadia because of the great amount of energy they store and the length of the fault zone that slips, compared to fault zones or segments that slip more frequently. Episodic tremor and slip events are slow slip events that generate "tremors" (minor seismic vibrations) that generate non-earthquake seismic signatures (Rogers and Dragert, 2003). They are not damaging but are recorded by seismographs and provide clues as to where future margin rupture earthquakes might occur by acting as an indicator of stress loading along a megathrust fault (Rogers and Dragert, 2003). Margin rupture episodic tremor and slip events happen along convergent plate boundaries where stress builds up along the continental margin until a frictional threshold is exceeded. When the threshold is exceeded the tectonic plates “bounce back” to an unstressed position.

The Cascadia margin is 1100 km long, and is locked for the vast majority of that distance (Hyndman and Wang, 1993). Margin ruptures are typical of subduction zones, and produce the largest earthquakes on record. The rupture is a result of the locked portion of the margin giving way producing a large earthquake. When a subduction thrust fault is locked, elastic strain builds in the direction of subduction causing crustal contraction (Wang, 2000). The rupture releases all the stored energy, and decompression causes crustal extension.

Schulz (2015) defines a partial margin rupture (PMR) as a rupture that occurs along 50-70% of the subduction zone. While a rupture of 50-70% of the margin is clearly a “partial” margin rupture, smaller margin ruptures do happen and are also more frequent, and happen more frequently at the southern end of the Cascadia margin (Priest et al., 2014; Figure 10). If a PMR, as Schulz defines it, were to occur along the southern half of the CSZ, we could expect an earthquake between magnitudes 8.0-8.6. Smaller ruptures will result is smaller earthquakes, as the magnitude is directly proportional to the length of the rupture.

Using an empirical fault area versus magnitude relation, Hyndman and Wang (1995) state the magnitude of an earthquake is directly proportional to ruptured fault surface area. According to Schulz (2015), Goldfinger et al, (2003), and Priest et al., (2014), a full or near-full margin rupture (FMR) would correspond to an earthquake between magnitudes 8.7-9.2. An FMR producing a magnitude 8.7-9.2 earthquake corresponds well with the findings of Wallace (1970), which found that a FMR would result in an M9 earthquake.

Recurrence intervals, calculated by Priest et al. (2014), were found for both partial and full margin ruptures based on turbidites from the past 10,000 years found off the coast of the Pacific Northwest (Goldfinger et al., 2003; Priest et al., 2014). Overall, the recurrence interval for a margin rupture along the CSZ is about 240-245 years, which was found on the basis of 41 events over the 10,000 year period (Priest et al., 2014; Schulz, 2015). Considering that a margin rupture of any length hasn't happened in over 300 years, Schulz (2015) says that we are overdue for a PMR. That would be correct had the paper not defined a PMR as 50-70% of the CSZ length, and having a magnitude between 8.0-8.6. The recurrence interval for an event along the CSZ of magnitude 8.0 and above is approximately 417 years, based on there being 24 events of M8+ in the past 10,000 years (Priest et al., 2014). This suggests that the Cascadia subduction zone is not overdue for an earthquake of that magnitude, but is about 75% of the way through that recurrence interval, assuming that past earthquake recurrence intervals are a good indicator of when future earthquakes will occur.

The recurrence interval for a FMR is more than 500 years. According to Priest et al. (2014) the recurrence interval for an FMR is between 500 and 530 years. Goldfinger et al. (2003) find a 1-1 correspondence between turbidites occurring, on average, every 655 years and M9 earthquakes. There is evidence from turbidites and subducted forests on the western North American margin, and a recorded "orphan tsunami" in Japan that

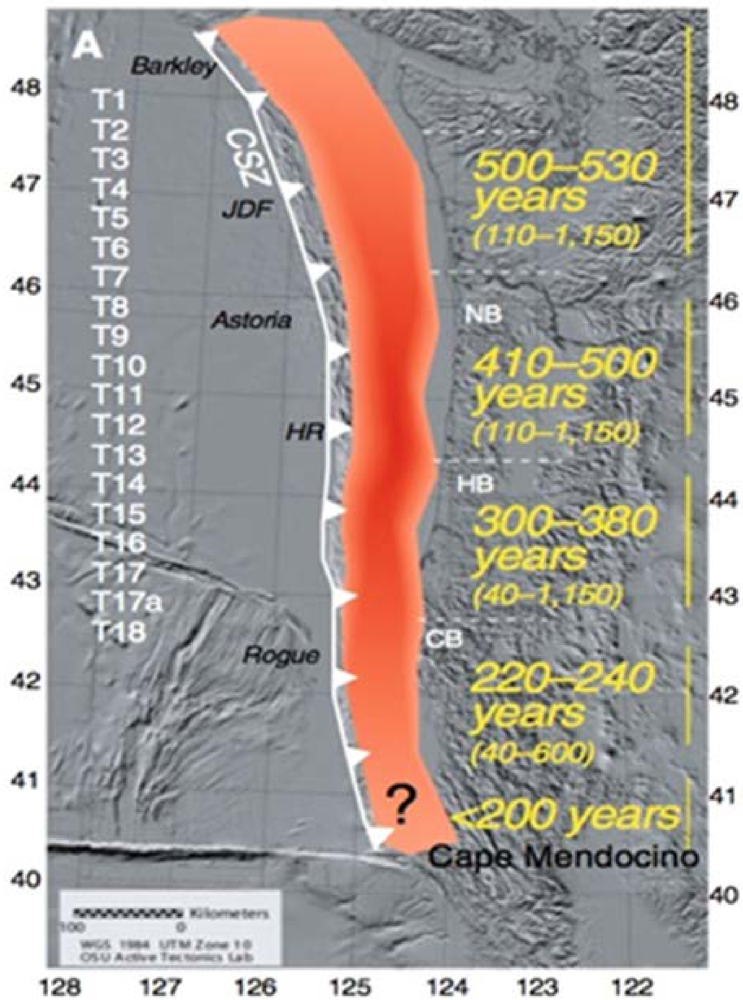

Figure 10: Average recurrence times for different inferred segments of the Cascadia subduction zone based on offshore turbidites. From Priest et al. (2014).

suggest the last full margin rupture occurred in the year 1700. This is the last margin rupture of any length along the Cascadia margin.

San Andreas Transform Region

The SAF is a right-lateral transform fault marking the boundary between the Pacific and NA plates. Relative motion along the SAF is northwest-southeast oriented, with the Pacific moving northwest relative to the North American plate. As mentioned previously, the SAF was once much shorter, but has lengthened over time as portions of the oceanic slab subducted under NA (Atwater, 1970).

The San Andreas region covers an area in this study from 30°-40°N (Figure 1), and from two different longitude ranges depending upon the sub-region in question. The northern San Andreas (NSA) sub-region ranges from 35°-40°N and 115°-124°W (Figure 1, Region 4), while the southern San Andreas (SSA) covers 30°-35°N and 113°-122°W (Figure 1, Region 5). A latitudinal cutoff at 35°N is used here somewhat arbitrarily so as to divide the SAF region into two sub-regions of approximately the same size. The longitude cutoff values were made based on the geometry of the SAF and its surrounding faults.

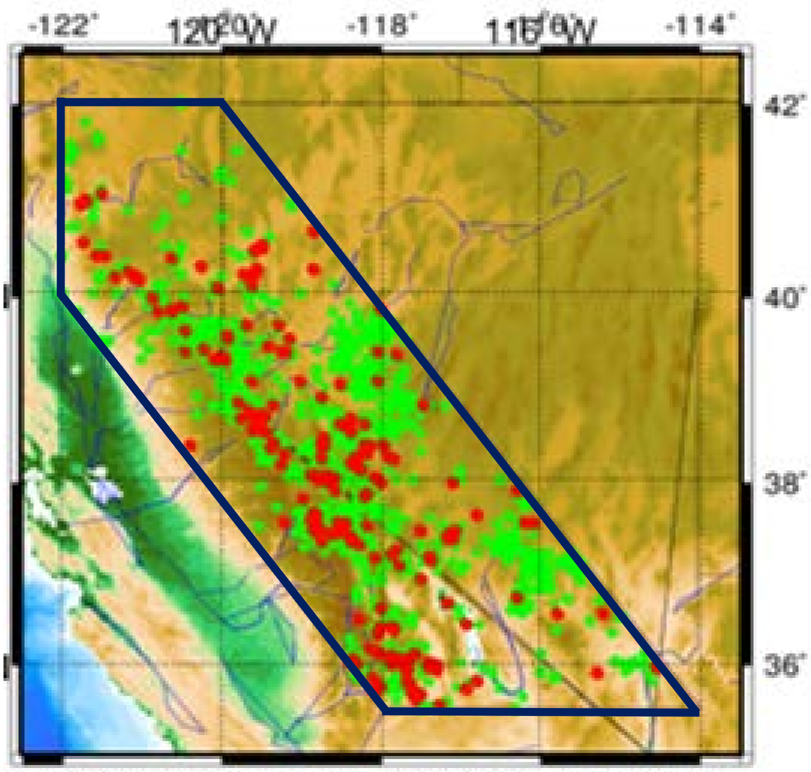

Figure 11: Seismicity of the Walker Lane Belt, outlined by the blue polygon, for earthquakes of M3.5+ for the 1999-2000 date cutoff. Note San Francisco Bay located at 38°N on the far left-hand side of the figure.

Figure 12: Major faults in the San Francisco Bay area. Yellow portion of the Hayward Fault is the section that slipped during the 1868 Hayward earthquake. Dot size represents the present relative population of major cities in the area. Courtesy of dailymail.co.uk.

It is important to note that what I have labeled as the San Andreas region for the purpose of this study covers more than just the SAF and its branch faults. The San Andreas region is broad and essentially covers an area from the coast through central Nevada. The Walker Lane Belt (WLB), which is designated by the area inside of the blue polygon in Figure 11 and runs along the eastern side of the Sierra Nevada's, is also part of the San Andreas region, as defined here, despite not being immediately related to the SAF. This was done because the WLB is a series of left-stepping transtensional faults (Wesnousky, 2005), and since the faults are transform faults they are more closely related to San Andreas transform movement than they are to WHR extensional movement despite the slight extension found in the WLB (Figure 12).

Deformation and Faulting in the San Andreas Region

Schwartz and Coppersmith (1984) segment the SAF north-south in terms of the percentage of creep observed along certain portions of the fault, breaking it up into northern, central, south central, and southern segments. In this thesis, I divided the SAF into four segments as well, partially based Schwartz and Coppersmith's work, but also based on fault geometry. I subdivide the system into a northern segment, calling it San Andreas North (SAN) running from 37.5°-40°N, a central segment (SAC) from 35.5°-37.5°N, a portion from 33.5°-35.5°N which I will also refer to as the San Andreas Bend (SAB), and a southern portion (SAS).

Wallace (1970) breaks down the SAF into even smaller segments based on creep rates (Figure 13). There are two segments that Wallace shows as possibly locked. The first segment is from Cape Mendocino to Los Gatos (Figure 13, orange portion) at the very northern end of the SAF, and the second being from Cholame to Cajon pass (Figure 13, yellow portion), the site of the great 1857 earthquake. These two areas of the SAF have been relatively inactive and show almost no creep. The central portion of the SAF is an area with a high creep rate (Teyssier, 1995; Wallace, 1970; Schwartz and Coppersmith, 1984) with estimates ranging from 2-5 cm/yr depending on the segment (Wallace, 1970), 32 ± 2 mm/yr (Schwartz and Coppersmith, 1984), and 34 mm/yr

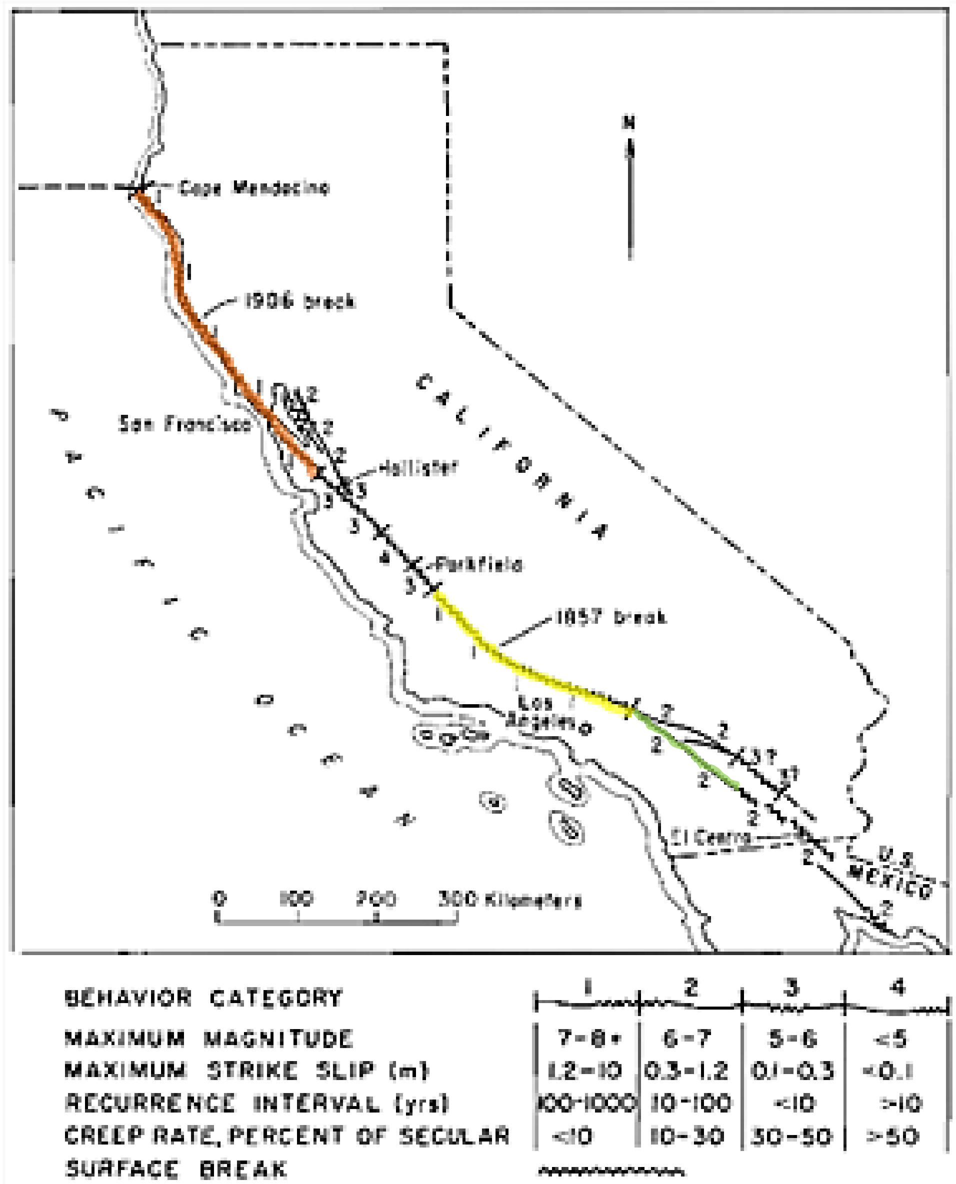

Figure 13: Map of California and the San Andreas Fault showing fault behavior as a percentage of creep. Proposed locked portions of the fault, Cape Mendocino to Los Gatos and Cholame to Cajon Pass, shown in orange and yellow respectively. San Jacinto Fault shown in green. From Wallace (1970).

(Teyssier, 1995). Other segments of the fault described by Wallace show little creep compared to the central portion of the SAF, and also shows little to no creep on an important branch of the SAF, the San Jacinto fault system.

Mount and Suppe (1987) studied the central portion of the SAF in greater detail, focusing on heat flow and estimating shear stress along this portion of the SAF. They find that due to anomalous heat flow and seismic energy radiation that the shear stress along this portion of the SAF is extremely low, only 10-20 MPa. This could account for the high creep rate seen in the central SAF. Zoback et al. (1987) also find low levels of shear stress, between 10-20 MPa, based on conductive heat flow in boreholes located near the SAF.

The San Andreas Fault system has many branch faults. In the northern half of the SAF system we have the Rodgers Creek, Hayward and Calaveras faults (Figure 12). In the southern half of the SAF system we have the Garlock, San Jacinto and Elsinore faults (Figure 2).

Seismicity in the San Andreas Region

The SAF is a transpressional tectonic boundary comprised of many fault segments with very high seismicity; certain portions of the 800 mile long (Schulz and Wallace, 1989) SAF are more seismically active than others. Seismicity along the SAF is much more prevalent in the southern half of the region than in the northern half. The northern half of the San Andreas includes significant branch faults like the Hayward, Rodgers Creek, and Calaveras faults (Figure 12; Brocher et al., 2008), but lacks bends, and also lacks major WLB faulting.

The largest earthquake to strike the San Andreas region in historical times was the M7.9 Fort Tejon earthquake of 1857. The majority of earthquakes of magnitude five or higher occurred in the southern half of the region, and the majority of the southern half's earthquakes occurred in the SAS sub-region (Figure 14).

Field et al. (1999) estimated the maximum magnitude for earthquakes on the San Andreas to be M7.99. Schulz (2015) states that, based on rupture length, the maximum magnitude possible on the SAF would be about M8.2. Wyss (1979), and Wells and Coppersmith (1994) go into detail about these calculations. The USGS estimates it to be M8.3 based on fault area (length and depth), but this would involve the entire SAF rupturing at once, which they state is highly unlikely (Earthquake Facts, 2015). Kijko

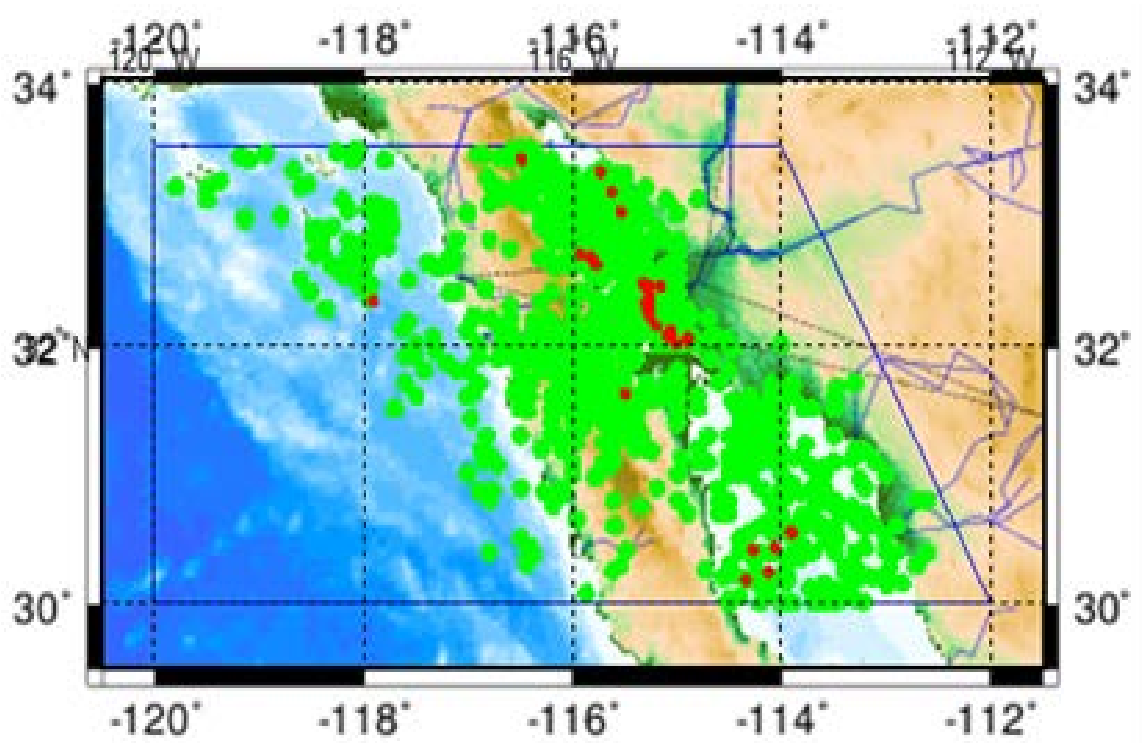

Figure 14: CS analysis of the SAS sub-region, outlined in the blue polygon, of M5+ events for the 1999-2000 date cutoff. Thirty-six out of thirty-six Post-Cat events were successfully forecasted.

(2004) found the maximum magnitude for southern Calfornia to be about 8.31, 8.32 and 8.34 based on when earthquake magnitudes are distributed according to the doubly-truncated Gutenberg-Richter relation, when the empirical magnitude distribution deviates moderately from the Gutenberg-Richter relation, and when no specific type of magnitude distribution is assumed, respectively.

Magnitude 5 earthquakes occur approximately six to eight times per year along the SAF based on the recurrence intervals found in the Uniform California Earthquake Rupture Forecast, models 2 and 3 (UCERF2, UCERF3), respectively. During the 255 year catalog used in this thesis M5 earthquakes are actually more prevalent in the northern half of the region, as opposed to the southern half which shows a greater number of M5+ earthquakes in recent years. This illustrates how difficult it is to forecast characteristics of future seismicity based on past seismicity, but as will be seen below there does seem to be at least hints of stable long-term patterns in CS predictability

The Western Hinterland “Continental Extension/Intraplate” Region

The Western Intraplate Hinterland Region of the WUS is a broad area of extension fueled by the collapse of the North American Cordillera, and relative movement of several blocks of the North American continent. While the WHR is broadly associated with the plate boundary deformation of the SAF, and localized contraction or rotation in Washington State and Oregon respectively (McCaffrey and Goldfinger, 1995) because of the collapse of the previously thickened crust, this study categorizes it as an “intraplate” region because it does not lie on or near a major plate boundary as the other two regions, Cascadia and SAF, of this study do.

Deformation and Faulting in the Western Intraplate Hinterland Region

Hammond and Thatcher (2004) outline six areas of differing tectonic deformation within in the WHR region, of which I will discuss the first four: (1) east-west extension in the Wasatch Fault zone, (2) low-rate east-west extension near the Utah-Nevada border, (3) low-rate east-west contraction between 114.7°-117.9°W, (4) extension normal to and strike-slip motion across the N10°E Central Nevada Seismic Zone. Numbers 5 and 6 of Hammond and Thatcher’s six part tectonic regime I have included in the San Andreas region, so I will not describe them here.

Yellowstone and the surrounding Snake River Plain (Figure 15), and the associated volcanism and extension there is another area of interest. Yellowstone is a mantle hotspot where volcanic intrusions accommodate crustal extension in the area at depth. The North American continent is migrating over the hotpot, as evident from the Snake River Plain, an area of low-lying terrain almost completely basaltic in nature that appears to be moving southwest. The movement may not have always been to the southwest though. Change in motion may have been due to topographic swell caused by either a hot upper mantle or by some component of buoyancy from depleted upper mantle (Parsons et al., 1998).

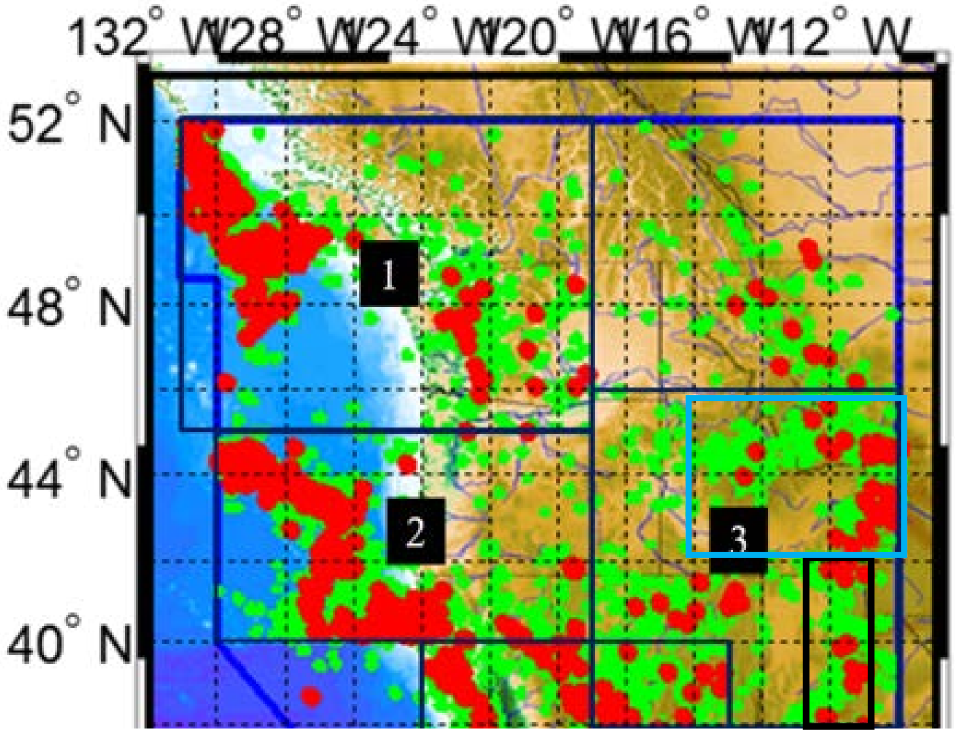

Figure 15: The Wasatch Fault zone (WFZ) is a small fault zone in the southeastern corner of the WHR. The WFZ is outlined by the black rectangle. Yellowstone and the Snake River Plain outlined in blue.

In the northwest Snake River Plain (NWSRP) and the northern WHR in general is one of the most actively extending parts of the region, and seismic activity there is quite high due to that extension. Here, "brittle extension is accommodated by tilt-block faulting on several faults, forming half-grabens", (Parsons et al., 1998).

Seismicity in the Western Intraplate Hinterland Region

The Wasatch Fault zone (WAS) is an area on the eastern edge of the WHR (Figure 15) that is characterized by periodic earthquakes. The WAS has not ruptured during historic times (Schwartz and Coppersmith, 1984). The recurrence intervals of magnitude 7 events found for different segments of the WAS range between 400-666 years

(Schwartz and Coppersmith, 1984). Schwartz and Coppersmith note that, “based on segment lengths, down-dip fault width, and average displacement per event” the highest magnitude event on the Wasatch could be between M7.0 and M7.5. Therefore, despite its low seismicity, and lack of large earthquakes in historic times, the WAS might still be deadly, at least according to the conclusions of Schwartz and Coppersmith.

The Snake River Plain is nearly aseismic, with some of the largest earthquakes recorded within the plain being of only M1.5 (Parsons et al., 1998), but on both the east side and the northwest side of the plain there is quite a lot of seismicity. The aseismic nature of the Snake River Plain is somewhat paradoxical since it is in an area of active extension. It is possible that because of the basaltic intrusions that the plain became strong enough to resist extensional deformation, or that it is too weak to fail by faulting because of the thermal input from the hotspot (Parsons et al., 1998).

The eastern side of the Snake River Plain (ESRP) is also an area with more seismicity than the other sub-regions of the WHR. Earthquakes in this sub-region reached magnitudes as high as M7.5 (the 1959 Hebgen Lake earthquake), and smaller earthquakes are quite abundant here for an intraplate region.

The number of earthquakes surrounding the Snake River Plain is likely attributable to the diffuse network of extensional faults surrounding the Yellowstone hotspot and the Snake River Plain (Parsons et al., 1998). Basaltic crust makes its way to the surface in the Snake River Plain through dikes, and the areas surrounding the region need to extend outward, either northward or eastward in the case of the NWSRP and

ESRP, to accommodate the strain caused by the basaltic intrusions. Because the network of faults in the NWSRP and ESRP are diffuse though, we shouldn't expect a high level of CS predictability there.

"Cellular Seismology" and Earthquake Forecasting and Prediction

One of the many methods used in the study of earthquake forecasting is a spatial investigation and evaluation tool known as "Cellular Seismology" (CS), invented by Kafka (2002, 2007). CS analyzes the relationship between past earthquakes and more recent earthquakes in an attempt to discern the extent to which locations of past seismicity delineate zones where future earthquakes are likely to occur.

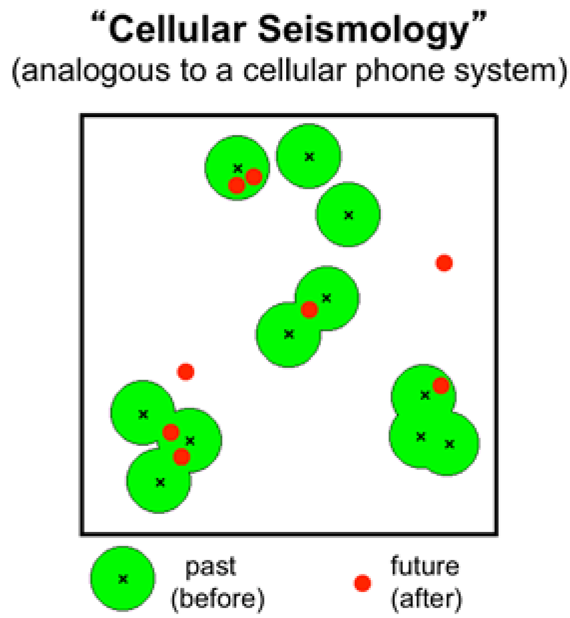

Figure 16: Hypothetical scenario showing how cellular seismology works. Pre-Cat earthquakes cover a certain percentage of area of the map, with a given radius from the epicenter. Post-Cat earthquakes shown in red. If the red dots fall within the green area covered by Pre-Cat earthquakes, we call that a hit. If the red dots fall outside the green area, we call that a miss.

Various studies by Kafka and his students and other colleagues have found that, on average, plate boundaries tend to show a higher level of CS predictability than intraplate areas (e.g., Kafka, 2002, 2007; Kafka et al., 2014). As described previously, "CS predictability" is the term used herein to refer to the measure of the extent to which past locations of earthquakes delineate zones where future earthquakes are likely to occur in a given region.

One of the goals of this study is to determine whether the same pattern of higher CS predictability found in plate boundary zones versus intraplate zones is true for the WUS and the various sub-regions of the WUS that are analyzed in this study. The more general goal is to investigate the variation of CS predictability among the various tectonic sub-regions of the WUS described in the proceeding background section. CS will thus be used to investigate the extent to which seismicity in the Cascadia region, the San Andreas region, and the Western Intraplate Hinterland Region accurately shows a delineation of where future earthquakes are likely to occur based on previous earthquakes. CS is also used to find and compare seismicity relationships between regions/sub-regions that contain a subduction zone, transform boundaries, mid-ocean ridges, and broad areas of extension.

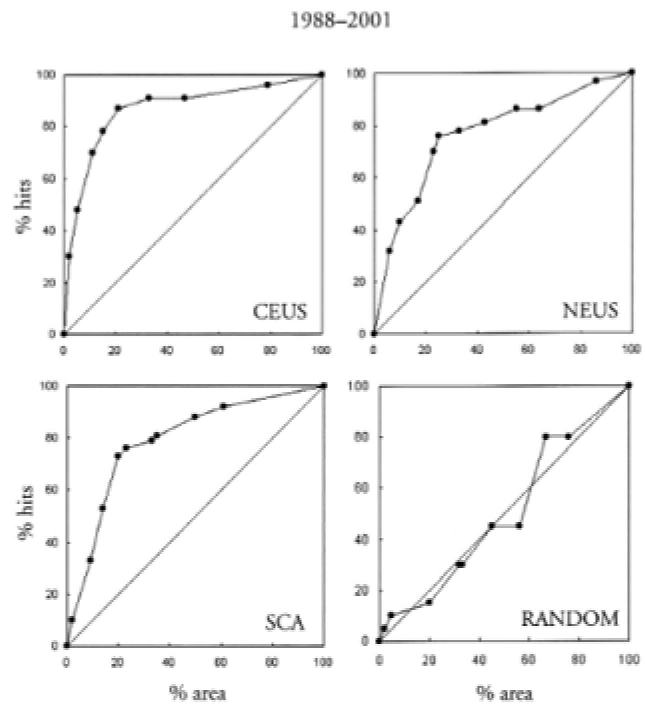

Figure 17: Percentage of hits as a function of percentage of map area covered by Pre-Cat earthquakes for the central eastern US (CEUS), northeast US (NEUS), and southern California (SCA), as well as a random distribution for a hypothetical region.

CS is of very simple design, but has been found by Kafka and Ebel (2007, 2011) to yield results comparable to the more complicated method of "Pattern Informatics" used by Rundle et al. (2007), Tiampo et al. (2002) and Holliday (2006, 2007).

CS divides an earthquake catalog into a "before" sub-catalog (or "Pre-Cat") and an "after" sub-catalog (or "Post-Cat") (Figure 16; Kafka, 2007). The Pre-Cat and Post-Cat data are mapped and analyzed to see how many of the Post-Cat earthquakes occurred near the Pre-Cat earthquakes, which we refer to here as the level of "CS predictability", with a defined radius from each epicenter representing "near". In other words, the area surrounding the Pre-Cat epicenters covers a subset of the area of the study region. If the Post-Cat earthquakes fall within that area, we call that a "hit". If they do not fall within that area we call that a "miss". Each regional Pre-Cat data set has its own radius corresponding to a given amount of percentage of map area.

Kafka and colleagues have investigated the effect of varying the percentage of map area in CS studies, and have found that 33% map area is a convenient metric for comparing CS predictability in different regions (e.g., Kafka, 2002; Kafka, 2007; Kafka et al., 2014). In the CS analyses in this study, 33% map area is, therefore, chosen as a useful and convenient metric for comparison of regions, but 33% does not have any particular physical significance. Theoretically, covering 33% of the map will result in a CS hit percentage of 33% if the Post-Cat seismicity is uniformly distributed spatially (Kafka, 2002). That is, 33% of the Post-Cat earthquakes will fall within the 33% area of the map covered by Pre-Cat radii for a given CS analysis. This usually turns out not to be the case, especially for plate boundaries. In many studies by Kafka and his colleagues using 33% map area, more than 33% of Post-Cat earthquakes are hits, indicating that, for many types of tectonic regions, there is a preference for future earthquakes to occur near past earthquakes.

Covering 33% of the map area will result in different CS results should the area in question be different in spatial extent. Consider an area where seismicity is highly localized. If that area is the only place where seismicity happens and we are covering 33% of the map area, we should expect a higher level of CS predictability when we zoom out away from the seismic area, and lower CS predictability when zoomed in. Even though we are covering 33% of the map area in both cases, when we are zoomed out to a larger total area, that 33% also covers a larger spatial extent then when we are zoomed in, resulting in higher levels of CS predictability. However, zooming out to a larger sub-region, means that to cover 33% of the map area it is necessary to make the CS circle radii larger, thus likely raising the percentage of hits. Thus, using percentage of area as the CS predictability metric (rather than for example, CS radius) mitigates the effect of regions being different sizes; see Kafka (2007) for further discussion of this issue.

The USGS has developed a method for the forecasting of earthquakes in California, the “Uniform California earthquake rupture forecast”, or UCERF (Field and Milner, 2008), for which there have been three different reports thus far: UCERF1 (2006, not used in this study), UCERF2 (2008), and UCERF3 (2015). In contrast to CS, UCERF uses information about faults and ruptures to determine the likelihood of a specific magnitude event happening along a fault or in a specific region of California for a given time period; 30 years in the case of UCERF3. The UCERF models give “estimates of the magnitude, location, and likelihood of earthquake fault rupture throughout California” (Field and Milner, 2008; Field 2015). UCERF3 is run using two models: an “Earthquake Rupture Forecast, which tells us where and when the Earth might slip along the state’s many faults, and a Ground Motion Prediction model, which estimates the subsequent shaking given one of the fault ruptures. The results of UCERF3 forecast that both the northern and southern halves of the San Andreas are more than 90% likely to have a M6.7+ event in the next 30 years, 93% and 95% respectively (Figure 18). M6.7 was chosen based on the 1994 Northridge earthquake. CS is primarily a spatial (i.e. location) based analysis of future earthquakes, as it doesn’t deal with their likelihood. CS, and this thesis specifically, also just begin to ascertain the relationship between magnitude and future earthquake likelihood by systematically varying the magnitude cutoffs for the regions analyzed.

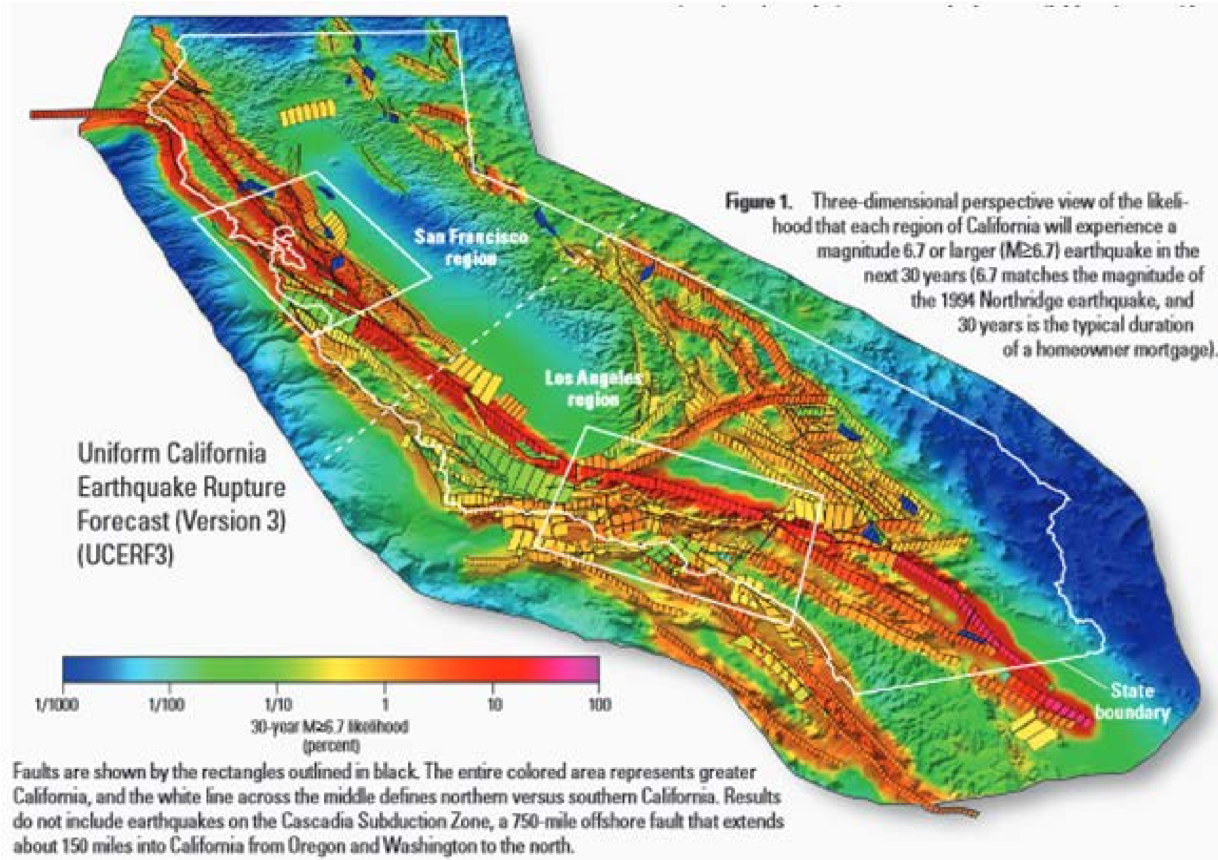

Southern California region

Magnitude (greater than or equal to)	Average repeat time (years)		30-year likelihood of one or more events		Readiness
5	0.24	(0.7)	100%	(1.0)	1.0
6	2.3	(0.9)	100%	(1.0)	1.0
6.7	12	(1.5)	93%	(1.0)	1.0
7	25	(1.4)	75%	(0.9)	1.1
7.5	87	(1.2)	36%	(0.9)	1.2
8	522	(0.4)	7%	(2.5)	1.3

Northern California region

Magnitude (greater than or equal to)	Average repeat time (years)		30-year likelihood of one or more events		Readiness
5	0.24	(0.7)	100%	(1.0)	1.0
6	2.4	(0.9)	100%	(1.0)	1.0
6.7	12	(1.2)	95%	(1.0)	1.0
7	25	(1.2)	76%	(1.0)	1.1
7.5	92	(0.9)	28%	(1.1)	1.0
8	645	(0.8)	5%	(1.4)	1.1

Figure 18: UCERF3 analysis of the seismic hazard of California. Likelihoods of specific magnitude earthquakes for the northern and southern San Andreas given on the right. From Field (2015).

Data Collection and Analysis Methods

All earthquakes in my catalog are either taken courtesy of the constantly updated earthquake database of the USGS through the end of 2014, or they were provided from the work of Chambless and Kafka (2014, Chambless Senior Thesis, Boston College), which was from a separate USGS record (USGS Earthquake Hazards website, 2008). The current USGS website contains information on earthquakes dating as far back as the mid 1800's. The catalog of Chambless and Kafka (2015), obtained from the USGS Earthquake Hazards website, includes additional earthquakes dating back to 1769 the oldest dates contained within my catalog.

The CS method was implemented for the entirety of the WUS area stated in the introduction. This overall map area is then decreased slightly in size by the use of a polygon, created in Matlab, that cuts out most of the Pacific ocean in the southwestern portion of the map regions, as there are not many reported earthquakes in that area of the map (Figure 19).

Earthquakes from sources in the above three regions of study were then deleted based on whether or not they fell within the area of the aforementioned polygon, and only those earthquakes within the polygon are analyzed here using the CS method.

Computer programs written in Matlab and C (by Dr. Alan Kafka) were modified for the specific regions and sub-regions covered in this study to analyze Pre-Cat and Post-Cat data for the study area. Locations of the Pre-Cat and Post-Cat earthquakes were plotted, and hit percentages were calculated using separate Matlab codes.

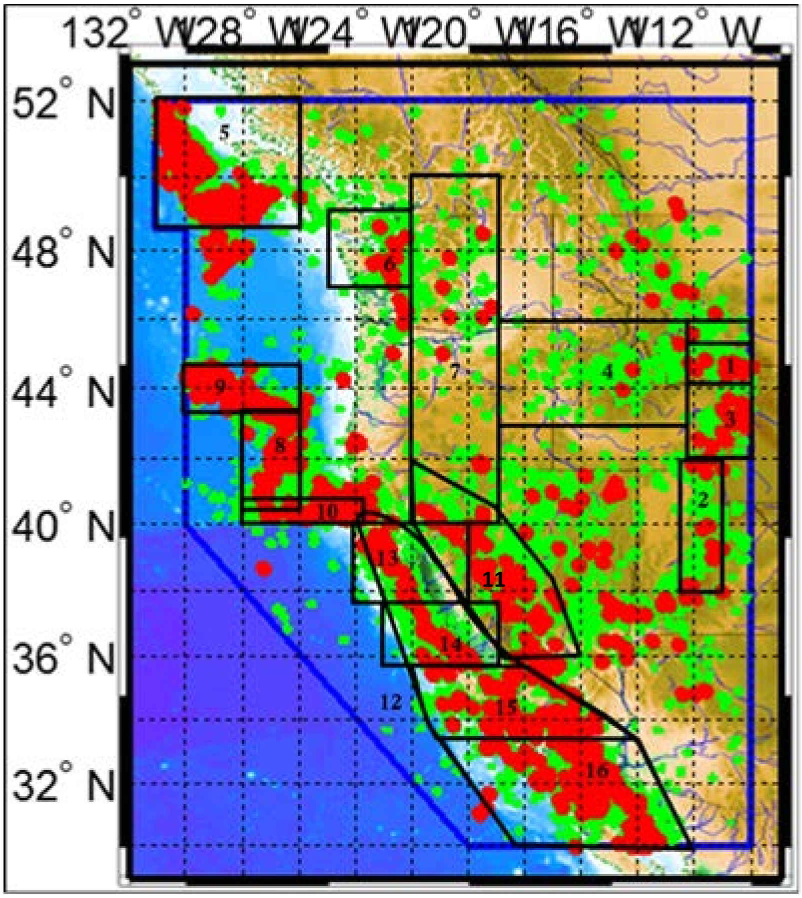

Figure 19: Map of the smaller sub-regions. Sub-region areas outlined in black. Numbers correspond to with the sub-regions listed in Table 3.

Three regions (described above) were created and analyzed. The preliminary calculation of the CS predictability was conducted to test the sensitivity of the chosen regions. Based on this initial calculation, I observe that the CS method did not yield any statistically significantly distinguishable differences between the Cascadia and the SAF regions in terms of the level of CS predictability. Consequently, smaller sub-regions were chosen for analysis to test for smaller-scale differences in CS predictability based on the respective tectonic regions. Twenty-one sub-regions were created (Figure 1; Figure 19), at least three per tectonic region, based on tectonic features, geometries, and plate boundaries.

Sub-region	Number	Longitude Range	Latitude Range	Region
Western Hinterland (WHR)	N/A	110°-119°W	38°-46°N	WHR
Northern Juan de Fuca (NJDF)	N/A	119°-131°W	45°-52°N	NJDF
Southern Juan de Fuca (SJDF)	N/A	119°-130°W	40°-45°N	SJDF
Northern San Andreas (NSA)	N/A	115°-124°W	35°-40°N	NSA
Southern San Andreas (SSA)	N/A	113°-122°W	30°-35°N	SSA
Yellowstone (YS)	1	110°-111.2°W	44.18°-45.03°N	WHR
Wasatch (WAS)	2	111°-112.5°W	38°-42°N	WHR
Eastern Snake River Plain (ESRP)	3	110°-112°W	42°-46°N	WHR
Northwest Snake River Plain (NWSRP)	4	112°-119°W	43°-46°N	WHR
Explorer Plate (EXP)	5	126°-131°W	48.5°-52°N	NJDF
Seattle (SEA)	6	122°-125°W	47°-49°N	NJDF
Cascades (CAS)	7	119°-122°W	40°-50°N	NJDF, SJDF
Gorda Ridge (GR)	8	126°-128°W	40.5°-43.10°N	SJDF
Blanco Fracture Zone (BFZ)	9	126°-130°W	43°-44.5°N	SJDF
Mendocino Fracture Zone (MFZ)	10	123.5°-128°W	40°-40.7°N	SJDF
Walker Lane Belt (WLB)	11	116°-122°W	35.5°-42°N	SJDF, NSA
Entire San Andreas (ESA)	12	112°-124°W	30°-40°N	NSA, SSA
San Andreas North (SAN)	13	120°-124°W	37.5°-40°N	NSA
San Andreas Central (SAC)	14`	119°-123°W	35.5°-37.5°N	NSA
San Andreas Bend (SAB)	15	114°-122°W	33.5°-35.5°N	NSA, SSA
San Andreas South (SAS)	16	112°-121°W	30°-33.5°N	SSA

Table 1: List of sub-regions, their corresponding number from Figure 19, Longitude and Latitude ranges, and their respective sub-region.

Sub-catalogs were created for each of these sub-regions by including all earthquakes in the catalog that fall within the respective bounding polygons that define the individual sub-regions. Similar to the a priori treatment of the full dataset, the Pre-Cat and Post-Cat earthquakes were plotted, hit percentages were calculated, and the results analyzed.

A list of all the sub-regions, their corresponding identification number in figure 19, their latitude and longitude grids, and the major tectonic sub-region(s) they belong in is given in Table 3:

Time Cutoffs

To investigate the effect the length and timing of the Pre-Cat has on the results of the study, the earthquake catalog was divided into two sub-catalogs (Figure 20), which were evaluated based on Pre-Cat-Post-Cat date cutoffs. The first set of analyses for the entire WUS, and all of the sub-regions, was run using a date cutoff of 2007-2008. All Pre-Cat earthquakes in this first set of analyses included earthquakes from 1769

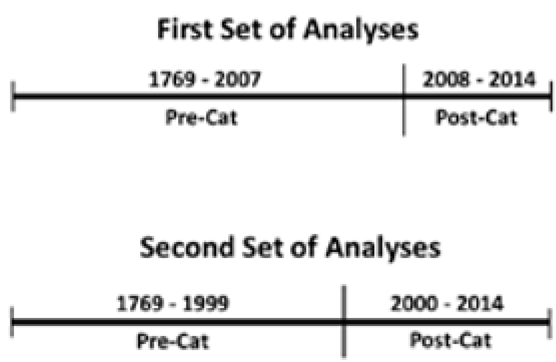

Figure 10: Visual representation of the date cutoffs between the Pre-Cat and Post-Cat for both sets of analyses.

through 2007, and earthquakes between the years 2008-2014 were included in the Post-Cat catalog. The second set of analyses lengthened the Post-Cat catalog time period, extending it back to the year 2000, with a resulting Post-Cat covering the years 2000-2014. This basically doubled the amount of time in the Post-Cat catalog, and gave a second set of results to compare to the first in an effort to try to discern systematic differences in CS predictability patterns between the two Post-Cats.

By doubling the Post-Cat date range, one might expect about twice as many Post-Cat earthquakes if the level of activity in the WUS was close to being constant. This turned out to be the case for most of the study area, but not for all of it. Doubling the Post-Cat date range also allows for possible additions to the higher end of the magnitude range for the Post-Cat data set. Larger magnitude earthquakes do not occur as often as smaller ones, and therefore have longer recurrence intervals. Doubling the length of the Post-Cat date range increases the probability of large earthquakes occurring during the time period of the Post-Cat, and therefore might lead to more high magnitude earthquakes in the catalog for some sub-regions.

The initial range of years was chosen somewhat arbitrarily in terms of seismicity and tectonics, but was more purposefully chosen for statistical reasons. The goal was to find a range of years long enough that the Post-Cat catalogs for the sub-regions analyzed yielded (as best as possible) enough earthquakes to draw statistically meaningful conclusions from the results. If there are not enough earthquakes in the catalog, then the results of the analysis may not be statistically reliable indicators of the true level of CS predictability for a given area. To investigate that issue, statistical significance tests were performed after all of the hit percentage results were found, to find out if the difference between hit percentages of any combination of two sub-regions was significantly lower, higher, or different than the rest. The date cutoff of 2007-2008 was chosen with the goal of making sure there were at least 15 Post-Cat earthquakes in the sub-catalogs for every sub-region. This date cutoff provided at least 16 Post-Cat earthquakes for any of the regions or sub-regions. The second date range was chosen to double the time period for the Post-Cat sets.

Magnitude Cutoffs

The completeness of the earthquake catalog, or lack thereof, plays a role in determining the low-end magnitude cutoff for the study (Cinella and Kafka, 2012: Cinella, J.R., Boston College Master's Thesis). Low magnitude earthquakes, below M3 for instance, are sometimes too small to be detected and located by the configuration of a seismic network at a given time. Having an accurate accounting of earthquakes in the catalogs is crucial for determining recurrence intervals for specific magnitude events in the study area. The catalog used in this study contains a total of 17,802 earthquakes, and thousands of earthquakes per region. Each sub-region analyzed also must contain enough Post-Cat earthquakes to perform statistically meaningful analyses for different magnitude ranges, and are therefore also analyzed for completeness. If an analysis for a specific sub-region did not yield enough Post-cat earthquakes to provide meaningful results at the M3.5+ level for the 2007-2008 date cutoff, those sub-regions ended up not being analyzed here. In other words, if a specific sub-region had less than 15 Post-Cat earthquakes for the 2007-2008 date cutoff, they were not analyzed further.

Earthquakes of magnitude lower than 3.5 were completely eliminated from this study. This was done: (1) because the catalog contained enough higher magnitude earthquakes to be able to conduct a study in a statistically meaningful way; and (2) to eliminate a low magnitude tail-off of the recurrence rate created by lower magnitude events not being recorded by seismometers or reported in the case of historical earthquakes. Even when allowing for an M3.5 magnitude cutoff, the lower magnitude events don't exactly follow the Gutenberg-Richter relationship relating magnitude to number of earthquakes of that magnitude (Sornette and Sornette, 1999), which will be discussed more in the next section. If earthquakes lower than M3.5 were included in the catalog, the linearity of the recurrence plots would have been diminished and we could not be confident that we were seeing a true representation of the rate of seismicity for those lower magnitude events.

A high-end magnitude cutoff was not used, as we were trying to determine the extent to which the highest possible magnitude events are forecasted successfully in the WUS. These are, of course, the earthquakes of most concern for hazard assessment (see fundamental question #2). Instead, magnitude ranges were chosen on the basis of moving the low-end of the cutoff up in magnitude in intervals 0.25 until there were no Post-Cat earthquakes left for that specific sub-region. For instance, the Post-Cat catalog for the 2007-2008 date cutoff did not include a single earthquake above M7.25. Therefore analyses would start for all Post-Cat earthquakes M3.5 and above, the next analysis would only contain Post-Cat earthquakes of M3.75 and above, the third would only contain Post-Cat earthquakes of M4 and above, and so on, until you reached the analysis for M7.25 and above, at which point you would produce a result containing no Post-Cat earthquakes. Statistically meaningful Post-Cat results should contain at least 10-15 earthquakes, and/or follow the best-fit recurrence line which will be discussed further in the next section. By varying the minimum magnitude I was then able to assess whether or not CS results differed based on threshold magnitudes (e.g., Cinella and Kafka, 2012).

The Pre-Cat catalog for each analysis was not changed with a low-end magnitude cutoff like the Post-Cat was, it was kept at M3.5+ throughout the analyses. Changing the Pre-Cat magnitude cutoff for each analysis would have possibly produced results that would have been difficult to interpret as the radius for the Pre-Cat earthquakes would have changed with each individual analysis. On the other hand, the Pre-Cat catalog, and thus the Pre-Cat radius, was changed for each individual sub-region. It is fundamental to the concept of CS that the Pre-Cat radius is based on the size of the area being analyzed, and as the area changes, so must the Pre-Cat radius so that all regions are analyzed for the same percentage of map area, 33% in this study (e.g. Kafka, 2002, 2007). Because of this, even though the northern San Andreas sub-region may have a Pre-Cat radius of 14 km, some of the smaller sub-regions, like the SAN, which is a sub-region located within the NSA sub-region, may have a smaller Pre-Cat radius because of the smaller total area covered by the map. Despite the Pre-Cat earthquakes covering 33% of the map in every sub-region, since the map is of a different size in each case, so too is the Pre-Cat radius. This may lead to significant differences in the level of CS predictability between an overall region and it's subsequent sub-regions.

Some sub-regions, or larger regions, did not have Post-Cat earthquakes reaching M7, or even M6, and therefore the analyses stopped at an upper magnitude level whenever there were no Post-Cat earthquakes left, and the highest magnitude earthquake for that sub-region had been analyzed. For some sub-regions the high-end cutoff was less than M5. Given that one of the major motivations for this study is to identify regions where large, damaging earthquakes could potentially occur in the future, what is the significance for this study in sub-regions where no large earthquakes have occurred recently? While these sub-regions may not directly provide meaningful results for addressing this question (i.e. fundamental question #2), they can however provide additional insight. For example, if the Pre-cat catalog has higher magnitude earthquakes (M5+) for those sub-regions, why doesn't the Post-Cat? Is this due to a lull in high magnitude activity? Is the recurrence interval too long for the Post-Cat to have yet realized the occurrence of the maximum possible magnitude earthquake? Or is it due to random variation in seismicity? All of these effects are possible, and they are fundamental limitations for all seismicity-based earthquake analysis and forecasting studies. This is a consequence of attempting to understand the earthquake process, which occurs over thousands to millions of years, within the confines of the limited range of dates from which we have reliable earthquake catalogs.

Recurrence Intervals

Gutenberg-Richter plots, referred to here as recurrence interval graphs were made, and intervals calculated, for each of the sub-regions and for the WUS as a whole. The Gutenberg-Richter relationship expresses the relationship between magnitude M, and number of earthquakes of magnitude M or greater. This relationship is expressed by the equation:

$$\mathrm{Log}_{10} N = a - bM$$

where N is the number of events of magnitude M or larger, and a and b are constants based on the study area (e.g., Sornette and Sornette, 1999). Data modeled by this equation usually shows a linear, or nearly linear trend. In an idealized Gutenberg-Richter relationship that line would have a slope of -1. If the slope was -1, then there is a ten-fold decrease in the number of events N, of magnitude M, as M increases by 1 (i.e. there are ten times fewer earthquakes of magnitude 6 as there are magnitude 5). In reality the slope of the line has typically been observed to range from about -0.5 to -1.5.

Recurrence interval plots were made using all of the earthquakes in the catalog (Pre-Cat and Post-Cat), for the WUS and each of its respective sub-regions. Because the catalog goes back to 1769, covering over 250 years, recurrence intervals could be found for most magnitudes in each region. Recurrence intervals for some of the higher

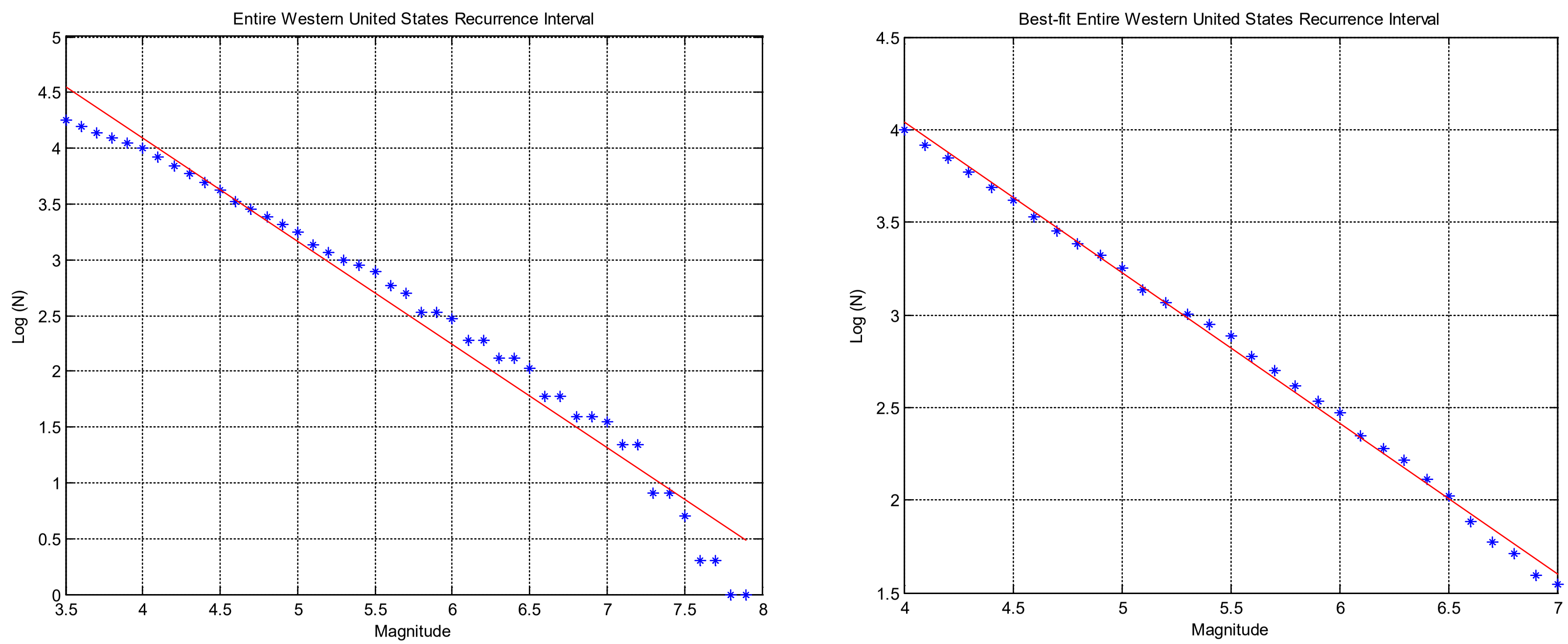

Figure 21: Recurrence plots for the western United States. Left; entire catalog, right; best-fit magnitude range plot.

magnitude earthquakes were not able to be accurately determined due to the paucity of those large magnitude seismic events.

Taking the entire catalog into account there still ended up being some deviation from a perfect linear relationship at either end of the magnitude range for the WUS (Figure 21a). In an effort to adjust for this effect, along with recurrence intervals for the entire catalog, M3.5 and above, a second recurrence plot was made for each sub-region to find the best range of magnitudes within which the data followed close to a linear trend (Figure 21b).

Statistical Significance Testing

In order to ascertain whether or not the differences in levels of CS predictability for two sub-regions are significantly different, or if the level of CS predictability are significantly lower or higher, statistical significance tests were performed. Two-tailed testing was done to find out if the CS results for two sub-regions were statistically significantly different, meaning, could the observed difference in the level of CS predictability of one sub-region vs. another sub-region be explained by some effect other than random variation.

One hypothesis of this study, stated previously, is that the level of CS predictability would be lower for the WHR region than for either the SAF or the Cascadia regions because the WHR is not near a plate boundary. If the CS results do show that the WHR predictability is lower, as expected, testing for statistical significance between the WHR and the other regions is the next step in determining whether or not the results for the WHR are meaningful. Determining whether or not the significance test shows that the level of CS predictability for the WHR is significantly lower than that of the other regions will allow me to glean more insight regarding CS predictability differences amongst plate boundary versus intraplate regions.

Testing for the levels of CS predictability between the Cascadia region and the SAF, and then finding out whether or not those results are statistically significantly different is also a major part of this study, as these results will give us insights into fundamental question #3: How does the type of plate boundary affect the success rate of the forecast?

Analyses were performed between all twenty-one of the sub-regions, using both 2007-2008 and 1999-2000 date cutoffs.

The first step was to calculate the z-score for each of the combinations of sub-regions. These calculations were run using Matlab. The equation used to find these z-scores is

$$Z = \frac{rX - rY}{\sqrt{r(1-r)\left(\frac{1}{X} + \frac{1}{Y}\right)}}$$

Where X and Y are the number of earthquakes in sub-region X and sub-region Y, rX and rY are the hit percentages for sub-region X and sub-region Y, and r is the combined hit percentage for both sub-region X and sub-region Y.

Z-scores were found for both the 2007-2008 and the 1999-2000 values of number of earthquakes and their respective hit percentages. After all of the z-scores were calculated, a z-score to p-value chart was used to find the p-values for each of the sub-region combinations. A summary of these results are presented in Table 4 (2007-2008 p-values) and in Table 5 (1999-2000 p-values).

RESULTS

CS Analysis of the Entire Western United States

For the most part, CS hit percentages are quite high in the WUS. We can see that the Cascadia region and the SAF have percentages of successful forecasts (levels of CS predictability) of more than 90% (Table 2, Table 3). The WHR shows a lower level of CS predictability, but is still quite high at more than 70% (Table 2, Table 3).

The differences in results between the Cascadia and SAF regions were very subtle. As will be seen below, the region with the higher hit percentage for a certain date cutoff as well as different magnitude ranges changes depending on the date cutoffs for the Pre-Cat and Post-Cat. The Cascadia region has a higher overall hit percentage for the 2007-2008 date cutoff while the SAF is higher for the 1999-2000 date cutoff. The WHR is lower than the Cascadia region and SAF for both date cutoffs, but as will be seen below, the hit percentage changes quite a lot when one of the sub-regions within the WHR region is taken out of the picture.

Sub-Region	2007-2008 Hit Percentage M3.5+	2007-2008 Hit Percentage M5+
Whole Area	96.6	97.1
NJDF	98.0	94.7
SJDF	94.8	96.6
WHR	83.4	50.0
NSA	90.2	85.7
SSA	97.3	96.8
EXP	92.1	97.1
MFZ	83.7	100.0
BFZ	91.6	90.2
GR	67.9	100.0
CAS	92.6	-----
SEA	76.9	-----
YS	70.8	-----
ESRP	80.8	-----
NWSRP	100.0	-----
WAS	6.3	-----
ESA	85.2	93.6
SAN*	83.1	0.0
SAC*	88.9	0.0
SAB	84.8	100.0
SAS	95.6	100.0
WLB	79.2	83.3

Table 2: List of hit percentages, M3.5+ and M5+, for the whole study area and each of the sub-regions for the 2007-2008 date cutoff. NJDF is the northern Juan de Fuca sub-region, SJDF is the southern Juan de Fuca sub-region, WHR is the WHR, NSA is the northern San Andreas, SSA is the southern San Andreas, EXP is the Explorer Plate, MFZ is the Mendocino Fracture zone, BFZ is the Blanco Fracture zone, GR is Gorda Ridge, CAS is Cascadia, SEA is Seattle, YS is Yellowstone, ESRP is the eastern Snake River Plain, NWSRP is the northwest Snake river Plain, WAS is the Wasatch Fault zone, ESA is the entire San Andreas sub-region, SAN, SAC, SAB, and SAS are the northern, central, bend and south sub-regions of the San Andreas respectively, and WLB is the Walker Lane Belt. Hit Percentages given to the nearest integer.

Sub-Region	1999-2000 Hit Percentage M3.5+	1999-2000 Hit Percentage M5+
Whole Area	94	94
NJDF	94	99
SJDF	90	91
WHR	79	62
NSA	87	95
SSA	92	98
EXP	93	94
MFZ	78	79
BFZ	91	95
GR	54	82
CAS*	77	0
SEA	90	100
YS	68	-----
ESRP	82	50
NWSRP	78	50
WAS	21	-----
ESA	84	96
SAN	82	50
SAC	61	67
SAB	84	100
SAS	93	100
WLB	79	80

Table 3: List of hit percentages, M3.5+ and M5+, for the whole study area and each of the sub-regions for the 19992000 date cutoff. Hit percentages given to the nearest integer.

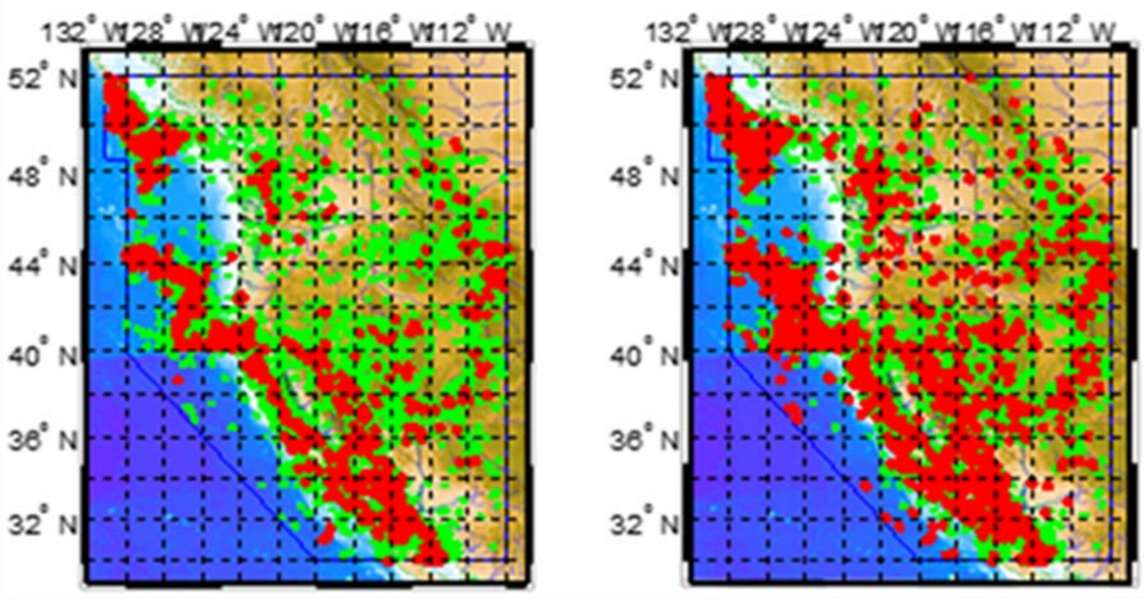

Figure 22: CS analysis of the entire WUS for M3.5+ seismic events. Left: 2007-2008 date cutoff, Right: 1999-2000 date cutoff. Green dots are Pre-Cat events covering approximately 33% of the map area outlined by the blue polygon. Red dots are Post-Cat events.

2007-2008 Date Cutoff

The analysis for the entire WUS using the 2007-2008 date cutoff was the first set of analyses run for this study. The Pre-Cat radius used in this set of analyses to cover 33% of the map area was 14.8 km (Figure 22a). The results showed that the WUS, in general, shows a very high hit percentage between past and recent seismicity. For M3.5

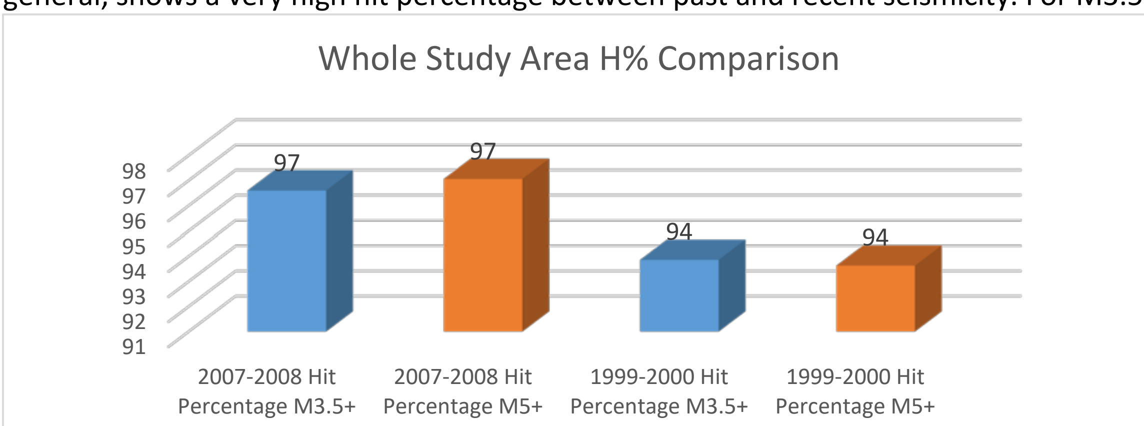

Figure 23: Hit percentage comparison for the entire WUS. M3.5+ percentages shown in blue. M5+ percentages shown in orange. Numbers above the bars are percentage of hits rounded to the nearest integer.

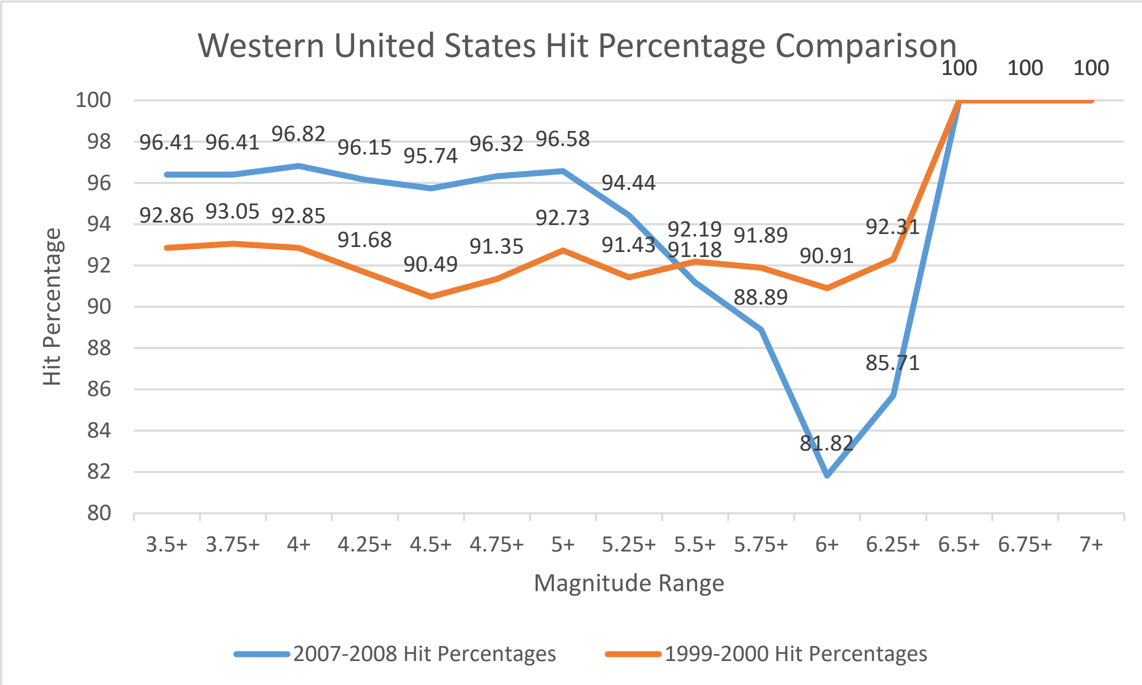

Figure 24: Progression of the entire WUS hit percentages with different magnitude cutoffs for both the 2007-2008 and 1999-2000 date cutoffs.

and above, 2,357 out of a possible 2,440 Post-Cat earthquakes fell within the designated Pre-Cat radius, a hit percentage of 96.6%.

For earthquakes of M5 and above the hit rate was slightly higher than the M3.5 and above trial. For M5 and above events the hit percentage was 97.1% (Figure 23), with 132 out of 136 possible earthquakes being hits. Numbers above the bars in Figure 23 are hit percentages rounded to the nearest integer, which is a reasonable level of resolution for comparison. As mentioned above, the Pre-Cat radius of 14.8 km did not change with magnitude (Figure 22a).

For earthquakes of magnitudes higher than the M5+ level, there was a slight drop-off in hit percentage. The percentage dipped to 86.7% for M6 and above (Figure 24). This percentage is still quite high and 13 out of 15 events of M6 and above were successfully forecasted using the CS method. The hit percentage increased slightly for earthquakes above M6.25+ and reached 100% for M6.5+ earthquakes, where 5 out of 5 events were successfully forecasted.

The recurrence interval plot for events M3.5+ shows a low-end deviation from a linear decrease starting at around M4.4 and continuing down to M3.5 (Figure 21a). Similar to the low-end deviation, a high-end magnitude deviation begins at around M7. It could be argued that it deviates at a lower magnitude than M7, but the number of earthquakes of magnitude M appears to have a clear dip below the best-fit line, starting at M7.3 (Figure 21a). To be more confident that I was using a magnitude range where the catalog is complete and the fit is linear, I chose M7 as the high-end cutoff, and M4 as the low-end cutoff, and proceeded to make a second recurrence plot for the WUS catalog for only this magnitude range (Figure 21b).

1999-2000 Date Cutoff

The 1999-2000 date cutoff for the entire WUS produced similar results to those of the 2007-2008 cutoff. For M3.5+ events. As expected, since there were roughly twice as many years in the Post-Cat catalog, there were roughly twice as many earthquakes in that catalog. The locations of 4,202 out of a possible 4,477 Post-Cat earthquakes were successfully forecasted. This gives us a hit percentage of 93.9%, slightly lower than that for the 2007-2008 cutoff. The Pre-Cat radius for this set of trials was 16.2 km (Figure 21b).

For M5+ earthquakes, locations of 235 out of 251 earthquakes were successfully forecasted, making for a hit percentage of 93.6%. Again, this is slightly lower than that of the 2007-2008 date cutoff.

Moving even higher in magnitude the same decrease in hit rate that we saw with the 2007-2008 cutoff might have been expected. There was a slight decrease (about 1%) compared to the 10% drop in the 2007-2008 cutoff. At M6+ there was a 92.3% hit rate, and at M6.5+ there is a jump to 100% successful forecasting (Figure 24). There were 10 earthquakes left in the Post-Cat at M6.5+.

The recurrence intervals are the same for this case as for the 2007-2008 cutoff since they use the same earthquake catalog covering the entire WUS, and for the entire time span of the study. In terms of actual yearly intervals for different magnitude events:

$$R_4 = 0.0255 \text{ years (9 days)}$$

$$R_5 = 0.1434 \text{ years (52 days)}$$

$$R_6 = 0.8064 \text{ years (294 days)}$$

$$R_7 = 7.19 \text{ years}$$

Where R_4 stands for the recurrence interval of M4+ events, etc. The recurrence intervals do not follow the ideal Gutenberg-Richter slope of -1.0, but the observed Gutenberg-Richter slope for this case, -0.85, which was determined by the recurrence intervals following a pattern where M(x+1) earthquakes were seen to be around seven times less likely to occur than M(x) earthquakes in the catalog, which is well within the global range of -0.5 to -1.5. Between magnitude 3.5 and magnitude 6, the earthquakes in the catalog appear to follow a pattern where a M(x) earthquake occurs approximately six times as often as a M(x+1) earthquake. The recurrence interval jumps from six times as often to nine times as often between R_6 and R_7, (i.e. M(x+1) is 9 times less likely to occur than M(x)). Based on this we can find the Gutenberg-Richter slope using the formula

$$N5 = 10^{\log(N6 + b)} = 6*N6$$

Where N5 and N6 are the number of magnitude 5 and magnitude 6 earthquakes in the catalog, and b is the slope we are looking for. Going forward

$$6*N6 = 10^{\log(N6)}*10^b = N6*10^b$$

$$b = \log(6) = 0.78$$

and for

$$9*N6 = N6*10^b$$

$$b = 0.95$$

meaning that instead of having a slope of -1, the Gutenberg-Richter slope is approximately -0.78 for the first case, and -0.95 for the second case. Since no M8 earthquakes occurred during my 255 year catalog, we can't find a precise recurrence interval for M8+ events, but based on the recurrence intervals between M6+ and M7+ events, an extrapolated estimate of R_8 is

$$R_8 \approx 65 \text{ years}$$

If 65 years is the recurrence interval for M8+ events, then there should have been at least three in the past 255 years in the WUS. This interval for M8+ events would also imply a recurrence interval for M9+ events of around 585 years, 70 years less than that of Goldfinger et al. (2003) who found a "1-to-1 correspondence between turbidites occurring every 655 years to M9 subduction zone earthquakes" in the Cascadia subduction zone. This 585 year interval also agrees well with the recurrence interval given by Priest et al. (2014) of 530+ years for a FMR (Figure 10).

CS Analysis of the Cascadia Subduction Region

Analysis of the Northern Cascadia Sub-region

2007-2008 Date Cutoff

The CS analysis of the northern Cascadia sub-region produced high rates of successful forecasts. Locations of 295 out of 305 earthquakes of M3.5+ were successfully forecast, yielding a hit percentage of 96.7%. The Pre-Cat radius was 18.2 km (Figure 25a).

For M5+ events the northern Cascadia sub-region produced a very high hit rate as well, having 37 out of 38 events successfully forecasted, i.e. a lower hit percentage of only 94.7%. Considering only 1 of 38 didn't fall within the Pre-Cat radius though, these

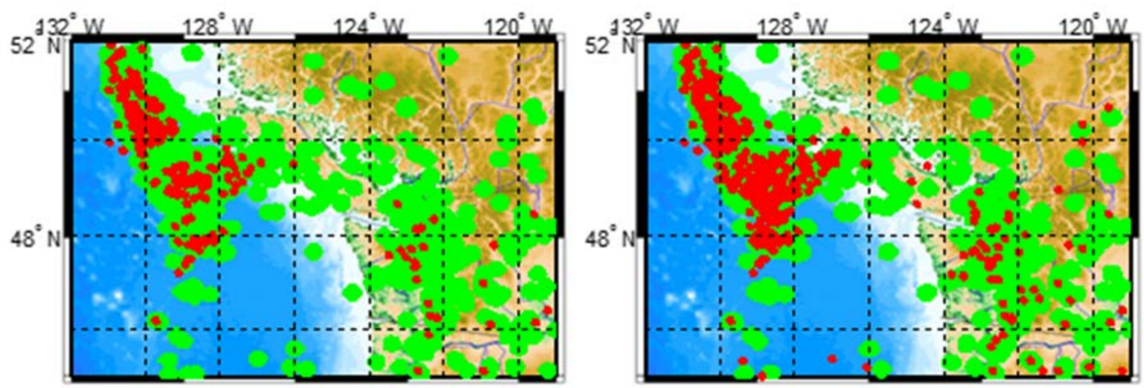

Figure 25: CS analysis of the Northern Cascadia (NJDF) sub-region for M3.5+ seismic events. Left; 2007-2008 date cutoff, Right; 1999-2000 date cutoff.

numbers are still quite high. Starting at M5.25+ all earthquakes are successfully forecasted, 17 of 17 events. 7 of 7 M6+ events in this sub-region were forecasted successfully.

1999-2000 Date Cutoff

The CS analysis of the northern Cascadia sub-region for the 1999-2000 date cutoff produced successful forecasts the locations of 671 out of 711 possible events of M3.5+. The hit percentage is 94.4%. The Pre-Cat radius used in this case to cover 33% of the map area is 19.5 km (Figure 25b).

Locations of 78 of 79 M5+ events were successfully forecasted giving a 98.7% hit percentage, one of the highest of any sub-region in this study. As with the 2007-2008

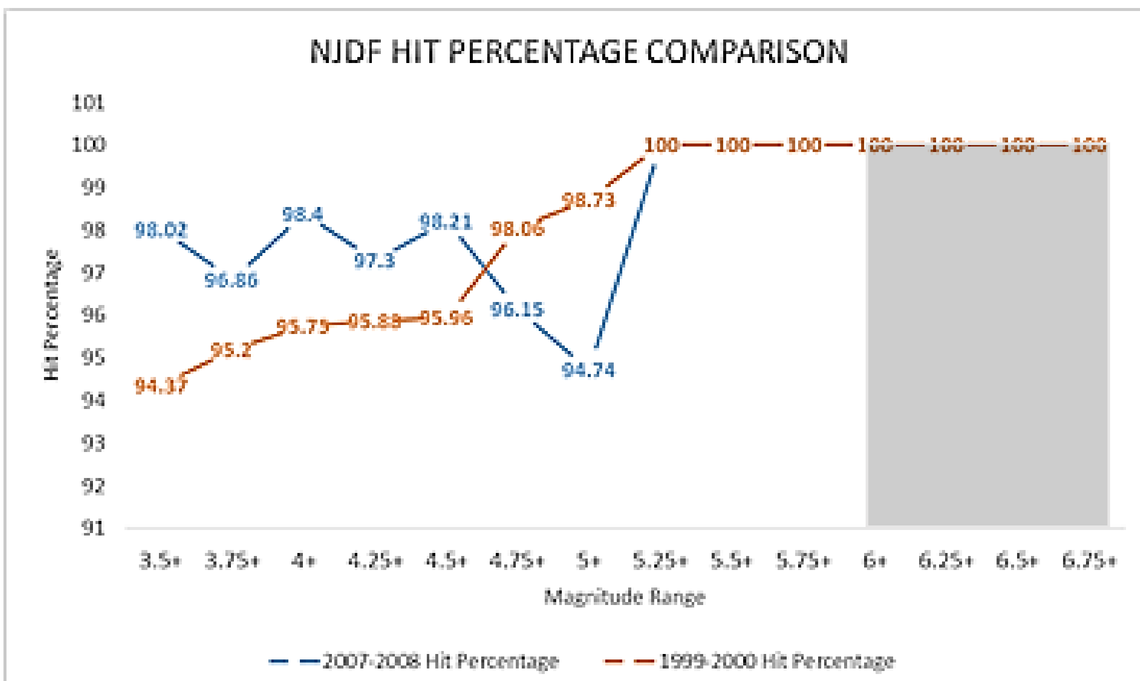

Figure 26: Progression of entire NJDF hit percentages with different magnitude cutoffs. Shading indicates magnitudes for which there are less than 15 Post-Cat earthquakes.

analyses, all earthquakes of M5.25+ were successfully forecasted, 37 in all. Locations of 11 out of 11 M6+ events were forecasted (Figure 26).

For northern Cascadia the recurrence interval plots start to deviate from a line starting at M4 on the low-end, and at M6.8 on the high end when using the entire northern JDF earthquake catalog (Figure 27a), therefore this range was chosen for my best-fit recurrence graphs (Figure 27b). The resulting recurrence intervals for the northern Cascadia sub-region are as follows:

R_4 = 0.2550 years (93 days)

R_5 = 1.61 years

R_6 = 11.9 years

R_7 = 128 years

Again, there are no M8+ events so finding that recurrence interval is not possible. There are also only 2 events of M7+ in this sub-region, therefore the 128 year recurrence interval for M7+ events here may not be entirely representative of the long-term trend.

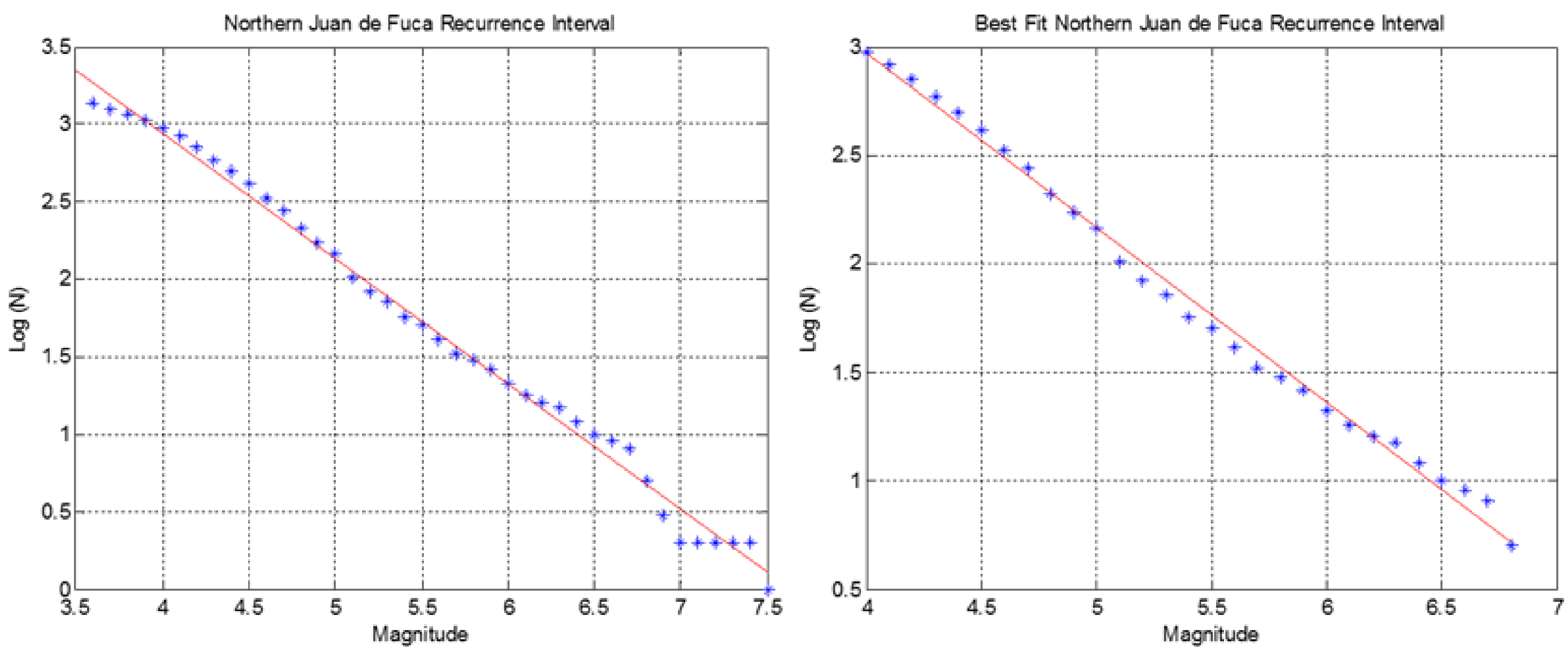

Figure 27: Recurrence plots for the Northern Cascadia (NJDF) sub-region. Left; entire catalog, right; best-fit magnitude range plot.

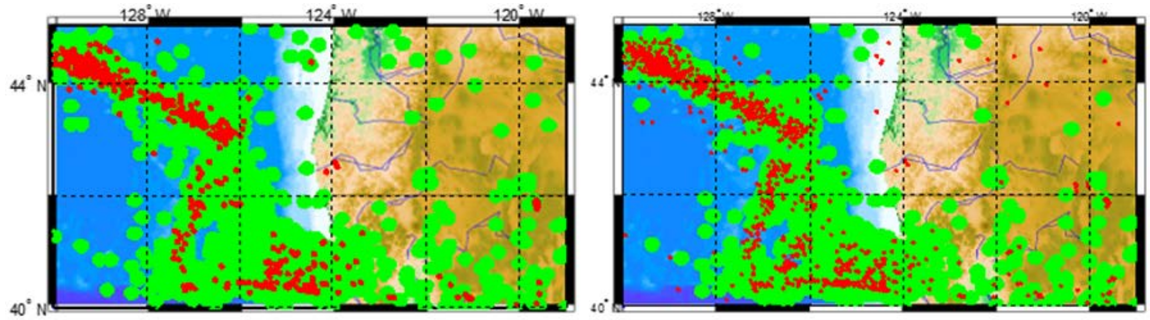

Figure 28: CS analysis of the Southern Cascadia (SJDF) sub-region for M3.5+ seismic events. Left; 2007-2008 date cutoff, Right; 1999-2000 date cutoff.

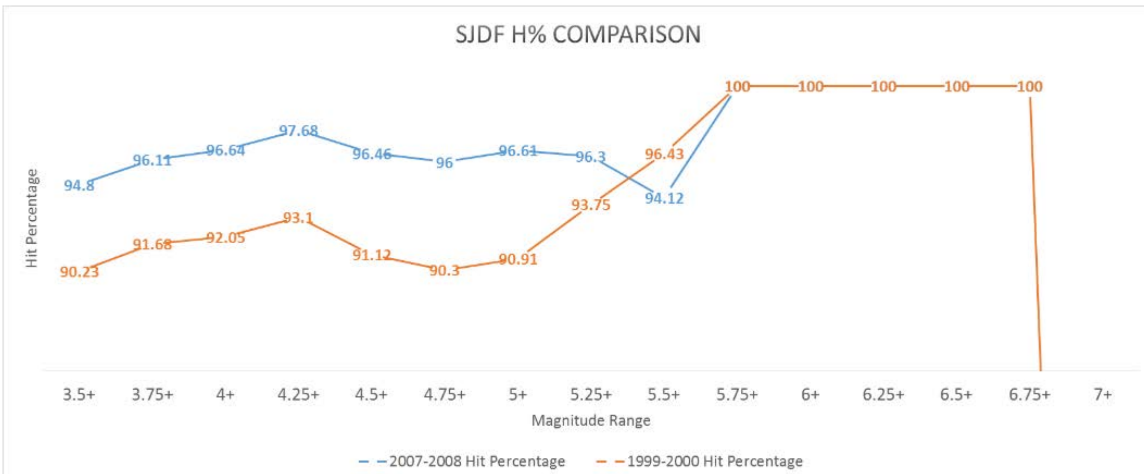

Figure 29: Progression of entire SJDF hit percentages with different magnitude cutoffs.

Analysis of the Southern Cascadia Sub-region

2007-2008 Date Cutoff

The CS analysis of the southern Cascadia sub-region produced high hit percentages, although not quite as high as the northern Cascadia sub-region. Locations of 509 out of 537 events of M3.5+ were forecasted successfully, giving us a 94.8% hit percentage (Figure 28a), about 3% lower than its northern counterpart.

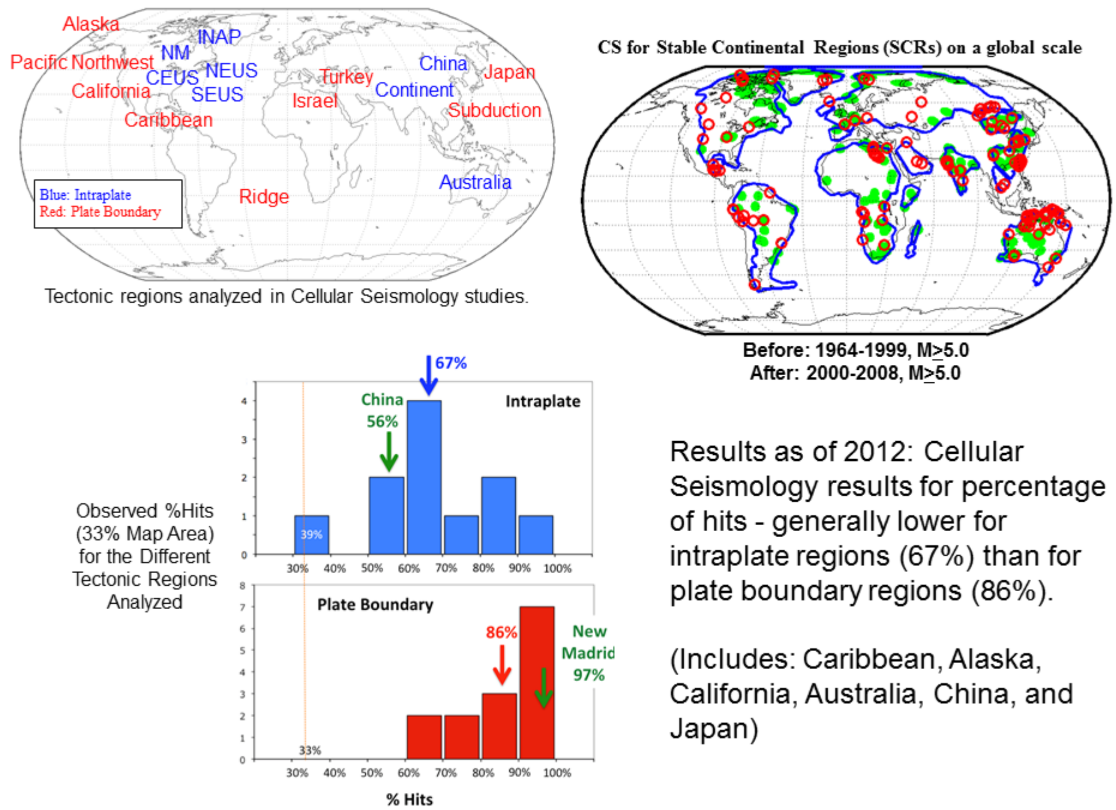

Figure 30: Comparison of intraplate versus plate boundary regions worldwide, courtesy of Dr. Alan Kafka. Regions studied given in blue/red in the top-left world map. CS result map given in top-right. Histograms of intraplate and plate boundary regions at the bottom. Average level of CS predictability for intraplate regions wordwide was found to be 67% while the average level of CS prediftability for plate boundary regions was found to be 86%.

57 out of 59 M5+ events were successfully forecasted, a hit percentage of 96.6%. This is a higher success rate than its northern counterpart. There is a 100% hit rate starting at M5.75+, and 4 out of 4 M6+ events were forecasted for that case.

1999-2000 Date Cutoff

The 1999-2000 date cutoff for the southern Cascadia sub-region produced lower hit percentages across the board than the 2007-2008 cutoff. Locations of 960 out of 1,064 earthquakes of M3.5+ were successfully forecasted, a hit percentage of only 90.2% (Figure 28b). While this is still a very high percentage in terms of typical CS predictability found by Kafka et al. (2014), and shown i Figure 30 below and Figure 74 in Discussion section, it is lower than the northern half of Cascadia.

M5+ events had a similar outcome as that of the catalog as a whole. Locations of 90 out of 99 events were forecasted successfully, a hit percentage of 90.9%. Percentages of around 90-92% were common until reaching magnitude M5.25+. Locations of 93.8% of events were successfully forecasted for M5.25, 96.0% for M5.5+, and 13 out of 13 events of M5.75+ were forecasted. Locations of eight out of eight M6+ events were successfully forecasted (Figure 29).

The southern Cascadia recurrence interval plot deviates from a line on the low-end at around M4, and at the high-end at M6.6 (Figure 31a). The best-fit recurrence line (Figure 31b) is therefore plotted using these values. The recurrence intervals for the southern Cascadia sub-region are:

$$R_4 = 0.1278 \text{ years (47 days)}$$

$$R_5 = 0.6405 \text{ years (234 days)}$$

$$R_6 = 4.04 \text{ years}$$

$$R_7 = 28.6 \text{ years}$$

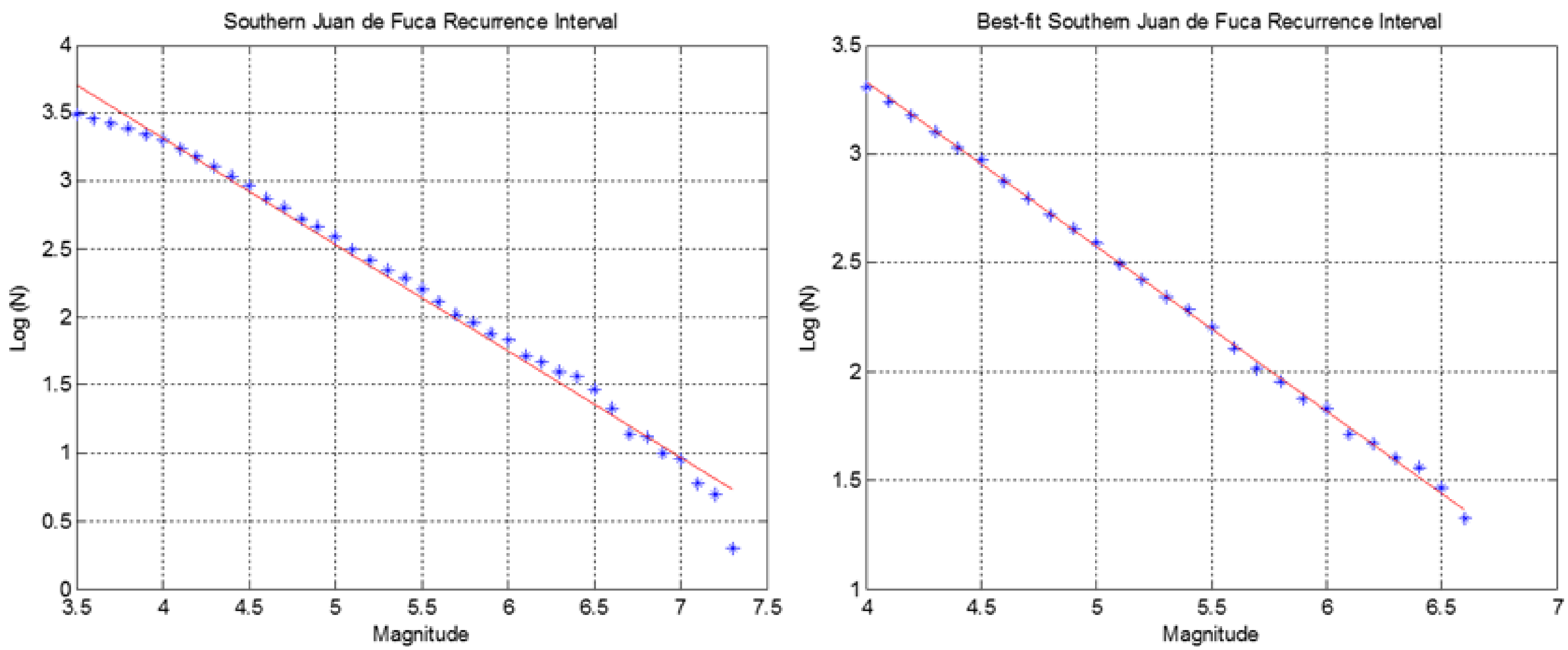

Figure 31: Recurrence plots for the Southern Cascadia (SJDF) sub-region. Left; entire catalog, right; best-fit magnitude range plot.

There are nine M7+ events in the southern Cascadia sub-region during the 255 year span of my catalog. The recurrence intervals are characterized by a Gutenberg-Richter slope of -0.85 to -0.90. Based on the interval for M7+ events, the extrapolated recurrence interval for M8+ events should be:

$$R_8 \approx 230 \text{ years}$$

This estimate is in very good agreement with the findings of Priest et al. (2014) who found a recurrence interval for the southern end of the Cascadia margin of 220-240 years. If these estimates are accurate, an M8+ earthquake might have occurred during this 255 year catalog, but given the uncertainties it is not necessarily surprising that we have not yet seen that earthquake occur.

Analysis of the Smaller Cascadian Sub-regions

Explorer Plate

The Explorer Plate sub-region is one that I would expect to show a very high level of CS predictability because of its number of plate boundaries and currently active fault zones in close proximity to one another, including a mid-ocean ridge segment, subduction zone, the Nootka fault and the Sovanco fracture zone which together provide a highly active zone of seismicity (Figure 32, The Cascade Episode). This, however, was not found to be the case. While the hit percentages are still high, they weren't any higher than other sub-regions of the Cascadia region.

Figure 32: The Explorer Plate, located at the northern end of the Cascadia region and its associated plate boundaries and fault segments. Triple junction near the bottom of the figure connects the Nootka fault, Sovanco fracture zone, and the Juan d Fuca ridge to the south. Courtesy of "The Cascade episode".

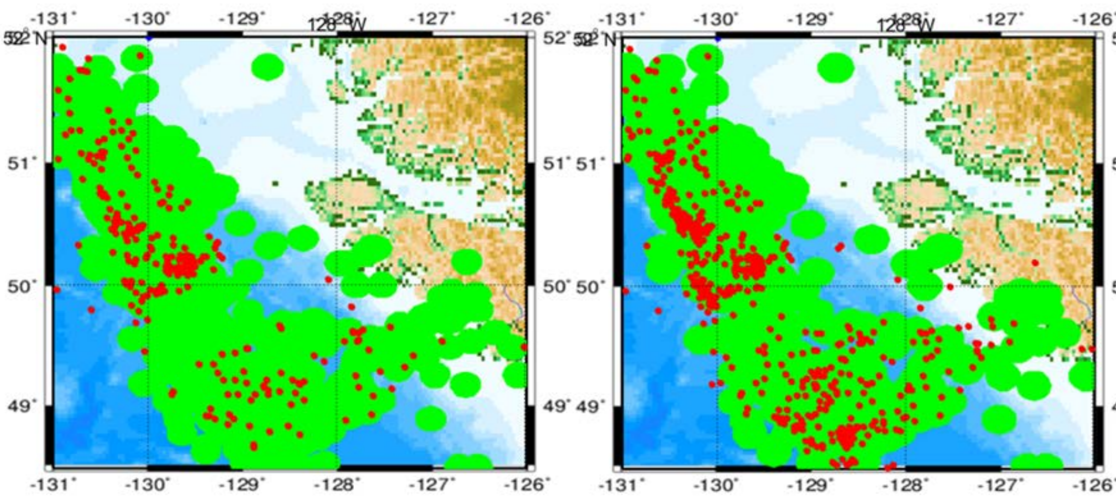

Figure 33: CS analysis of the Explorer Plate sub-region for M3.5+ seismic events. Left; 2007-2008 date cutoff, Right; 1999-2000 date cutoff.

2007-2008 Date Cutoff

Locations of 231 out of 251 earthquakes were successfully forecasted for the M3.5+ Post-Cat in the Explorer Plate sub-region. This is a hit percentage of 92.0%, lower than the northern Cascadia sub-region that the Explorer Plate sub-region belongs to. This is high, but again, a greater hit percentage was expected due to the number of plate boundaries and currently active faults in the sub-region. The Pre-Cat radius here is 11.8 km (Figure 33a).

For the M5+ Post-Cat, locations of 34 out of 35 earthquakes were successfully forecasted, a hit percentage of 97.1%. This is more along the lines of what was expected from this sub-region, given that its tectonic setting includes a number of well-defined plate boundaries and faults. Similar to previous sub-regions, all events of M5.25+ were successfully forecasted, including 7 out of 7 M6+ events.

1999-2000 Date Cutoff

The hit percentage for the entire catalog for the 1999-2000 date cutoff is higher than that of the 2007-2008 cutoff result. For the M3.5+ Post-Cat, locations of 510 out of 546 were forecasted. This is a hit percentage of 93.4%. The Pre-Cat radius was 13.4 km (Figure 33b).

The hit percentage for the M5+ cutoff was lower than the value from the 2007-2008 date cutoff. In this case, locations of 67 out of 71 events were successfully forecasted, yielding a hit percentage of 94.4%. In this analysis a 100% hit percentage was not observed until M6.5+. Nine out of ten M6+ events were successfully forecasted.

The recurrence plot deviates from a line at the low-end magnitude of M4, and the high-end magnitude of M6.5 (Figure 34a) The best-fit recurrence plot running from M4 to M6.5, providing a remarkable linear fit (Figure 34b). The recurrence intervals for the Explorer Plate sub-region are:

$$R_4 = 0.3602 \text{ years (131 days)}$$

$$R_5 = 1.81 \text{ years}$$

$$R_6 = 9.70 \text{ years}$$

There are no M7 events, but there was a single M7.2 event during the 255 year span. Because of the occurrence of only one M7+ earthquake, a recurrence interval could not be directly measured, but after extrapolating the best fit line, it is estimated to be:

$$R_7 \approx 50 \text{ years}$$

based on the recurrence interval values for the other magnitudes. If this estimate is correct, then more events of this size should have been expected in the 255 year catalog used in this study.

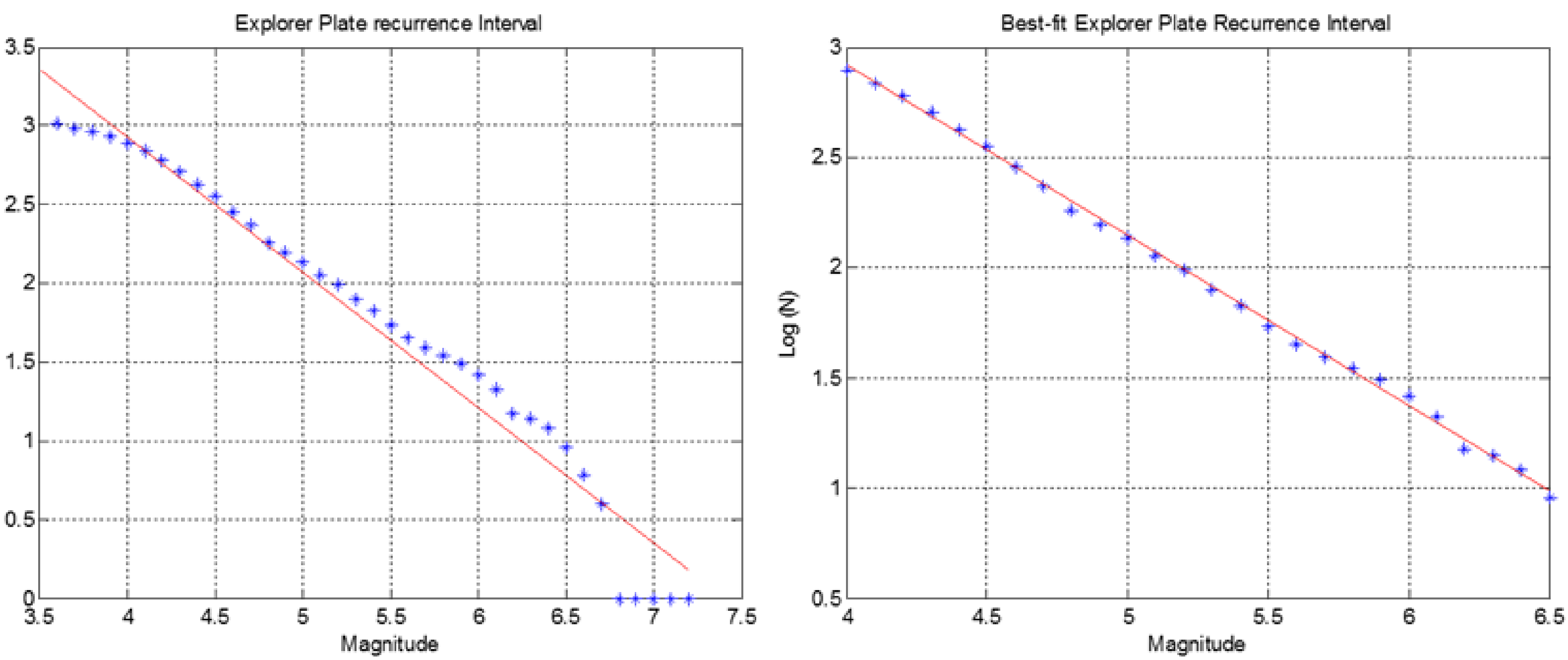

Figure 34: Recurrence plots for the Explorer Plate sub-region. Left; entire catalog, right; best-fit magnitude range plot.

Seattle Area

The Seattle sub-region is one of the smaller sub-regions in this study, and it has not experienced a lot of seismicity in recent years. Nonetheless, this is a very important sub-region to analyze because of the significance of the possibility of a major earthquake affecting a highly-populated, urbanized region (e.g. Seattle and Tacoma, WA) in this area.

2007-2008 Date Cutoff

The 2007-2008 date cutoff produced only 13 Post-Cat earthquakes for the Seattle sub-region. Of the 13 M3.5+ events, 10 were successfully forecasted, a hit percentage of 77.0%. This percentage is low compared to the other sub-regions in this study. There were no M5+ events for this date cutoff. The Pre-Cat radius here is 9.12 km (Figure 35a). Since this is a region of major seismic hazard concern, the observation that CS isn't a good indicator for this region is a cause for concern that there might be regions where future large earthquakes are lurking that aren't illuminated by past seismicity.

1999-2000 Date Cutoff

The 1999-2000 date cutoff also had a low number of earthquakes for this sub-region but it was high enough to make more significant conclusions about the Seattle sub-region. Out of the 30 Post-Cat earthquakes of M3.5+ for this set of analyses the locations of 27 were successfully forecasted. This is a 90.0% hit percentage. Again, even

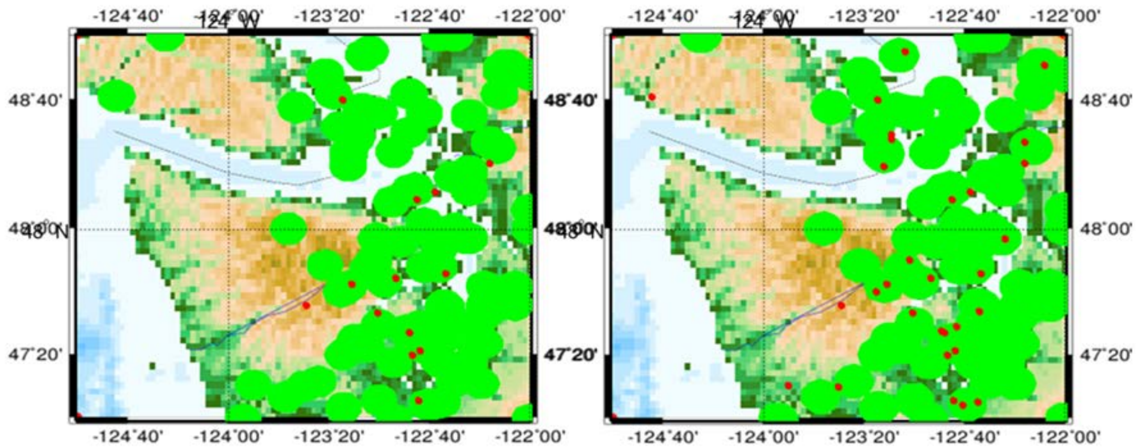

Figure 35: CS analysis of the Seattle sub-region for M3.5+ seismic events. Left; 2007-2008 date cutoff, Right; 1999-2000 date cutoff.

90.0% is low compared to the other regions analyzed so far. The Pre-Cat radius is 9.92 km for this case (Figure 35b).

In this region, a 100% hit percentage starts at M4+, where 9 out of 9 events were forecasted. There are only two M5+ events for this sub-region, both of which were forecast successfully. One of those two events was a M6.8 event from 2001. Considering that there isn't a lot of recent seismicity in the area, and the fact that the seismicity that was recorded is generally below M4.5, this M6.8 event seems quite anomalous.

The recurrence interval plot for the Seattle sub-region (Figure 36a) follows a linear trend quite well for the low-end magnitude range. There aren't a lot of high magnitude earthquakes, so the recurrence interval plot seems to make systematic jumps relative to the best-fit line for the entire catalog. A better fit to the data would have been possible if there were slightly more mid-magnitude earthquakes in the catalog (i.e. M5-M6). These mid-magnitude earthquakes do not appear to happen as often, or may not inherently follow a linear trend, as is needed to maintain a good linear pattern in the sub-region.

Because of the lack of mid-magnitude events, I did not feel that a best-fit magnitude range yields true insight into the Seattle region. More specifically, as the best-fit was limited to earthquakes between M3.5-M5.5 (Figure 36b) the magnitude range is small and thus there is a great deal of uncertainty regarding inferences of future seismicity in the Seattle sub-region. The estimated recurrence intervals are:

$$R_4 = 3.77 \text{ years}$$

$$R_5 = 10.2 \text{ years}$$

$$R_6 = 42.6 \text{ years}$$

There are no M7+ events in the catalog for the Seattle sub-region, but after extrapolating the best-fit line of the other recurrence intervals, the M7+ recurrence interval is found to be:

$$R_7 \approx 170 \text{ years}$$

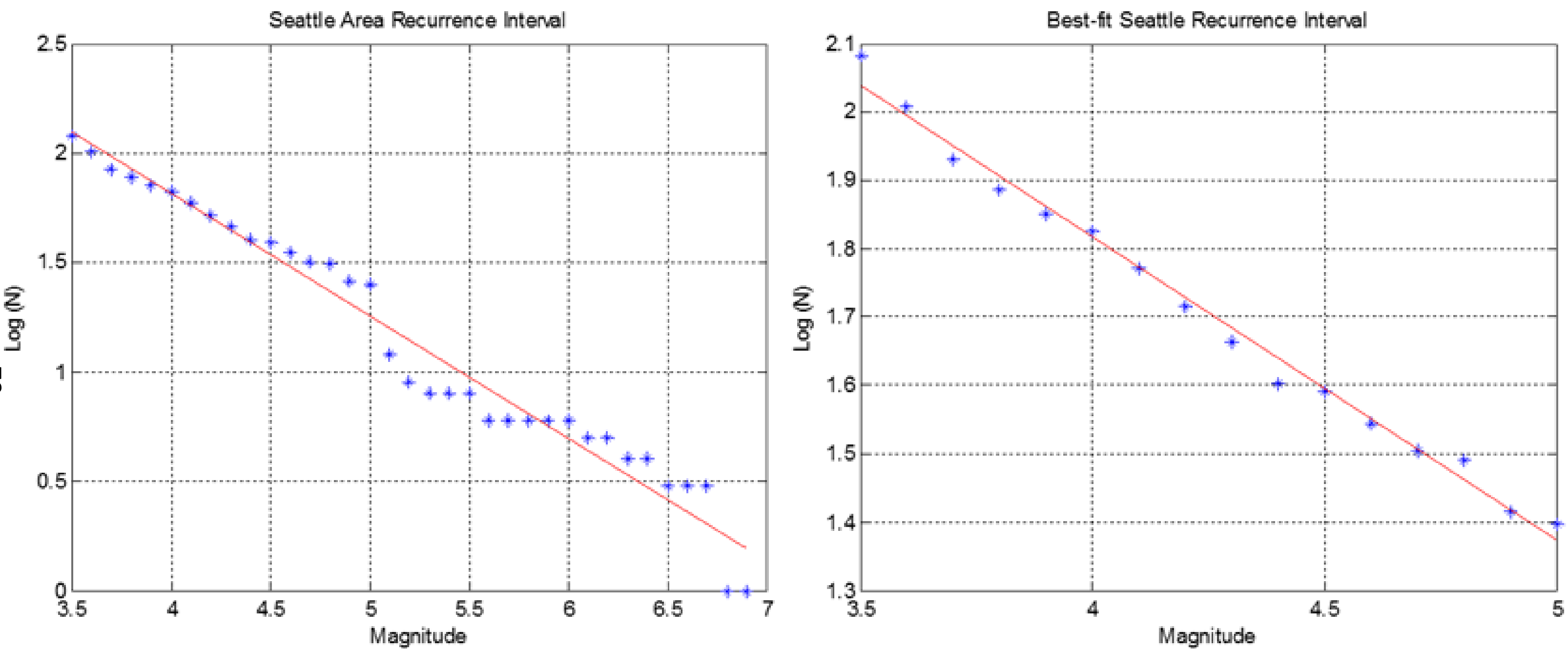

Figure 36: Recurrence plots for the Seattle sub-region. Left; entire catalog, right; best-fit magnitude range plot.

Cascade Volcanic Chain

This sub-region represents the volcanic chain known as the Cascades. Finding the level of CS predictability of earthquakes near the volcanic chain should provide insight into the earthquake hazard here, which is important because of the potentially devastating effects that a major earthquake in this region could have. There were a decent amount of earthquakes in this region for the Post-Cat time period, but not many M5+ earthquakes.

2007-2008 Date Cutoff

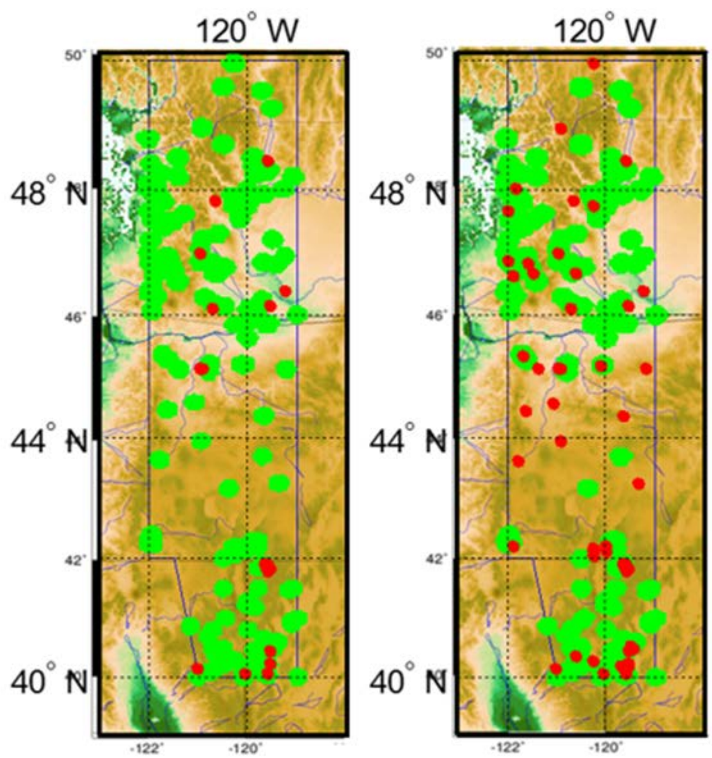

Figure 37: CS analysis of the Cascades sub-region for M3.5+ seismic events. Left; 2007-2008 date cutoff, Right; 1999-2000 date cutoff.

Locations of M3.5+ events were successfully forecasted 50 out of 54 times for the Cascades sub-region. This is a hit percentage of 92.6%. The Pre-Cat radius was 16 km (Figure 37a). As with the Seattle sub-region, the 2007-2008 date cutoff did not produce any M5+ events for the Cascades sub-region. Locations of four out of four M4.5+ events were successfully forecasted though.

1999-2000 Date Cutoff

For the 1999-2000 date cutoff, locations of 72 out of 93 M3.5+ earthquakes were successfully forecasted; a hit percentage of 77.4%. This is considerably lower than the 2007-2008 hit percentage. This considerable drop in hit percentage raises questions as to where these more recent earthquakes in the 2007-2008 catalog occurred and why they were forecast successfully compared to previous earthquakes in the 1999-2000 catalog.

M5+ events were not successfully forecasted here. There were two M5+ events for the Cascades sub-region. Both of these events fell outside the Pre-cat radius, which was 17.2 km (Figure 37b).

The recurrence plot shows a linear trend from M3.5+ to M6.2+, where there is a rapid drop in the number of events. After M6.2+ there is only a single event, of M7.4 for the 255 year catalog (Figure 38a). This singular event seems to be an anomaly. The best-fit recurrence line goes from M3.5+ to M6.2+, essentially covering all events with the exception of the M7.4 event (Figure 38b). The estimated recurrence intervals are:

$R_4 = 1.43$ years

$R_5 = 6.41$ years

$R_6 = 50.9$ years

There was only a single M7+ event so basing the recurrence interval on that one event would not provide a reliable result, but extrapolating from the recurrence intervals for M4, M5, and M6 earthquakes makes the M7 recurrence interval:

$R_7 \approx 400$ years

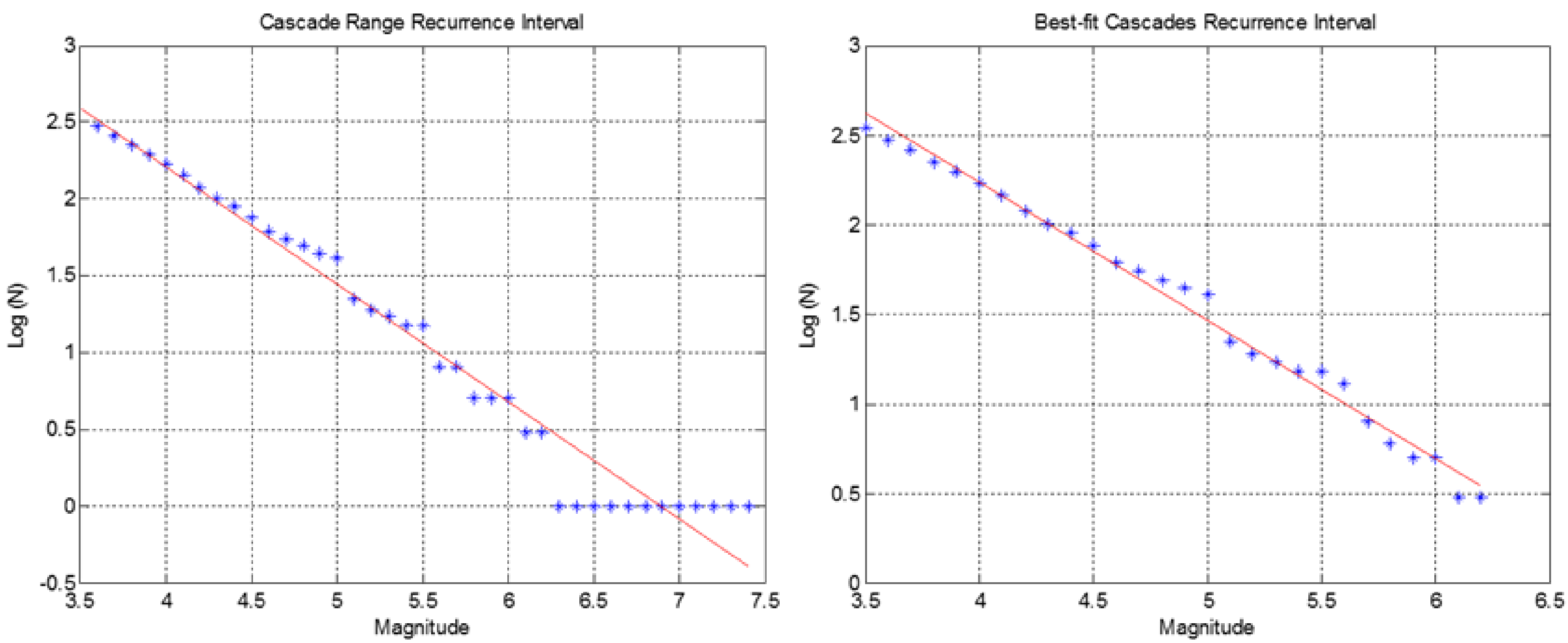

Figure 38: Recurrence plots for the Cascades sub-region. Left; entire catalog, right; best-fit magnitude range plot.

Gorda Ridge

The Gorda Ridge (GR) is the southernmost mid-ocean ridge segment present within the Gorda, Juan de Fuca, and Explorer plate sub-region. At its southern edge is the Mendocino fracture zone. The ridge runs adjacent to northern California and the Oregon coast.

2007-2008 Date Cutoff

Of the 53 M3.5+ events for the GR sub-region the locations of only 36 were forecasted with CS, producing a hit percentage of only 67.9%. Considering this is a plate boundary, one might expect a much higher hit percentage than 67.9%. Most of the

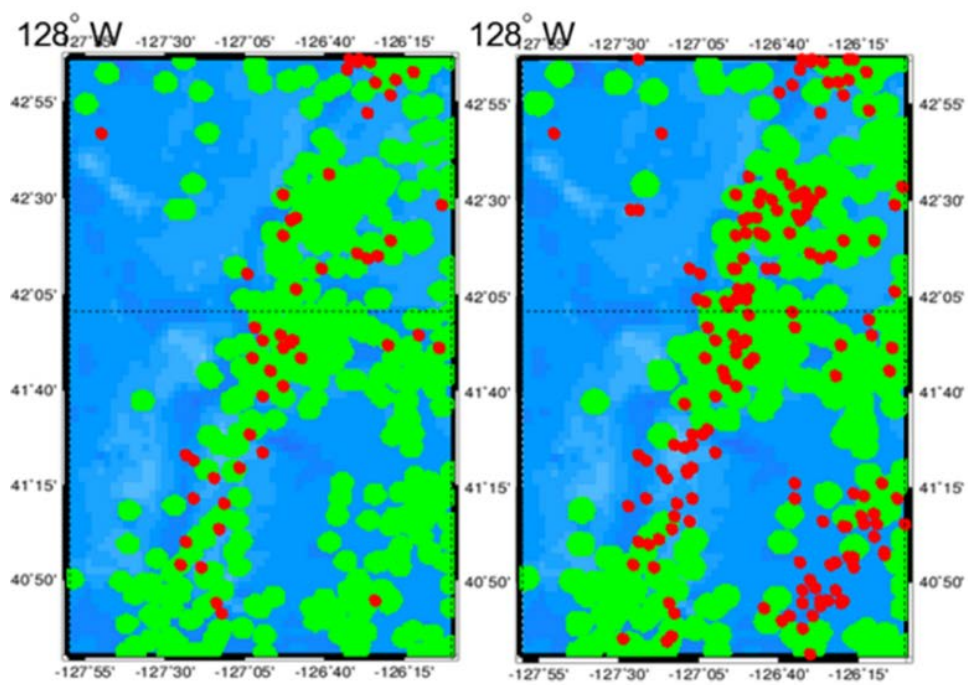

Figure 39: CS analysis of the Gorda Ridge (GR) sub-region for M3.5+ seismic events. Left; 2007-2008 date cutoff, Right; 1999-2000 date cutoff.

events seem to be quite scattered, suggesting, perhaps counterintuitively, that there isn't a persistent pattern to the seismicity along this active mid-ocean ridge segment. The Pre-cat radius was 5.1 km (Figure 39a).

There were four M5+ events, all of which were successfully forecasted. All of the events were below M5.75.

1999-2000 Date Cutoff

Only 90 of 166 events were forecasted successfully for this set of analyses. This corresponds to a 54.2% hit percentage. There is one section of the MOR segment that has produced recent earthquakes in a region that previously lacked sesimicity. There is a south-central portion of the ridge where there are almost no Pre-Cat earthquakes, but many Post-Cat events. At least 24 of the 76 misses can be attributed to this portion of the ridge, and to the area to its southeast in the direction that the plate is moving. Past seismicity can sometimes be a very poor indicator of where future earthquakes will occur, as illustrated by this case comprising a well-defined oceanic plate boundary region.

While the overall hit percentage is quite low, the M5+ hit percentage is a bit higher. 9 out of 11 events were successfully forecasted, 81.8%. There was a single M6+

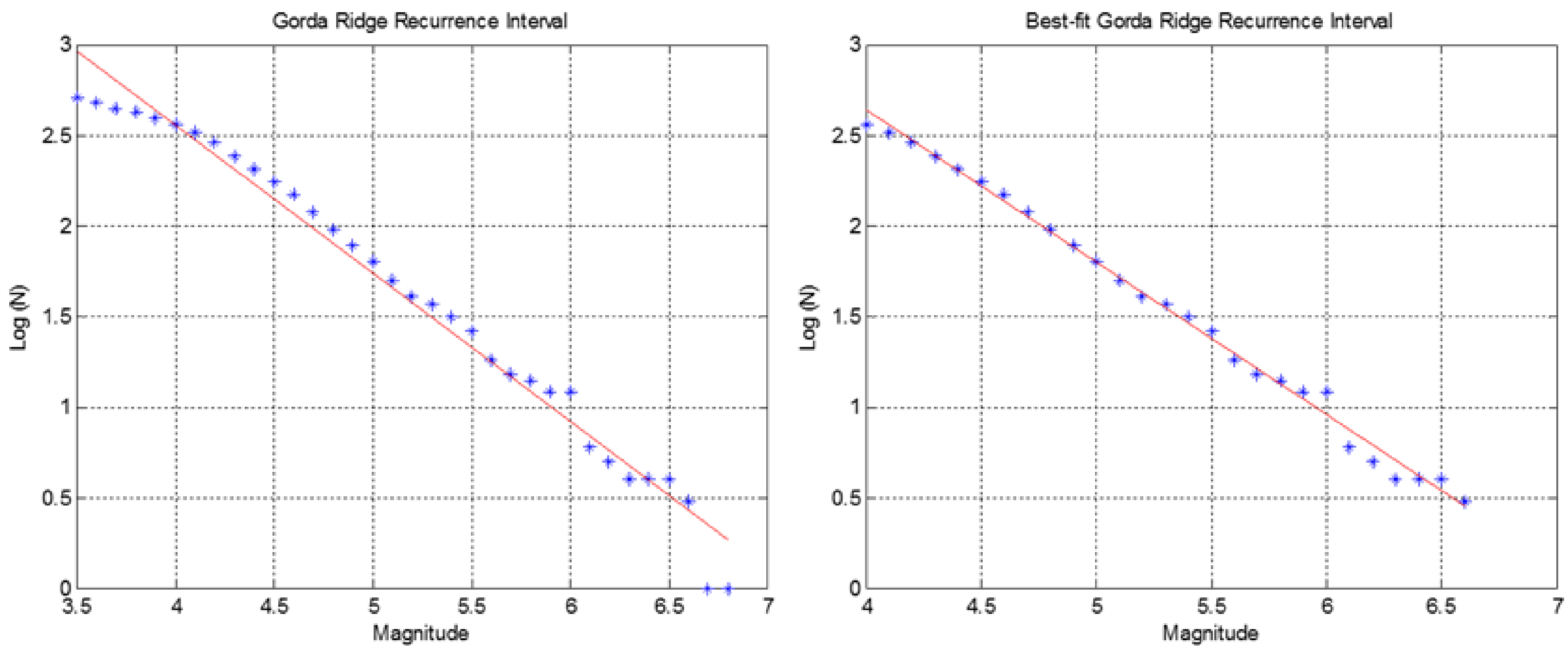

Figure 40: Recurrence plots for the Gorda Ridge (GR) sub-region. Left; entire catalog, right; best-fit magnitude range plot.

event for this sub-region, but it was not forecasted. The Pre-Cat radius was 6.16 km (Figure 39b).

The low-end deviation from a line for the recurrence plot starts at M4+. The high-end deviation starts at M6.6+ (Figure 40a). These are the low and high-end cutoffs for the best-fit recurrence plot for the sub-region (Figure 40b). The estimated recurrence intervals for the GR sub-region are:

$$R_4 = 0.718 \text{ years (262 days)}$$

$$R_5 = 4.04 \text{ years}$$

$$R_6 = 20.2 \text{ years}$$

There are no M7+ events on the GR, but the extrapolated value for the M7+ recurrence interval is

$$R_7 \approx 100 \text{ years}$$

If the recurrence interval is 100 years, we would expect (on average) at least two events during a time period comparable to that of the catalog used in this study.

Blanco Fracture Zone

The Blanco Fracture Zone (BFZ) is the transform fault connecting the GR to another MOR segment, the JDF ridge. The BFZ divides the Gorda microplate from the Juan de Fuca microplate.

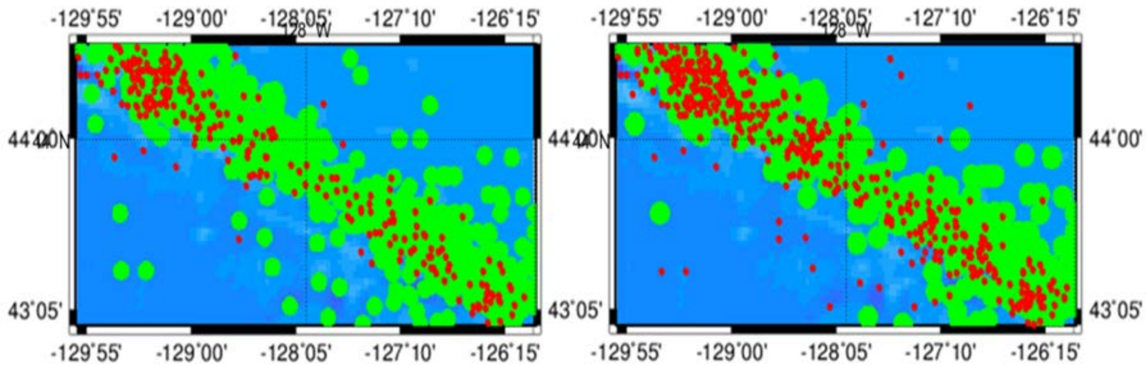

Figure 41: CS analysis of the Blanco Fracture Zone (BFZ) sub-region for M3.5+ seismic events. Left; 2007-2008 date cutoff, Right; 1999-2000 date cutoff.

2007-2008 Date Cutoff

For M3.5+ events on the BFZ, locations of 241 out of 263 were successfully forecasted for a 91.6% hit percentage. The Pre-Cat radius was 5.6 km (Figure 41a).

There were quite a few M5+ events on this transform fault, and most of them were successfully forecasted using the CS method. Locations of 37 out of 41 M5+ events were forecasted, a 90.2% hit percentage. There was a 100% hit percentage starting at M5.25+, where locations of all 15 events were forecasted. There were two M6+ events, both successfully forecasted.

1999-2000 Date Cutoff

Out of the 477 earthquakes of M3.5+ for this set of trials, locations of 434 were forecasted successfully. This provides a success rate of 91.0%. The Pre-Cat radius was 6.84 km (Figure 41b).

Despite doubling the Post-Cat date range there was no corresponding doubling of M5+ events. Only 17 new M5+ events were added to the previous 41 events. Out of the 58 M5+ events, 55 were successfully forecasted resulting in a 94.8% success rate. There was, however, a doubling of M6+ events, and all four were successfully forecasted.

As shown in figure 42a, we see a sharp roll-off from a linear pattern on the recurrence plot at M4.1+. The high-end starts to show roll-off around M5.6+. These two values provide the best-fit range for the recurrence plot (Figure 42b). The estimated recurrence intervals for the BFZ are:

$$R_4 = 0.360 \text{ years (131 days)}$$

$$R_5 = 6.22 \text{ years}$$

$$R_6 = 25.5 \text{ years}$$

There are no M7+ events, and the highest magnitude event for the 255 year catalog is only M6.5. Consequently, no extrapolation was performed to estimate a recurrence interval for M7+ events for the BFZ.

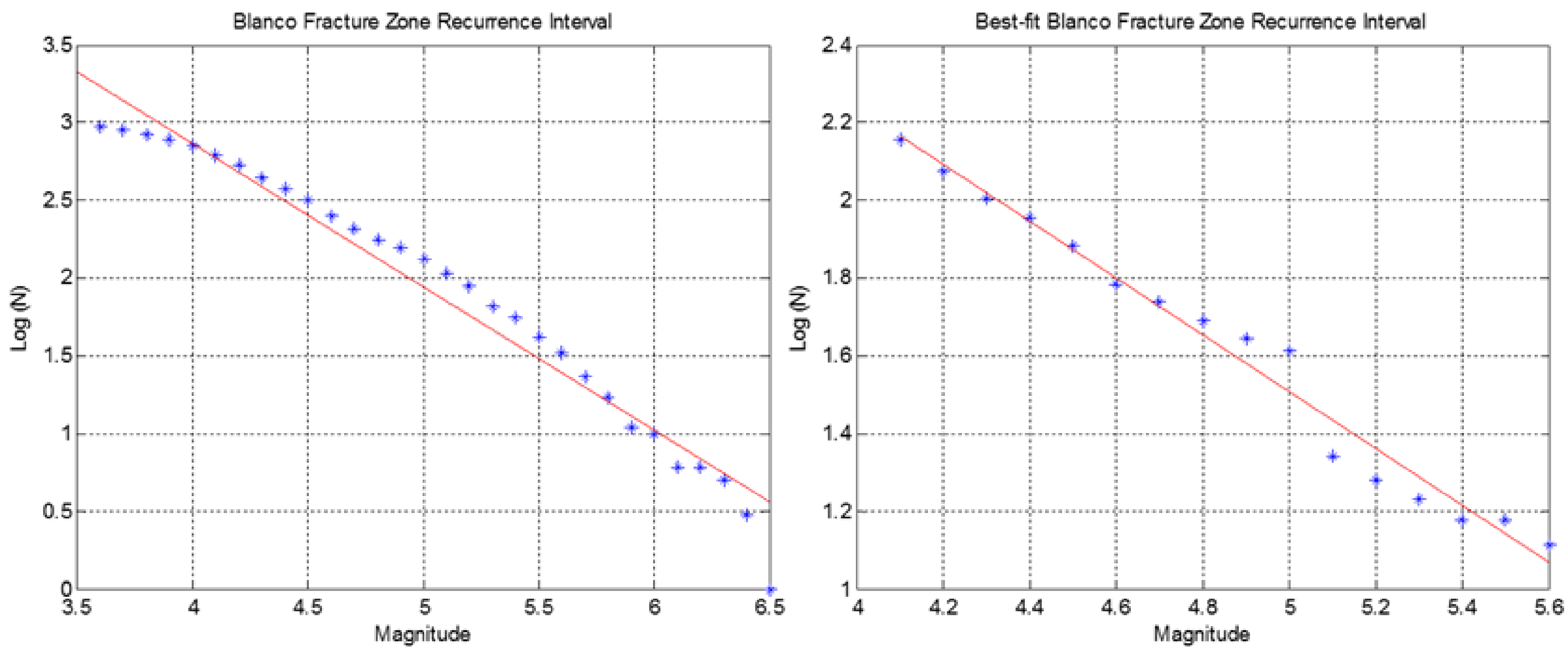

Figure 42: Recurrence plots for the Blanco Fracture Zone (BFZ) sub-region. Left; entire catalog, right; best-fit magnitude range plot.

Mendocino Fracture Zone

The Mendocino fracture zone (MFZ) is the transform fault at the very southern edge of the Cascadia region. It separates the Gorda plate from the Pacific plate, and is a right-lateral, transpressional fault. This sub-region also includes the Mendocino Triple Junction.

2007-2008 Date Cutoff

For M3.5+ events there was a success rate of 83.7%. Out of 104 earthquakes 87 were successfully forecasted. The Pre-Cat radius was 3.35 km (Figure 43a).

There was a 100% hit rate for the M5+ events. Eight out of eight events were forecasted. One M6+ events were forecasted successfully.

1999-2000 Date Cutoff

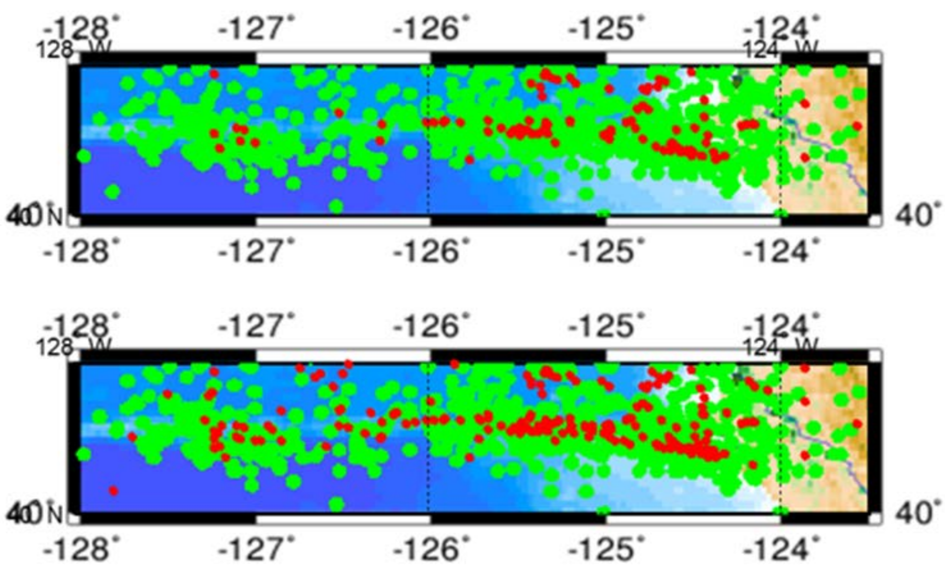

Figure 43: CS analysis of the Mendocino Fracture Zone (MFZ) sub-region for M3.5+ seismic events. Top; 2007-2008 date cutoff, Bottom; 1999-2000 date cutoff.

M3.5+ events were successfully forecasted 159 out of 205 times for the 1999-2000 date cutoff. This dropped the success rate down to 77.6%. The Pre-Cat radius was 3.5 km (Figure 43b).

There is also no longer a 100% success rate for M5+ events. Only 11 out of 14 M5+ events were successfully forecasted, a 78.6% success rate. Neither of the two M6+ events were forecasted successfully, meaning that the M6+ event that was a hit in the 2007-2008 catalog became a miss in this catalog.

The recurrence plot for the MFZ shows only slight deviation from the line at the low end of the magnitude range (Figure 43a). This deviation begins at M4+. The high-end deviation doesn't begin until M6.5+. The best-fit for the MFZ is plotted from M3.6+ to M6.5+ (Figure 44b). I chose M3.6 because even though there is some deviation from the linearity of the recurrence plot starting at M4+, the pattern is quite linear starting at M3.6+ and going to M6.5+. The estimated recurrence intervals for the MFZ are:

$$R_4 = 0.486 \text{ years (177 days)}$$

$$R_5 = 2.44 \text{ years}$$

$$R_6 = 9.47 \text{ years}$$

$$R_7 = 63.8 \text{ years}$$

The highest magnitude events on the MFZ were M7.2, but extrapolation based on the other recurrence intervals leads to the estimated recurrence interval for M8+ events to be:

$$R_8 \approx 320 \text{ years}$$

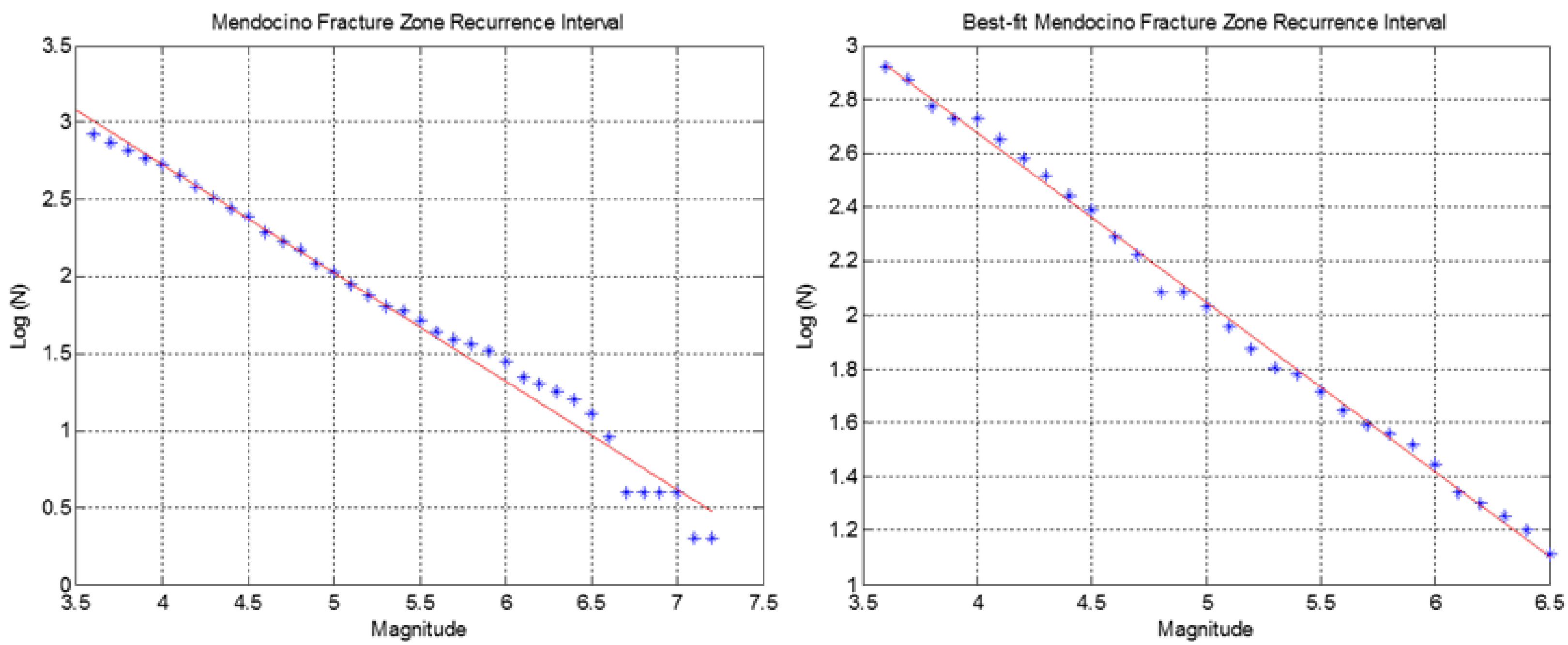

Figure 44: Recurrence plots for the Mendocino Fracture Zone (MFZ) sub-region. Left; entire catalog, right; best-fit magnitude range plot.

This estimate is about 60% longer than the estimate from 'EconScience' (<200), but it is for the MFZ, and not necessarily the CSZ margin. The eastward end of the MFZ is the CSZ margin however.

CS Analysis of the San Andreas Transform Region

Analysis of the Northern San Andreas Sub-region

2007-2008 Date Cutoff

The northern sub-region of the SAF (NSA) has a great amount of seismic activity. There are 367 earthquakes represented in the Post-Cat for M3.5+, and locations of 331 out of 367 of them were successfully forecasted, a hit rate of 90.2%. This is lower than that of either of the larger Cascadia sub-regions. The Pre-Cat radius was 7.1 km (Figure 45a).

There are not that many M5+ events for the NSA. Out of the seven M5+ events, six were successfully forecasted, an 85.7% success rate. There was one event of M6+, but it was not successfully forecasted.

1999-2000 Date Cutoff

The 1999-2000 date cutoff for the NSA showed an even lower hit percentage for the Post-Cat catalog. Out of 884 events of M3.5+, 770 were successfully forecasted. This is only an 87.1% success rate. The Pre-Cat radius was 7.6 km (Figure 45b).

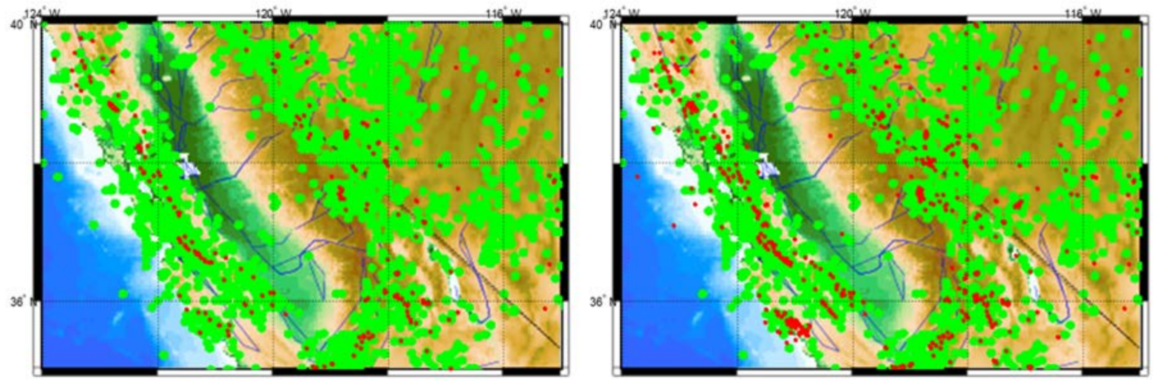

Figure 45: CS analysis of the Northern San Andreas (NSA) sub-region for M3.5+ seismic events. Left; 2007-2008 date cutoff, Right; 1999-2000 date cutoff.

Almost all of the M5+ events were successfully forecasted. Out of 19 events, 18 were hits, a success rate of 94.7%. Three out of four M6+ events were hits.

The recurrence plot for the NSA sub-region was quite linear (Figure 46a). There was low-end deviation starting around M4.5+, and high-end deviation at M7.6+. The best-fit recurrence plot ranges in between these two values (Figure 46b). There is a hump in the mid-magnitudes from M5+ to M6+ meaning that there were more mid-magnitude events than the linear trend would predict. Even in the best-fit plot there is roll-off at the lower magnitudes, starting at M5+. The estimated recurrence intervals are:

R_4 = 0.081 years (29 days)

R_5 = 0.454 years (166 days)

R_6 = 2.55 years

R_7 = 25.5 years

There are no M8+ earthquakes in the catalog, but judging from R_6 and R_7, R_8 is likely about 255 years, which is the length of this earthquake catalog. This leads to the possibility that a magnitude 8 earthquake could occur soon in this region.

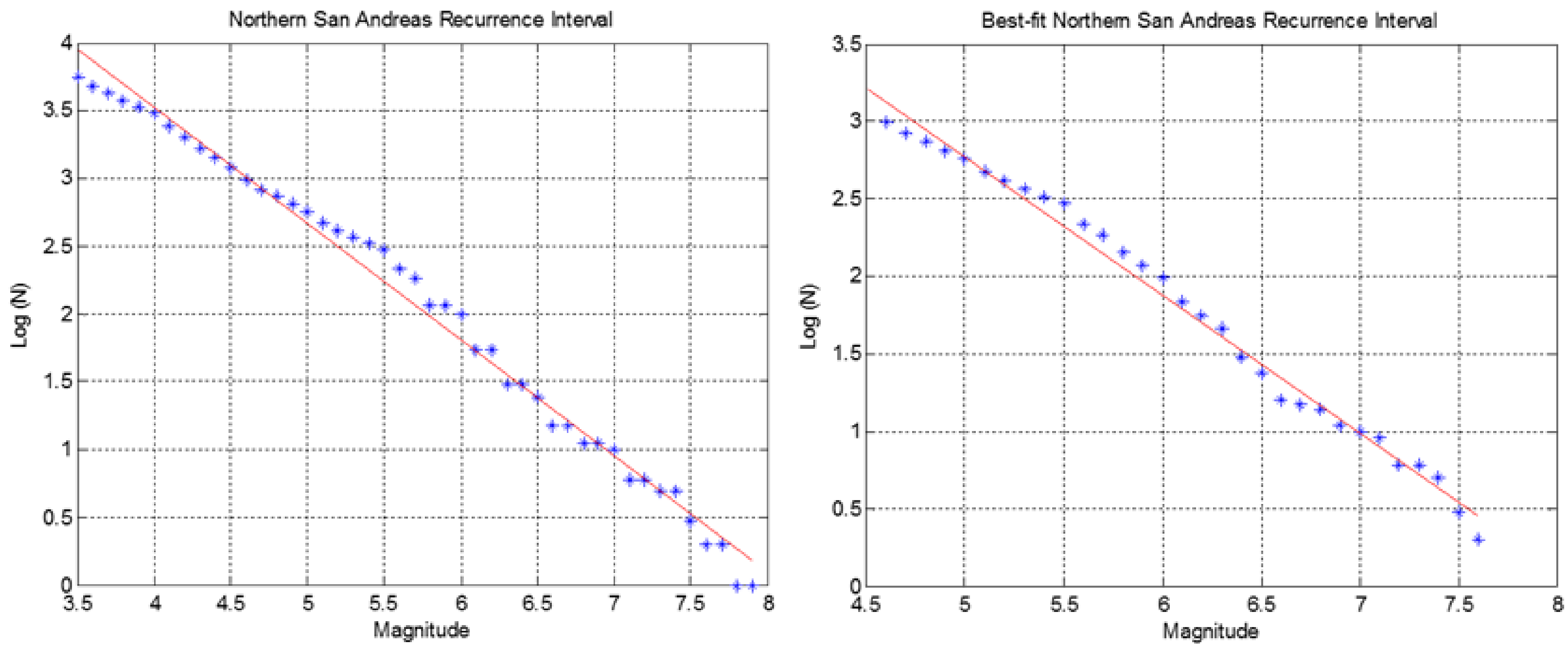

Figure 46: Recurrence plots for the Northern San Andreas (NSA) sub-region. Left; entire catalog, right; best-fit magnitude range plot.

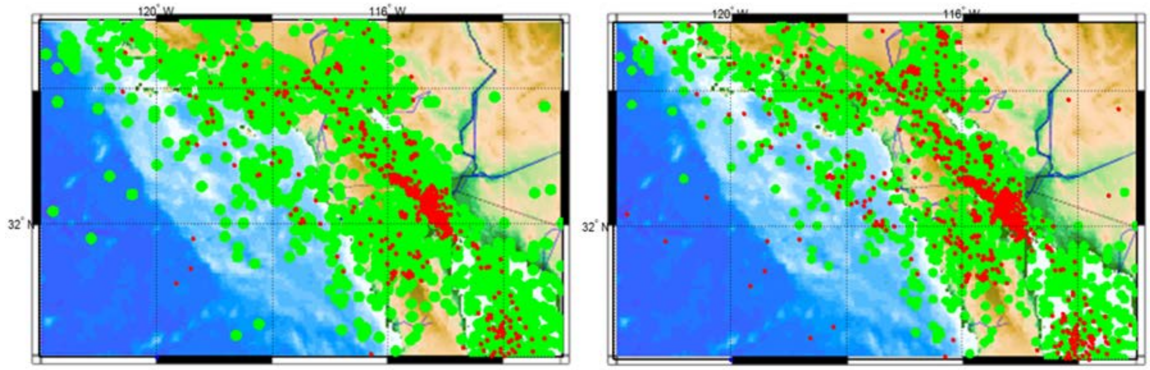

Figure 47: CS analysis of the Southern San Andreas (SSA) sub-region for M3.5+ seismic events. Left; 2007-2008 date cutoff, Right; 1999-2000 date cutoff.

CS Analysis of the Southern San Andreas Sub-region

2007-2008 Date Cutoff

The southern San Andreas sub-region (SSA) had the most Post-Cat earthquakes of any of the larger sub-regions. For events of M3.5+, locations of 1,057 out of 1,086 were successfully forecasted. This is a hit rate of 97.3%. This is the second highest out of any sub-region for the 2007-2008 date cutoff (Table 2). The Pre-cat radius was 9.2 km (Figure 47a).

There were 31 Post-Cat earthquakes of M5+, 30 of which were successfully forecasted. This gives a hit rate of 96.8% for the 2007-2008 date cutoff, which is the highest hit percentage of any sub-region analyzed. One out of two M6+ events were successfully forecasted. There was a single M7+ event which was a hit.

1999-2000 Date Cutoff

For the 1999-2000 date cutoff the locations of 1,371 out of 1,489 events were successfully forecasted, giving a hit rate of 92.1%. While this is still very high, it is 5% lower than the 2007-2008 value. The pre-cat radius was 9.92 km (Figure 47b).

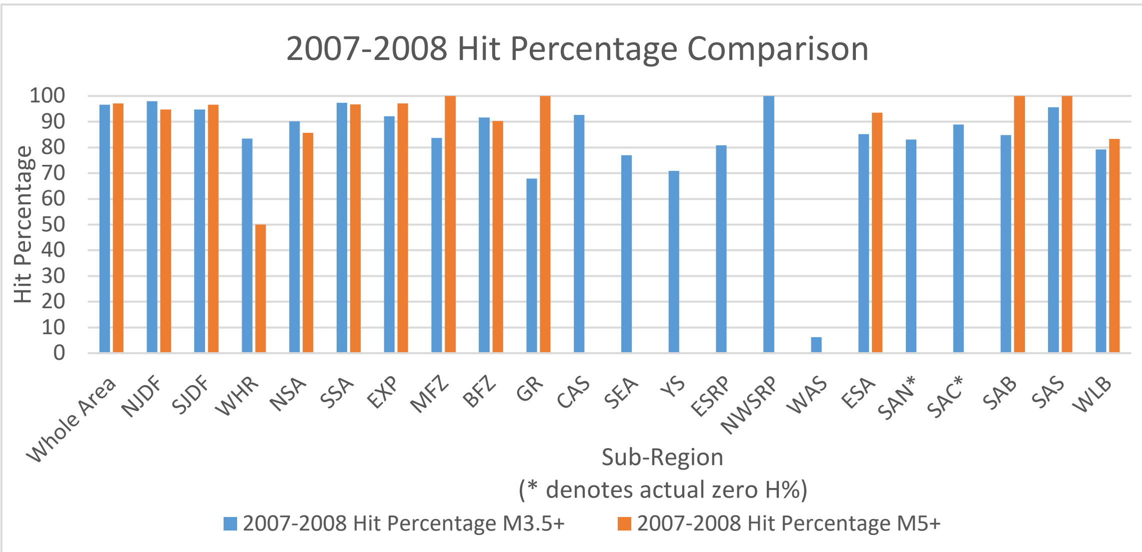

Figure 48: Hit Percentages for each of the sub-regions for M3.5+ (blue) and M5+ (orange) for the 2007-2008 date cutoff.

Of the 43 M5+ events, 42 were hits, giving a 97.7% success rate, the second highest of any sub-region, after the northern JDF. Only one of two M6+ events were successfully forecasted.

The recurrence plot for the SSA sub-region is remarkably linear, possibly due to greater seismic network coverage. There is slight deviation at a low-end magnitude of M4+, and the high-end deviation begins at M7.1+ (Figure 49a). The best-fit recurrence plot runs from M4+ to M7+ (Figure 49b). The estimated recurrence intervals for the SSA sub-region are:

$$R_4 = 0.097 \text{ years (35 days)}$$

$R_5 = 0.641$ years (234 days)

$R_6 = 4.04$ years

$R_7 = 25.5$ years

My extrapolated estimate for the recurrence interval of M8+ events based on the other recurrence intervals is:

$R_8 \approx 155$ years

Once again, based on the results of these analyses, the San Andreas seems to be overdue for a M8+ event, however M8+ events on the San Andreas are extremely rare.

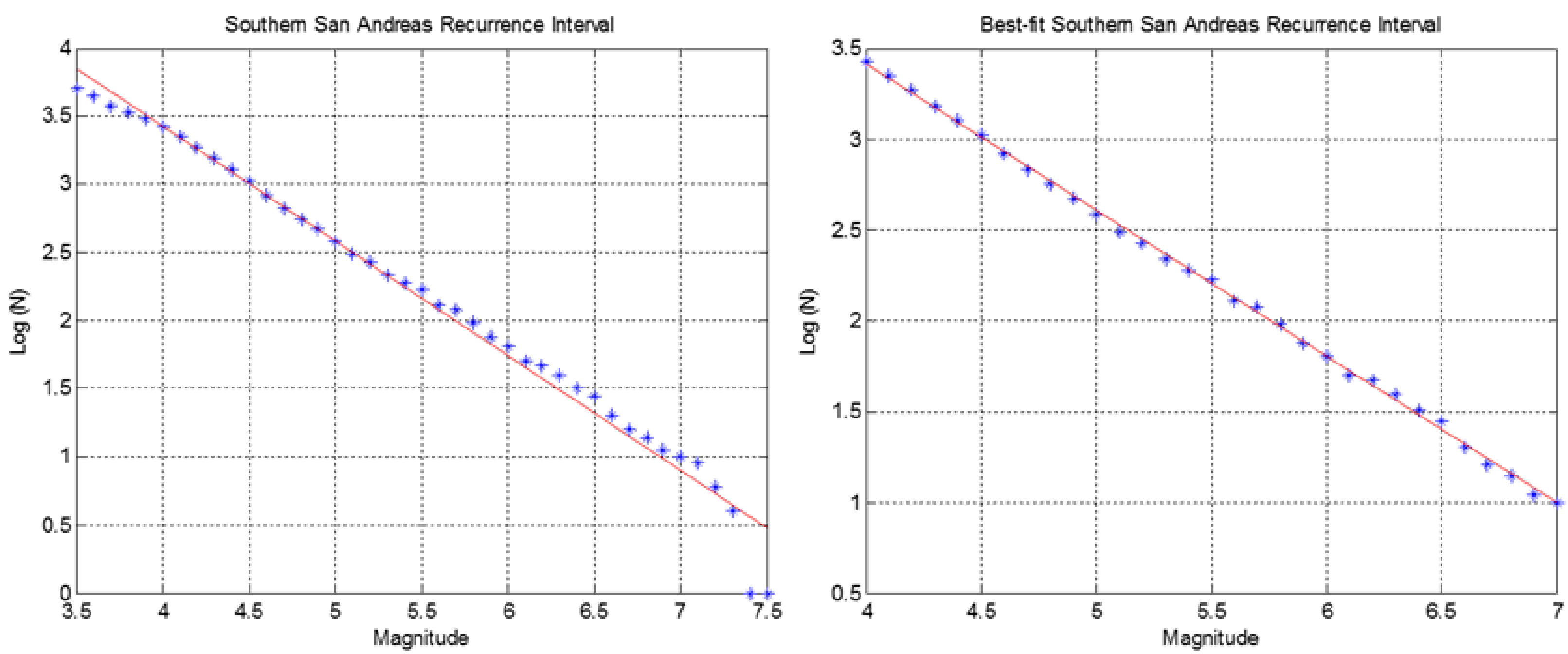

Figure 49: Recurrence plots for the Southern San Andreas (SSA) sub-region. Left; entire catalog, right; best-fit magnitude range plot.

Analysis of the Smaller San Andreas Sub-regions

Entire San Andreas

The "Entire San Andreas" (ESA) sub-region comprises the San Andreas and its main branch faults as the only faults considered in this sub-region. In the NSA and SSA sub-regions, parts of the Walker Lane Belt were analyzed along with the SAF. This sub-region looks at only the SAF, in its entirety (Figure 50).

2007-2008 Date Cutoff

For the ESA sub-region, the locations of 1,054 out of 1,237 earthquakes were successfully forecasted. This is a hit rate of only 85.2%. The Pre-Cat radius for the SAF is 5.3 km (Figure 50a).

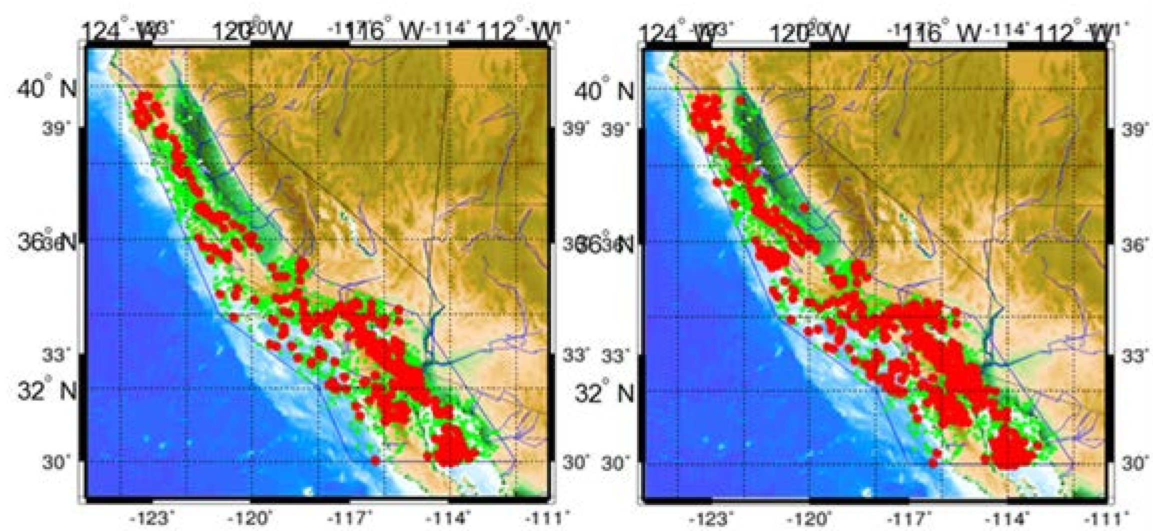

Figure 50: CS analysis of the entire San Andreas (ESA) sub-region for M3.5+ seismic events contained within the blue polygon. Left: 2007-2008 date cutoff, Right: 1999-2000 date cutoff.

For M5+ events on the SAF 29 out of 31 earthquakes were forecasted. This is a success rate of 95.6%. One of two M6+ events were successfully forecasted. There was a single M7+ event, which was a hit.

1999-2000 Date Cutoff

There were 1916 seismic events for the 1999-2000 date cutoff of M3.5+. Of these events 1612 were successfully forecasted. This is a success rate of 84.1%, almost identical to the 2007-2008 cutoff value. The pre-Cat radius is 5.78 km (Figure 50b).

For M5+ events 49 out of 51 were forecasted successfully, a success rate of 96.1%. Four out of five M6+ events were forecasted, and again, a single M7+ event was successfully forecasted.

The recurrence plot for the ESA sub-region has a low-end deviation starting at M4.5+, and a high end deviation stating at M7.4+ (Figure 51a). The best-fit recurrence plot uses these as its end-member values (Figure 51b). There is a relatively poor fit even between these magnitudes, as most of the values lie noticeably above or below the best-fit line. The estimated recurrence intervals for the entire SAF are:

R_4 = 0.045 years (17 days)

R_5 = 0.256 years (93 days)

R_6 = 1.50 years

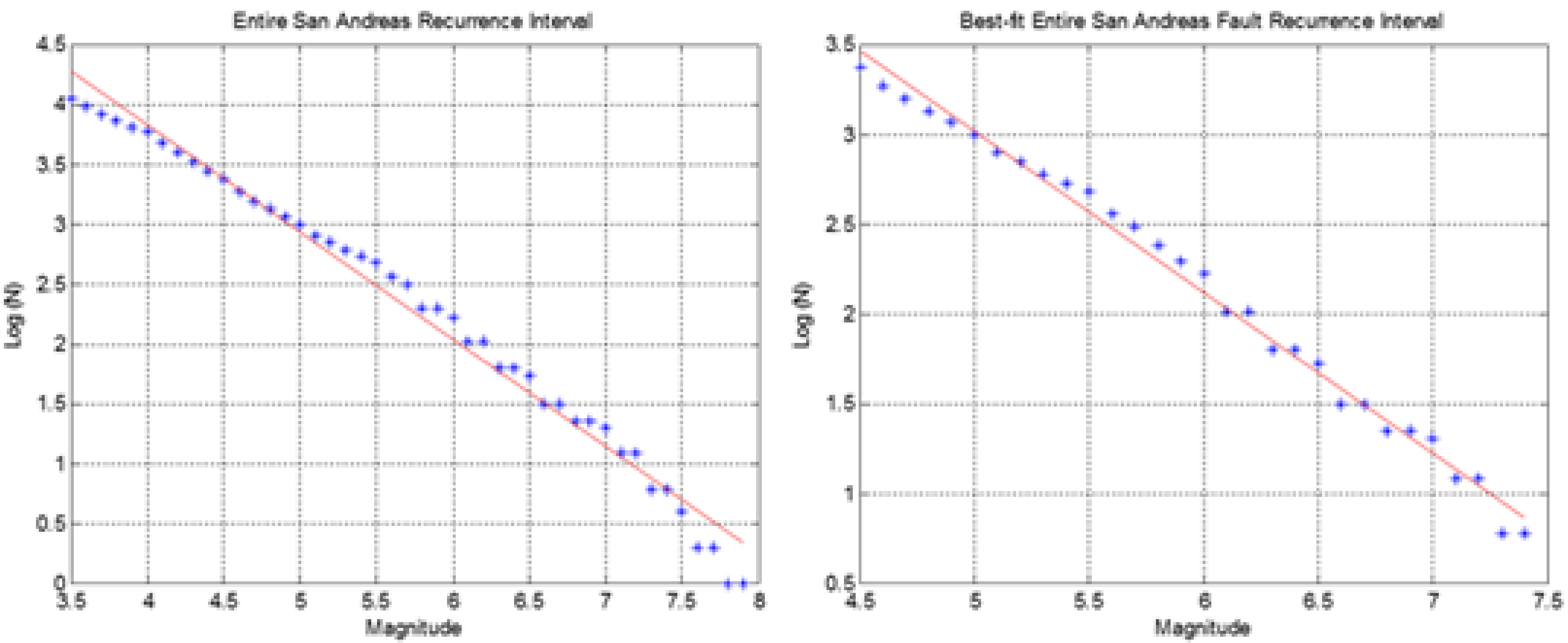

Figure 49: Recurrence plots for the entire San Andreas (ESA) sub-region. Left; entire catalog, right; best-fit magnitude range plot.

Figure 51: Recurrence plots for the entire San Andreas (ESA) sub-region. Left: entire catalog, right: best-fit magnitude range plot.

$$R_7 = 12.8 \text{ years}$$

My extrapolated estimate for M8+ events for the SAF is:

$$R_8 \approx 110 \text{ years}$$

This estimate is in good agreement with Wallace (1970) who finds a recurrence interval for M8 events of 102 years.

San Andreas North

2007-2008 Date Cutoff

For M3.5+ events in the San Andreas north (SAN) sub-region, locations of 64 out of 77 earthquakes were forecasted successfully. This is a hit rate of 83.1%. The Pre-Cat radius is 7.03 km (Figure 52a).

There was only a single M5+ event for the SAN sub-region, and it was not forecasted successfully. This single event was actually a M6+ event. There is a gap in magnitude from at least M4.7 to M6, meaning no Post-Cat earthquakes of M4.71 to M5.99 occurred in the SAN sub-region during the time period covered by the earthquake catalog used in this study.

1999-2000 Date Cutoff

Out of 161 total events for the SAN sub-region, locations of 132 events were successfully forecasted. This is a hit rate of 82.0%. The Pre-Cat radius is 7.04 km (Figure 52b).

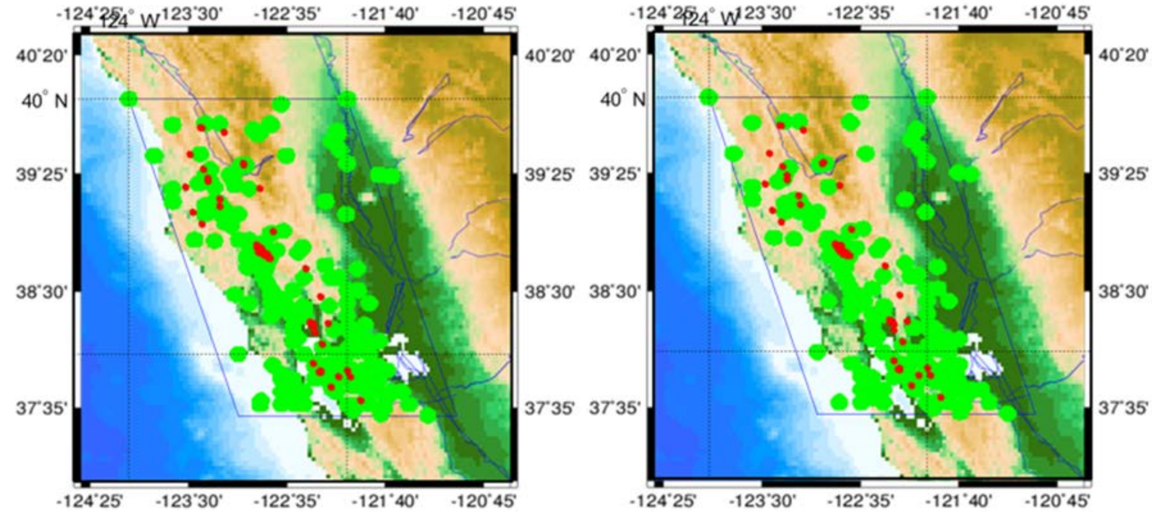

Figure 52: CS analysis of the San Andreas North (SAN) sub-region for M3.5+ seismic events contained within the blue polygon. Left; 2007-2008 date cutoff, Right; 1999-2000 date cutoff.

There is a hit rate of 50% for M5+ events. There were two events, and only one was forecasted successfully, and again, there is a single M6+ event.

The recurrence plot for the SAN decreases in “steps” once you reach M5.5+ (Figure 53a), because there are few events of higher magnitude in this sub-region. Even at lower magnitudes the SAN earthquakes do not show a very linear trend, but rather show a more curvilinear pattern. My estimate for the best-fit magnitude range is from only M3.5+ to M5+ (Figure 53b). The estimated recurrence intervals for the SAN sub-region are:

$$R_4 = 1.14 \text{ years}$$

$$R_5 = 6.55 \text{ years}$$

$$R_6 = 28.6 \text{ years}$$

$$R_7 = 128 \text{ years}$$

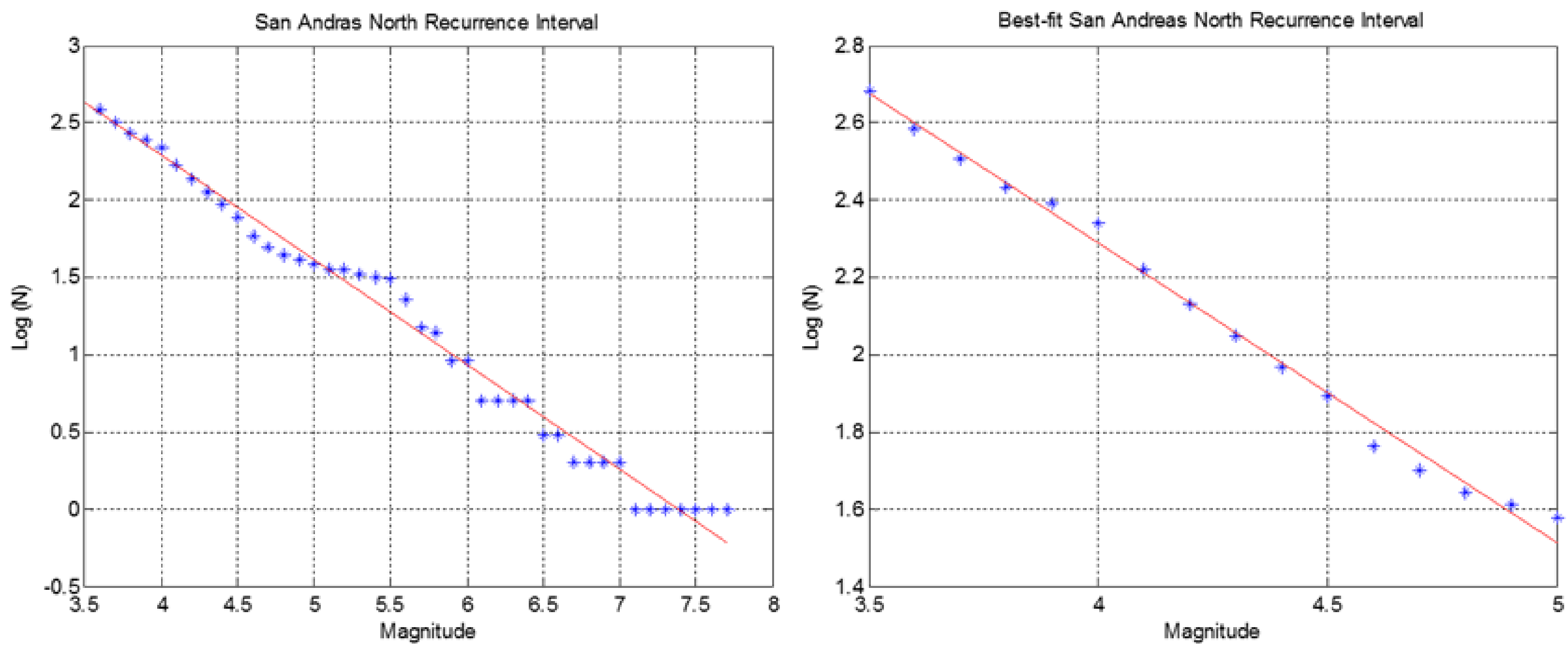

Figure 53: Recurrence plots for the San Andreas North (SAN) sub-region. Left; entire catalog, right; best-fit magnitude range plot.

The recurrence interval for M7+ events is based on only two events so it may not be representative of the sub-region over a longer period of time.

San Andreas Central

2007-2008 Date cutoff

Of the 72 M3.5+ events for the SAC sub-region, locations of 64 were forecasted successfully, a hit rate of 88.9%. The Pre-Cat radius is 3.16 km (Figure 54a).

Only a single M5+ event is present in the Post-Cat for the SAC sub-region using the 2007-2008 date cutoff. This single event is not forecasted successfully.

1999-2000 Date Cutoff

The SAC sub-region yields a major drop in hit percentage between the 2007-2008 cutoff and the 1999-2000 date cutoff. Only 170 out of 280 Post-Cat events were successfully forecasted. This is a low hit rate of only 60.7%. The Pre-Cat radius is 3.42 km (Figure 54b).

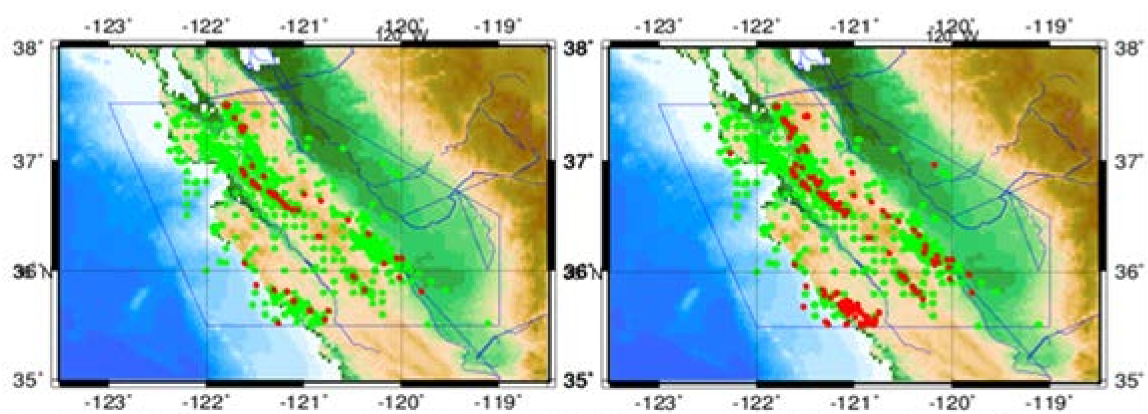

Figure 54: Cs analysis of the San Andreas central (SAC) sub-region for M3.5+ seismic events contained within the blue polygon. Left: 2007-2008 date cutoff, Right: 1999-2000 date cutoff.

Four out of six M5+ events were forecasted successfully. Two out of three M6+ events were hits. Both of these are 66.7% hit percentages.

The recurrence plot for the SAC sub-region has a big bump in seismicity between M5+ and M6+, then the number of events tapers off quickly (Figure 55a). The best-fit recurrence plot for the SAC sub-region (Figure 55b) runs from M3.5+ to M6+. The estimated recurrence intervals for the SAC sub-region are:

$$R_4 = 0.404 \text{ years (148 days)}$$

$$R_5 = 2.02 \text{ years}$$

$$R_6 = 6.41 \text{ years}$$

$$R_7 = 128 \text{ years}$$

The M7+ recurrence interval only includes two events over the 255 year catalog, thus the 128 year recurrence interval, but again, this may not be truly representative of the region over a longer period of time. There is a huge jump in number of years (20 fold) between events of M6+ and M7+, showing us that M7+ events are incredibly rare on this segment of the SAF.

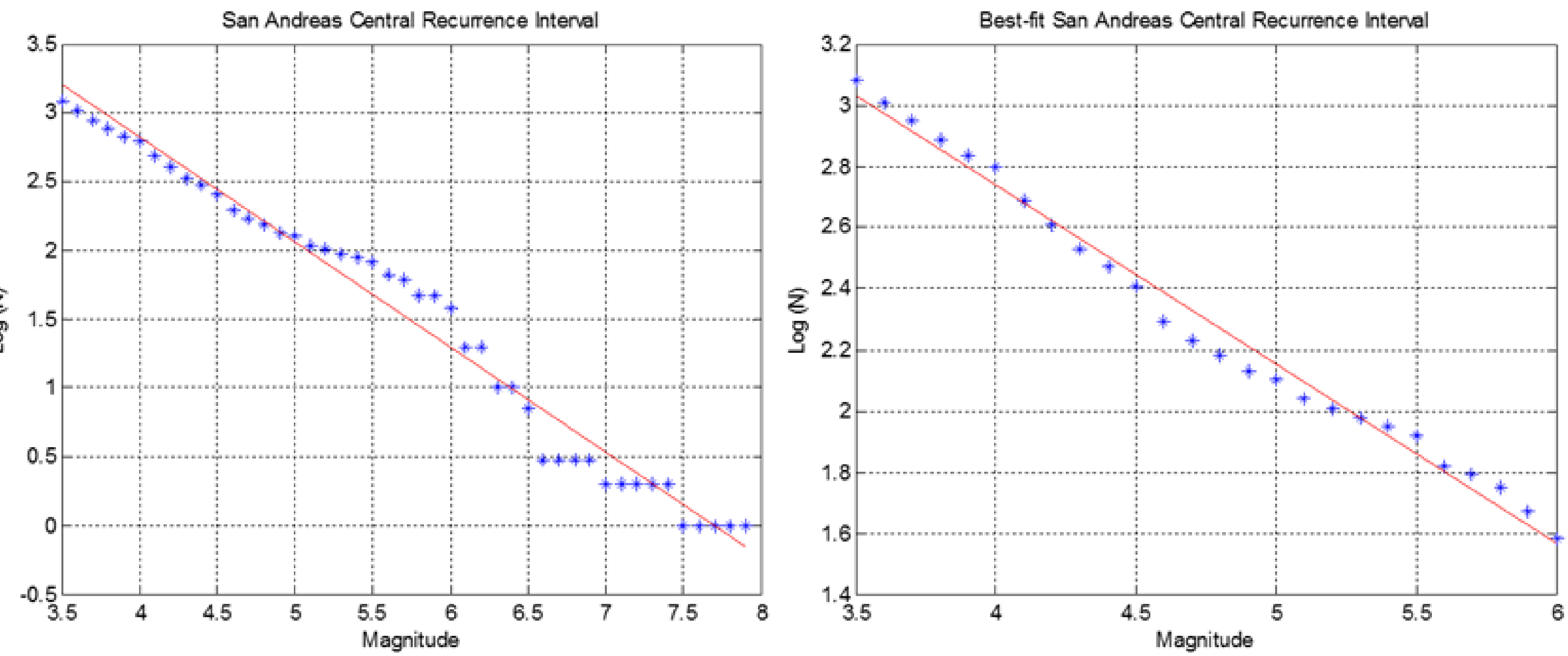

Figure 55: Recurrence plots for the San Andreas central (SAC) sub-region. Left; entire catalog, right; best-fit magnitude range plot.

San Andreas “Big Bend”

2007-2008 Date Cutoff

Of the 105 M3.5+ events in the SAB sub-region of the SAF, locations of 89 were successfully forecasted. This is a hit rate of 84.8%. The Pre-cat radius is 5.78 km (Figure 56a). There were only two events of M5+ in this analysis. Both are successfully forecasted.

1999-2000 Date Cutoff

For M3.5+ earthquakes on the SAB there is an 83.7% success rate. Out of 227 earthquakes 190 are forecasted successfully. The Pre-Cat radius is 5.79 km (Figure 56b).

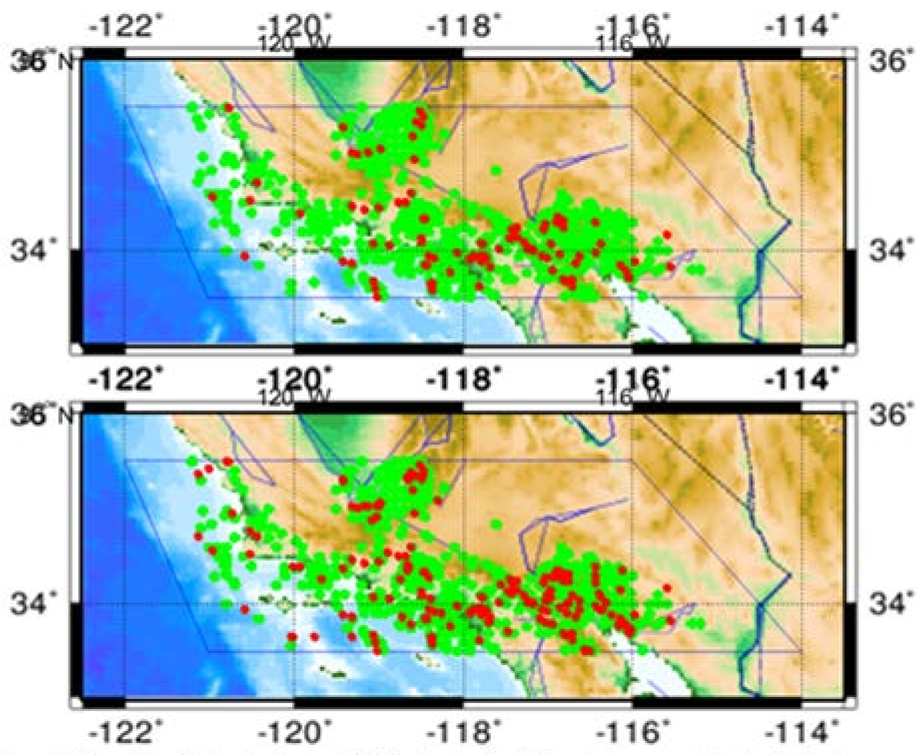

Figure 56: CS analysis of the San Andreas bend (SAB) sub-region for M3.5+ seismic events contained within the blue polygon. Top: 2007-2008 date cutoff, Bottom: 1999-2000 date cutoff.

There is a small spike in M5+ events. Doubling the years led to five more M5+ events in the Post-Cat. All seven of those events were forecast successfully. There are still no events of M6+.

There is almost no deviation on the low end of the magnitude range, even back to M3.5+, and only the large events greater than M7 show any sort of deviation at the high end of the magnitude spectrum. The recurrence plot for the SAB shows a very linear pattern from M3.5+ to M7+ (Figure 57a), which is where I start and stop the magnitude range for the best-fit recurrence plot (Figure 57b). The estimated recurrence intervals for the SAB are:

$$R_4 = 0.255 \text{ years (93 days)}$$

$$R_5 = 1.61 \text{ years}$$

$$R_6 = 8.06 \text{ years}$$

$$R_7 = 42.5 \text{ years}$$

Based on these recurrence intervals my extrapolated estimate is:

$$R_8 \approx 215$$

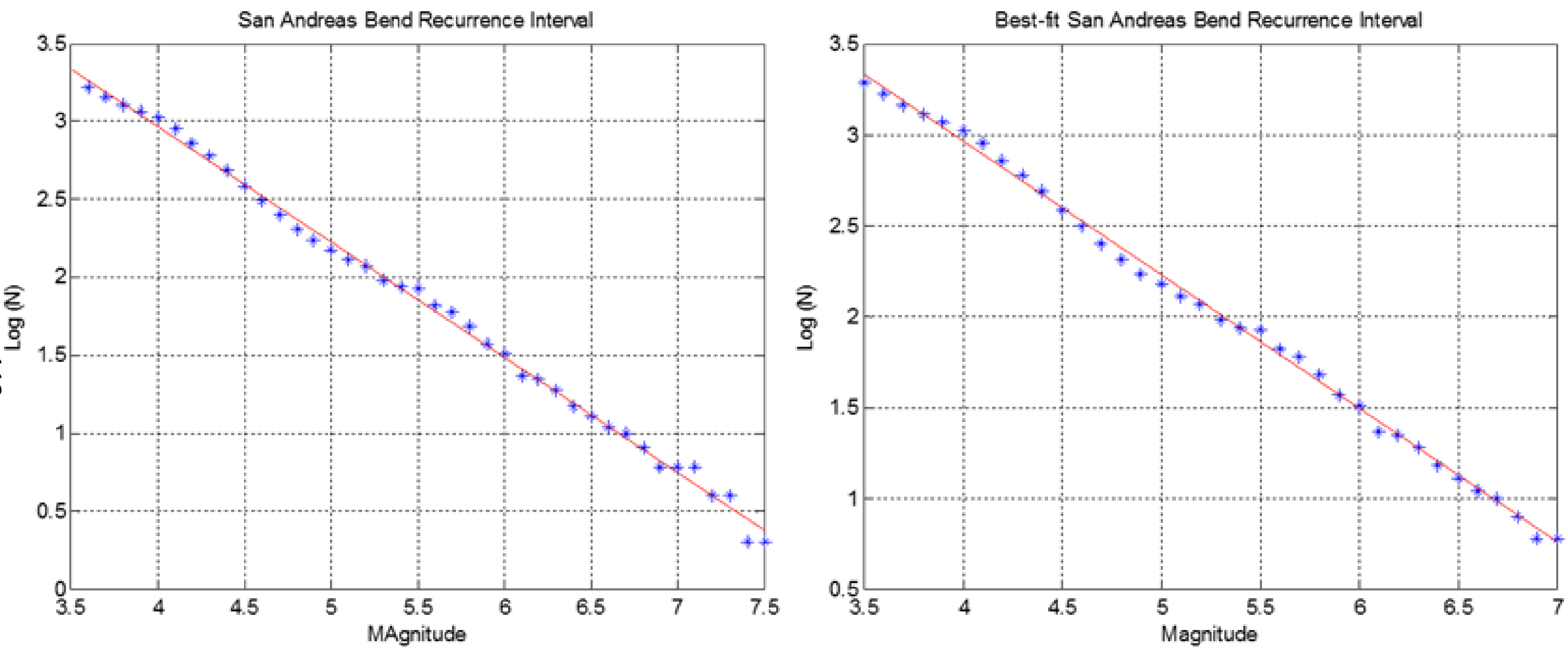

Figure 57: Recurrence plots for the San Andreas bend (SAB) sub-region. Left; entire catalog, right; best-fit magnitude range plot.

San Andreas South

2007-2008 Date Cutoff

The southern end of the SAF (SAS) is one of the most active sub-regions in the study. Of the 978 events in the Post-Cat, the locations of 935 are successfully forecasted. This is a 95.6% hit rate. The Pre-Cat radius is 7.26 km (Figure 58a).

100% of the M5+ events were successfully forecasted, 27 out of 27 events. There was a single M6+ event that was a hit.

1999-2000 Date Cutoff

There are a total of 1242 M3.5+ events in the 1999-2000 Post-Cat. Of these 1,242 events 1,160 were successfully forecasted; a hit rate of 93.4%. The pre-Cat radius was 7.65 km (Figure 58b).

Once again, 100% of the M5+ events were forecasted successfully; 36 events in total. The locations of every earthquake that has the potential to be damaging in this sub-region, which is characterized by a plethora of faults and seismic activity, was successfully forecasted using the CS method.

The recurrence plot for the SAS shows roll-off at the low end of the magnitude range starting at M4+, and at the high end of the magnitude range starting at M6.5+ (Figure 59a). These two values are used in the best-fit recurrence plot (Figure 59b). The estimated recurrence intervals for the SAS sub-region are:

R_4 = 0.143 years (52 days)

R_5 = 1.02 years

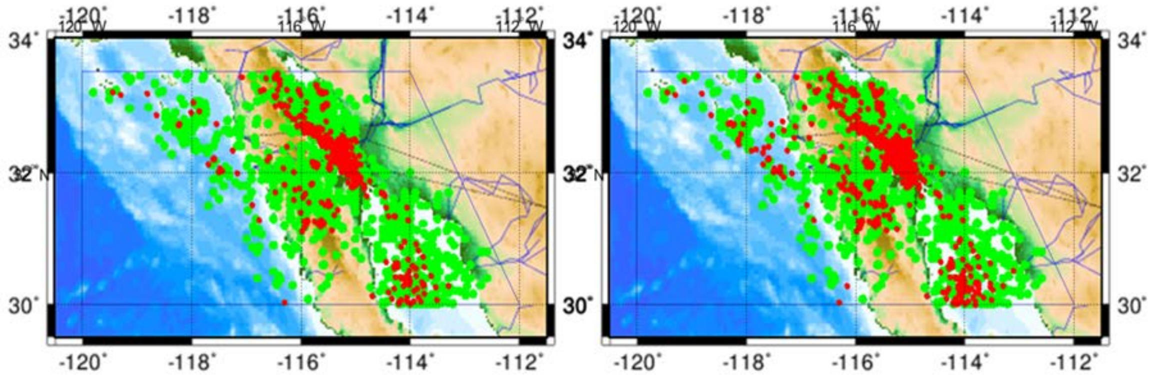

Figure 58: CS analysis of the San Andreas south (SAS) sub-region for M3.5+ seismic events contained within the blue polygon. Left; 2007-2008 date cutoff, Right; 1999-2000 date cutoff.

$$R_6 = 8.06 \text{ years}$$

$$R_7 = 84.5 \text{ years}$$

Based on these recurrence intervals the extrapolated estimate the recurrence interval for M8+ events is:

$$R_8 \approx 800 \text{ years}$$

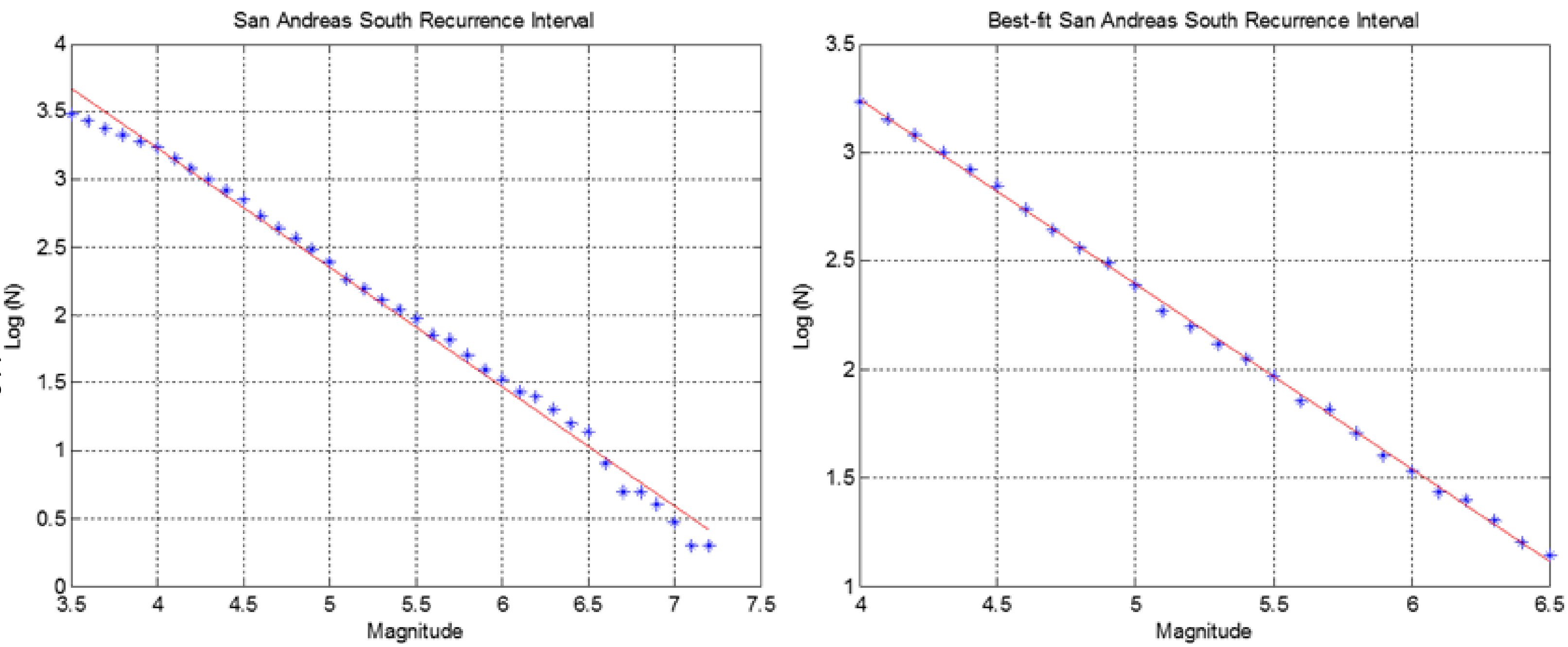

Figure 59: Recurrence plots for the San Andreas south (SAS) sub-region. Left; entire catalog, right; best-fit magnitude range plot.

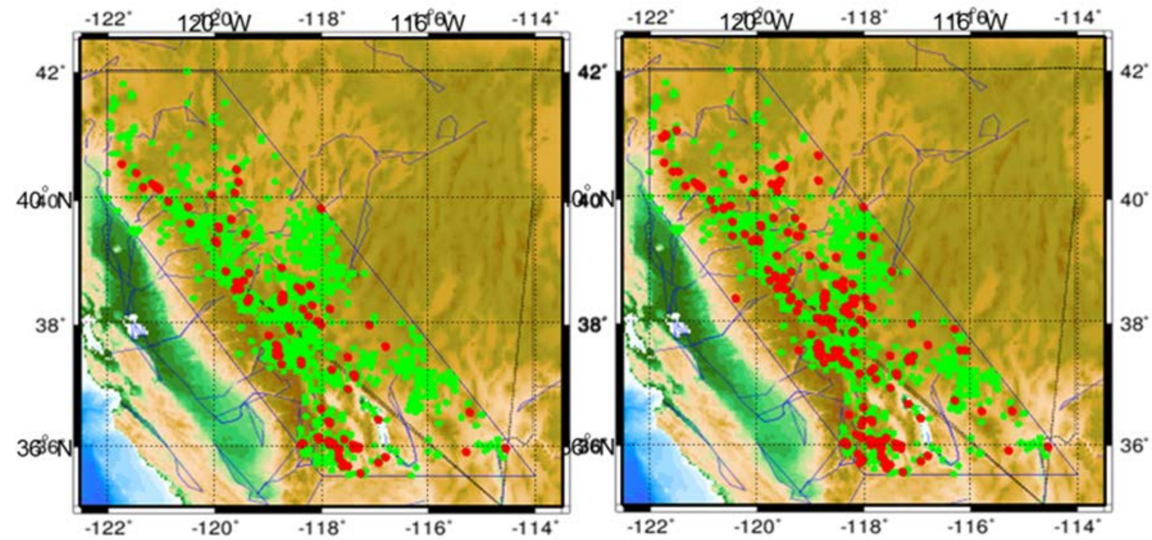

Figure 60: CS analysis of the Walker Lane Belt (WLB) sub-region for M3.5+ seismic events contained within the blue polygon. Left; 2007-2008 date cutoff, Right; 1999-2000 date cutoff.

Walker Lane Belt

2007-2008 Date Cutoff

For all of the events in the 2007-2008 Post-Cat for the WLB, the locations of 164 out of 207 are successfully forecasted, a hit rate of 79.2%. The Pre-Cat radius is 5.57 km (Figure 60a).

There were only six M5+ events in this catalog, and five of them were hits, an 83.3% success rate. There were no M6+ events.

1999-2000 Date Cutoff

The hit rate for the 1999-2000 date cutoff was almost exactly the same as the percentage for the 2007-2008 case. Out of 408 events, 324 were forecasted; a success rate of 79.4%. The Pre-Cat radius is 5.6 km (Figure 60b).

Starting at M5+, the success rate went down slightly. Eight of ten M5+ events were forecasted for an 80.0% success rate.

There is a bit of fluctuation in the higher magnitudes of the WLB's recurrence plot (Figure 61a) where the data does not follow the best-fit line well. I chose to make the best-fit plot from M3.5+ to M5.5+ (Figure 61b), cutting out the fluctuation at the higher magnitudes. The estimated recurrence intervals are:

R_4 = 0.140 years (51 days)

R_5 = 0.671 years (245 days)

R_6 = 5.58 years

R_7 = 51.0 years

Based on the other recurrence intervals, my extrapolated estimate for the M8+ recurrence interval is:

$R_8 \approx$ 500 years

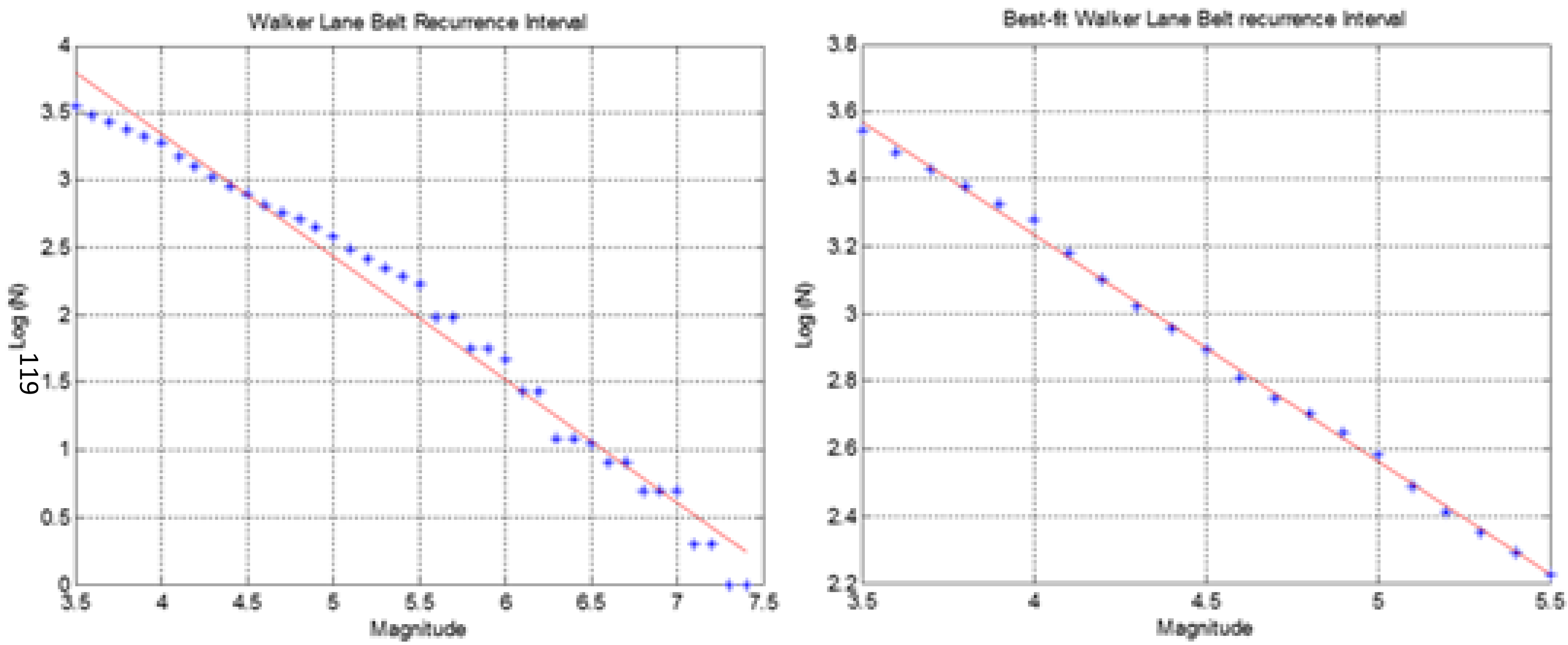

Figure 61: Recurrence plots for the Walker Lane Belt (WLB) sub-region. Left: entire catalog, right: best-fit magnitude range plot.

CS Analysis of the Western Intraplate Hinterland Region (WHR)

Analysis of the WHR

2007-2008 Date Cutoff

For M3.5+ seismic events in the WHR region, the locations of 131 out of 157 were successfully forecasted, a hit rate of 83.4%. This is higher than a few plate boundary sub-regions, despite being an "intraplate" region. The WHR has a higher hit percentage than the GR and the SAN sub-regions as well as the WLB. The Pre-Cat radius is 13.6 km (Figure 62a).

There were two M5+ events, one of which was a hit. There was a M6+ event, but it was not a hit.

1999-2000 Date Cutoff

The success rate for the 1999-2000 date cutoff was a little lower than the 2007-2008 value. Out of 353 events 278 were hits, a success rate of 78.7%. For the 1999-2000 catalog, the GR and the SAC sub-regions showed lower hit percentages than the WHR region despite being plate boundary sub-regions. The pre-Cat radius was 15.1 km (Figure 62b).

The success rate for M5+ events was quite low though. Only eight of thirteen events were hits. This is a hit rate of 61.5%. Again, there was a single M6+ event that was not successfully forecasted.

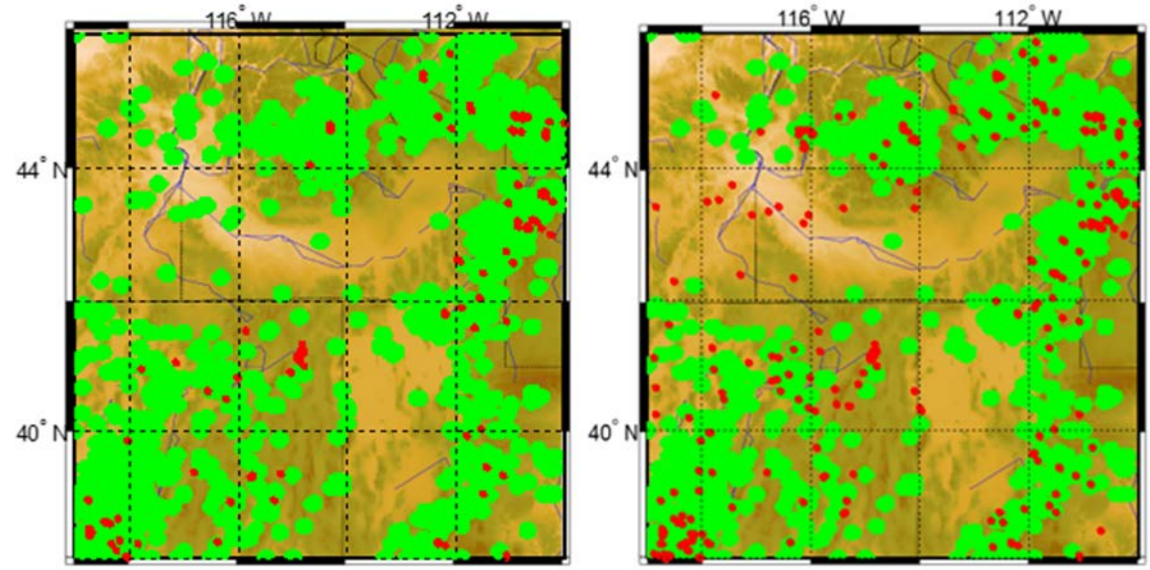

Figure 62: CS analysis of the Western Intraplate Hinterland Region (WHR) region for M3.5+ seismic events. Left; 2007-2008 date cutoff, Right; 1999-2000 date cutoff.

The recurrence plot for the WHR follows a clear linear pattern (Figure 63a). There is a sharp drop in seismicity at the high end of the magnitude range, but the lower end shows a good fit to the mid-magnitude seismicity. The best-fit recurrence plot goes from M3.5+ to M7+ (Figure 63b). The estimated recurrence intervals for the WHR region are:

R_4 = 0.203 years (74 days)

R_5 = 1.02 years

R_6 = 7.19 years

R_7 = 42.5 years

My extrapolated estimate of the recurrence interval for M8+ events is:

$R_8 \approx$ 255 years

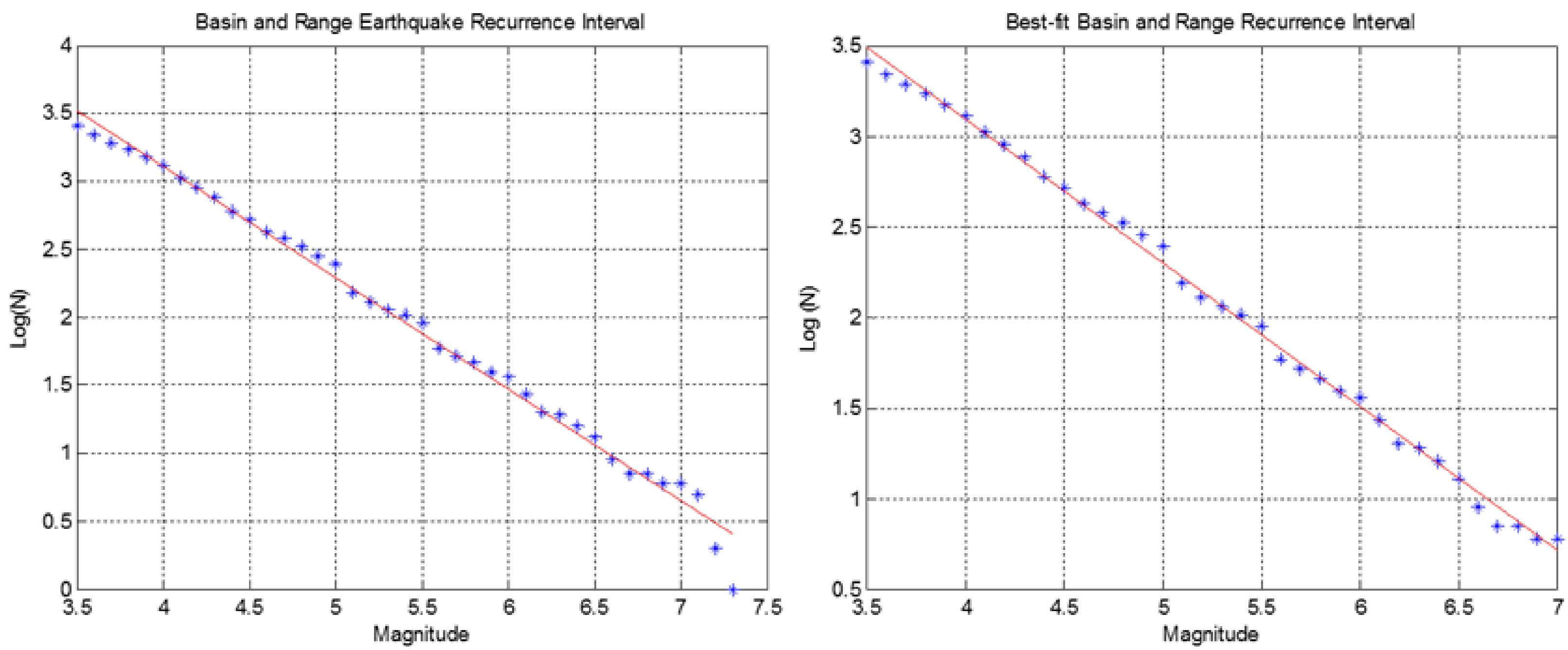

Figure 63: Recurrence plots for the Western Hinterland (WHR) region. Left; entire catalog, right; best-fit magnitude range plot.

Analysis of the Smaller Western Intraplate Hinterland Sub-regions

East Snake River Plain

2007-2008 Date Cutoff

The ESRP has an 80.8% hit rate for M3.5+ events. Of the 52 Post-Cat events, the locations of 42 were successfully forecasted. The Pre-Cat radius is 6.82 km (Figure 64a). There were no Post-cat events of M5+.

1999-2000 Date Cutoff

The hit rate for this date cutoff was about 1% higher than the 2007-2008 cutoff value. Locations of 72 of 88, or 81.8% of the earthquakes were forecasted successfully (Figure 64b).

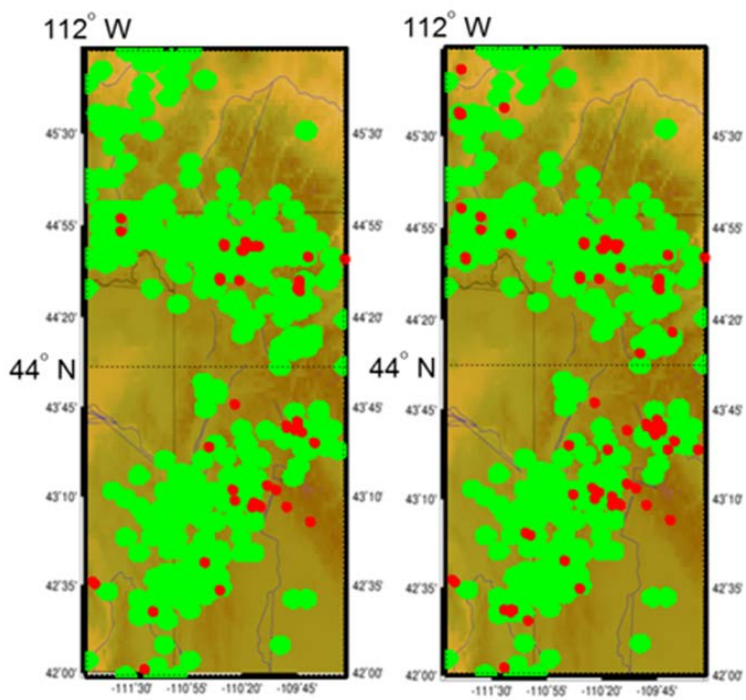

Figure 64: CS analysis of the east Snake River Plain (ESRP) sub-region for M3.5+ seismic events. Left; 2007-2008 date cutoff, Right; 1999-2000 date cutoff.

One of two Post-Cat events of M5+ were forecasted successfully. There were no M6+ events in the Post-Cat.

The recurrence plot for the ESRP is not very linear. There is a bit of a negative deviation from a linear trend in the mid-magnitudes, meaning there were less events than the best-fit line would have occurring for the time period, between M5+ and M5.7+ (Figure 65a). The best-fit plot for the ESRP goes from M3.5+ to M6.5+, despite the slump in the middle (Figure 65b). The estimated recurrence intervals for the ESRP are:

R_4 = 0.806 years (294 days)

R_5 = 5.09 years

R_6 = 32.1 years

There is only a single M7+ event in the catalog so the recurrence interval for M7+ events cannot be accurately found. My extrapolated estimate is:

$R_7 \approx$ 190 years

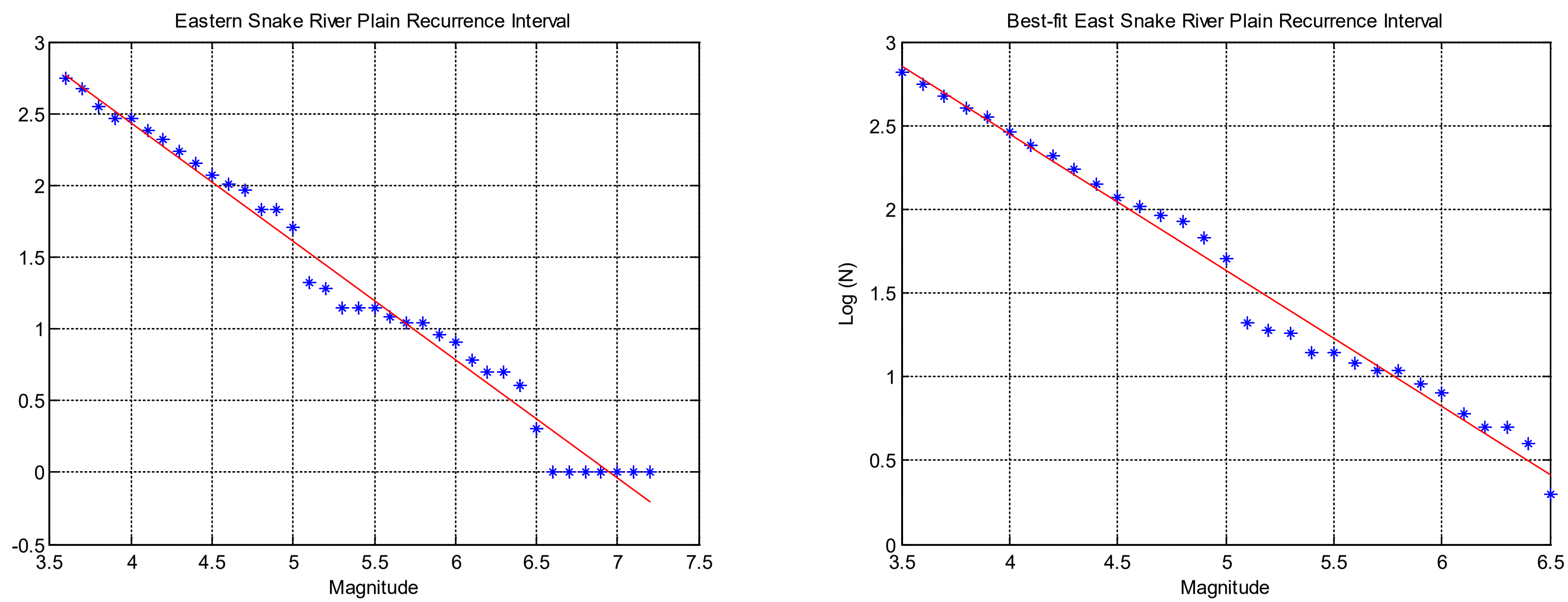

Figure 65: Recurrence plots for the east Snake River Plain (ESRP) sub-region. Left: entire catalog, right: best-fit magnitude range plot.

Northwest Snake River Plain

2007-2008 Date Cutoff

The NWSRP sub-region had very few Post-Cat earthquakes in the 2007-2008 catalog. There were only 14 events. The locations of all 14 events were successfully forecasted. The Pre-cat radius is 15.0 km (Figure 66a). There were no M5+ events for this set of analyses.

1999-2000 Date Cutoff

There was a 500% increase in the number of Post-Cat earthquakes just by doubling the Post-cat date range. There were 72 Post-cat earthquakes, 56 of which were

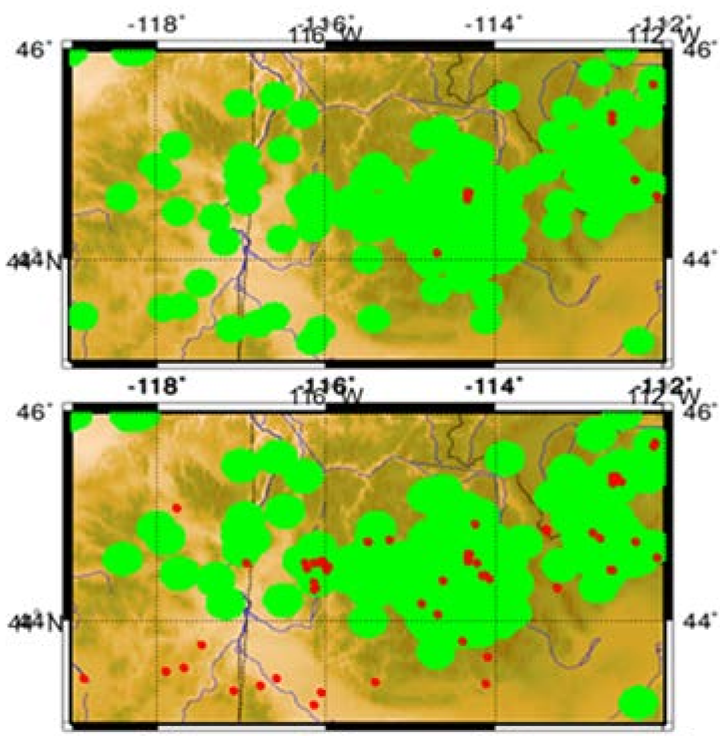

Figure 66: CS analysis of the northwestern Snake River Plain (NWSRP) sub-region for M3.5+ seismic events. Top; 2007-2008 date cutoff, Bottom; 1999-2000 date cutoff.

successfully forecasted. This is a hit rate of 77.8%. The Pre-cat radius is 18.6 km (Figure 66b).

There were four M5+ earthquakes, and only two of which were forecasted successfully. There were no M6+ events.

The recurrence plot for the NWSRP is linear until M6.2+ where it has high-end roll-off (Figure 67a). The best-fit plot for the NWSRP sub-region goes from M3.5+ to M6.1+ (Figure 67b). The estimated recurrence intervals are:

$$R_4 = 1.34 \text{ years}$$

$$R_5 = 9.05 \text{ years}$$

$$R_6 = 63.7 \text{ years}$$

There was only a single M7+ event, so the recurrence interval cannot be accurately estimated, but after extrapolation I estimate it to be:

$$R_7 \approx 445 \text{ years}$$

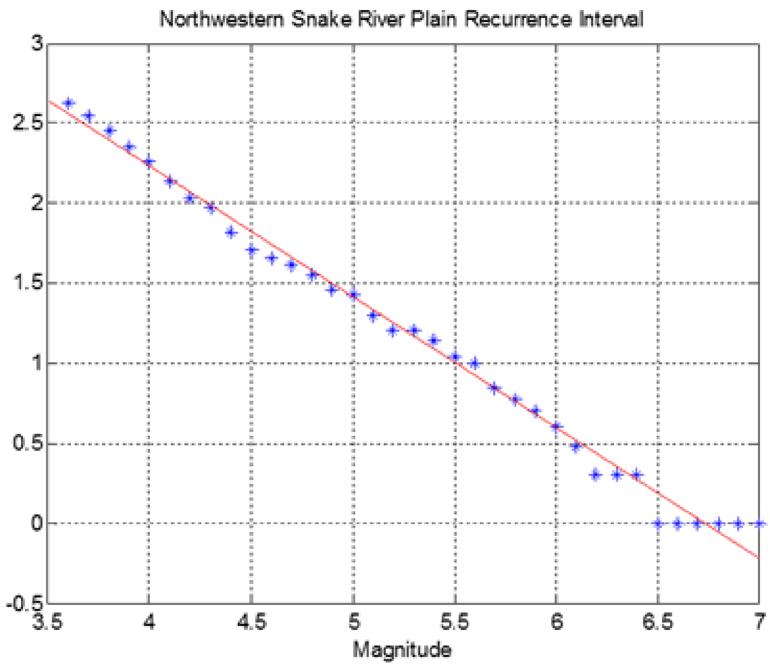

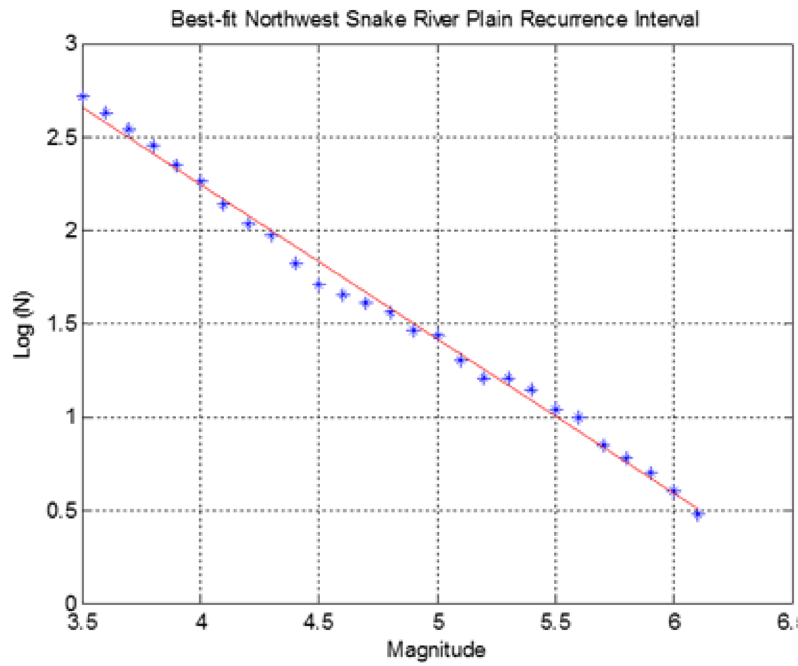

Figure 67: Recurrence plots for the northwestern Snake River Plain (NWSRP) sub-region. Left; entire catalog, right; best-fit magnitude range plot.

Wasatch Fault Zone

The WAS is the sub-region that shows the lowest hit percentages of any sub-region (Table 2 and Table 3 above) in this study. There were more misses than hits, or equal amounts of each on every analysis.

2007-2008 Date Cutoff

The 2007-2008 date cutoff for the WAS of M3.5+ events showed the lowest hit percentage for any sub-region. Only one of 16 events was a hit, just 6.3%. No other sub-

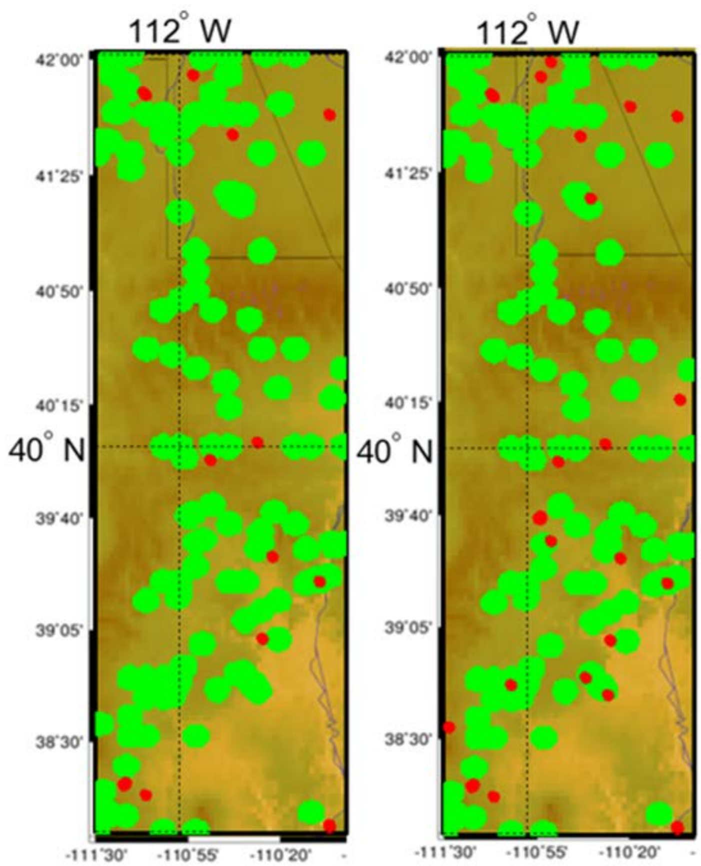

Figure 68: CS analysis of the Wasatch Fault Zone (WAS) sub-region for M3.5+ seismic events. Left; 2007-2008 date cutoff, Right; 1999-2000 date cutoff.

region, even the intraplate sub-regions come close to this value. The Pre-Cat radius is 7.03 km (Figure 68a). There were no M5+ events.

1999-2000 Date Cutoff

The hit percentage for the 1999-2000 date cutoff was a bit higher than for the 2007-2008 cutoff value. Of the 28 Post-cat events six were successfully forecasted, a 21.4% hit rate. This is still the lowest of any 1999-2000 date cutoff outcomes. There were still no M5+ events in the Post-cat. The Pre-Cat radius is 7.04 km (Figure 68b).

The recurrence plot for the WAS is not very linear and a best-fit plot wasn't calculated because the seismicity of this sub-region did not follow a linear pattern for the magnitude range of this study (Figure 69). The estimated recurrence intervals for the WAS are:

$$R_4 = 2.55 \text{ years}$$

$$R_5 = 7.19 \text{ years}$$

$$R_6 = 63.7 \text{ years}$$

It is difficult to estimate the recurrence interval for M7+ events. My extrapolated estimate is:

$$R_7 \approx 500 \text{ years}$$

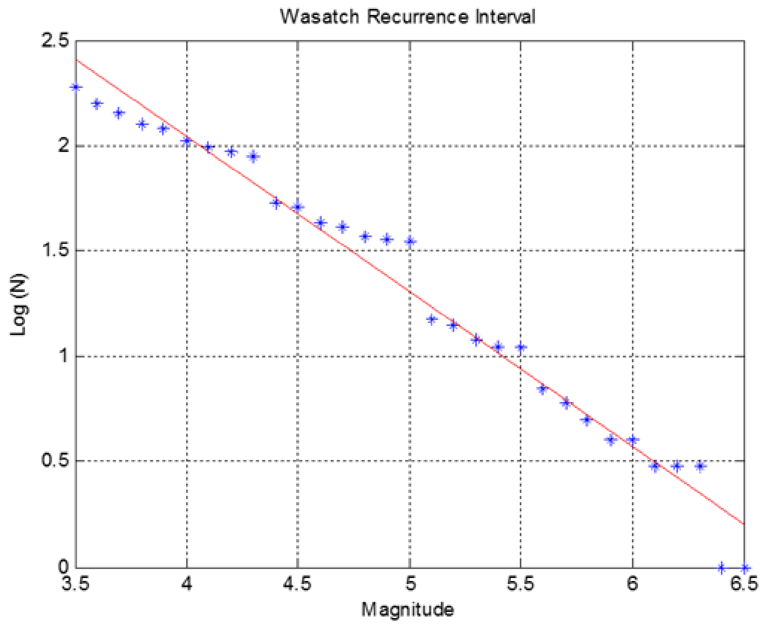

Figure 69: Recurrence plot for the Wasatch fault zone (WAS) sub-region. A best-fit plot was not possible for the WAS.

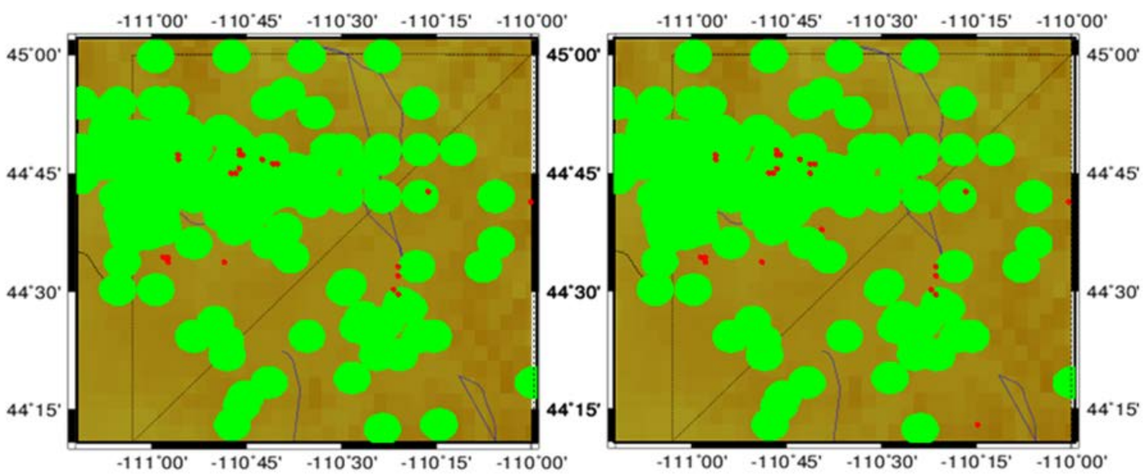

Figure 70: CS analysis of the Yellowstone (YS) sub-region for M3.5+ seismic events. Left; 2007-2008 date cutoff, Right; 1999-2000 date cutoff.

Yellowstone

2007-2008 Date Cutoff

Of the 24 events in the Post-Cat for the YS sub-region, 17 are hits, a hit rate of 70.8%. The Pre-cat radius is 3.86 km (Figure 70a). There are no M5+ events.

1999-2000 Date Cutoff

There were only four more events in this Post-Cat than there were in the 2007-2008 cutoff Post-Cat, even though the date range was doubled. Of the 28 events, 17 were successfully forecasted, a hit rate of 60.7%. Out of the four new earthquakes none were successfully forecasted. There were no M5+ events. The Pre-Cat radius is still 3.86 km (Figure 70b).

The recurrence plot for Yellowstone deviated from a linear pattern starting at M5+ (Figure 71a). The best-fit recurrence plot goes from M3.5+ to M5+ (Figure 71b). The estimated recurrence intervals for Yellowstone are:

$$R_4 = 2.12 \text{ years}$$

$$R_5 = 9.69 \text{ years}$$

$$R_6 = 63.7 \text{ years}$$

There is only a single M7+ event. My estimate for the recurrence interval of M7+ events is:

$$R_7 \approx 380 \text{ years}$$

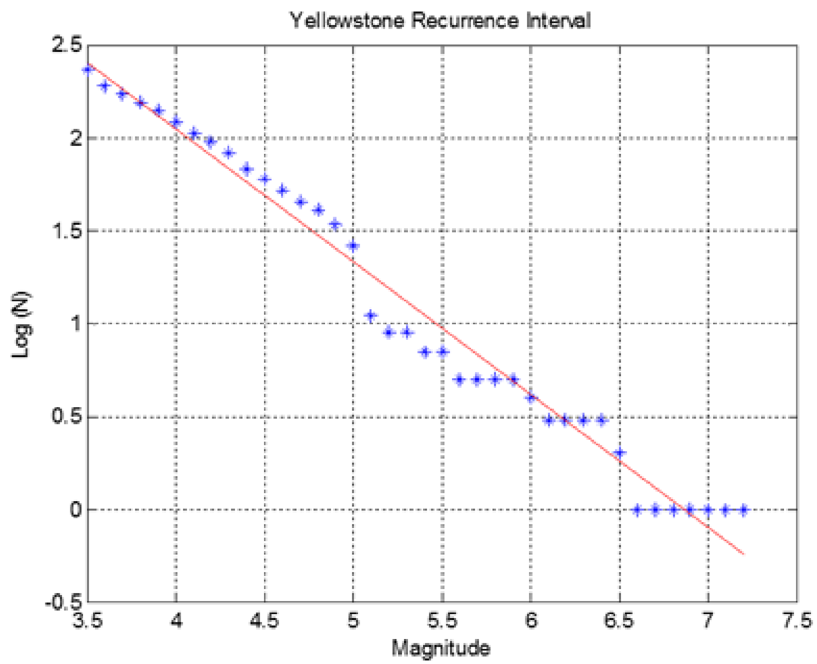

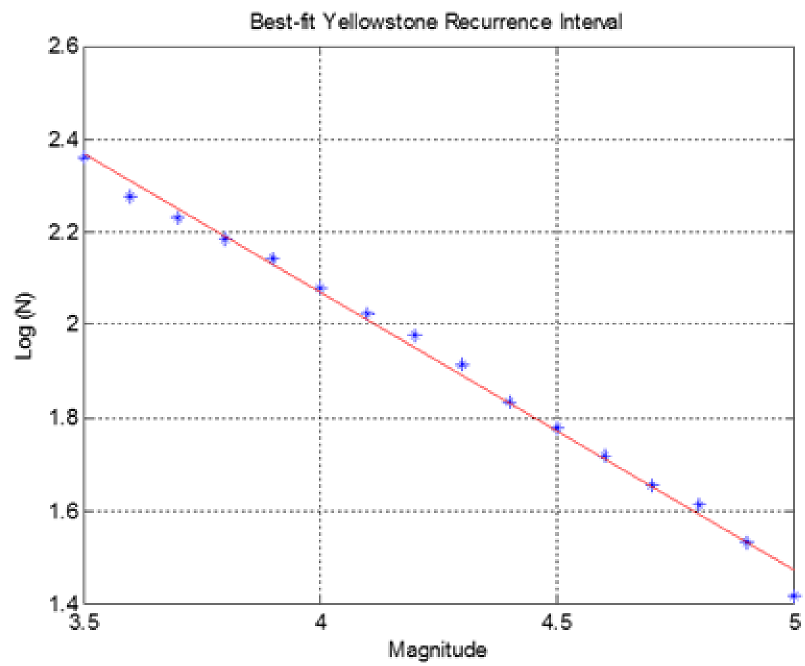

Figure 71: Recurrence plots for the Yellowstone (YS) sub-region. Left; entire catalog, right; best-fit magnitude range plot.

	NJDF	SJDF	WHR	NSA	SSA	EXP	YS	BFZ	MFZ	GR	SEA	WAS	ESRP	NWSR	CAS	ESA	SAN	SAC	SAB	SAS	WLB
NJDF	0.00																				
SJDF	0.32	0.00																			
WHR	0.05	0.09	0.00																		
NSA	0.14	0.23	0.81	0.00																	
SSA	0.18	0.69	0.96	0.89	0.00																
EXP	0.46	0.70	0.34	0.80	0.43	0.00															
YS	0.18	0.22	0.48	0.30	0.18	0.27	0.00														
BFZ	0.42	0.65	0.36	0.84	0.39	0.96	0.28	0.00													
MFZ	0.18	0.26	0.98	0.50	0.16	0.42	0.48	0.44	0.00												
GR	0.03	0.04	0.22	0.08	0.03	0.07	0.86	0.07	0.23	0.00											
SEA	0.44	0.50	0.78	0.60	0.45	0.56	0.81	0.57	0.78	0.67	0.00										
WAS	0.00	0.00	0.00	0.00	0.00	0.00	0.00	0.00	0.00	0.00	0.00	0.00									
ESRP	0.23	0.30	0.84	0.47	0.22	0.41	0.60	0.42	0.84	0.63	0.88	0.00	0.00								
NWSR	0.94	0.84	0.48	0.69	0.92	0.75	0.28	0.74	0.50	0.85	0.50	0.00	0.45	0.00							
CAS	0.70	0.87	0.50	0.85	0.73	0.97	0.30	0.94	0.54	0.89	0.57	0.00	0.48	0.79	0.00						
ESA	0.02	0.03	0.80	0.33	0.00	0.25	0.41	0.27	0.86	0.86	0.73	0.00	0.71	0.52	0.53	0.00					
SAN	0.22	0.30	0.98	0.52	0.21	0.44	0.51	0.46	0.97	0.73	0.80	0.00	0.87	0.50	0.54	0.83	0.00				
SAC	0.45	0.61	0.65	0.91	0.47	0.80	0.36	0.82	0.69	0.86	0.65	0.00	0.60	0.67	0.82	0.72	0.68	0.00			
SAB	0.21	0.31	0.90	0.58	0.20	0.48	0.45	0.50	0.92	0.80	0.75	0.00	0.78	0.53	0.59	0.96	0.90	0.75	0.00		
SAS	0.70	0.88	0.13	0.35	0.68	0.59	0.20	0.55	0.22	0.96	0.48	0.00	0.27	0.86	0.82	0.99	0.26	0.56	0.26	0.00	
WLB	0.02	0.03	0.62	0.14	0.01	0.11	0.62	0.12	0.65	0.66	0.92	0.00	0.90	0.35	0.28	0.34	0.71	0.38	0.57	0.02	0.00

Table 4: P-values for the 2007-2008 date cutoff. Values that are statistically significant at the 95% confidence interval are shown in red lettering and blue-backed rectangles. Sub-region initials shown in green rectangles.

	NJDF	SJDF	WHR	NSA	SSA	EXP	YS	BFZ	MFZ	GR	SEA	WAS	ESRP	NWSR	CAS	ESA	SAN	SAC	SAB	SAS	WLB
NJDF	0.00																				
SJDF	0.18	0.00																			
WHR	0.00	0.02	0.00																		
NSA	0.05	0.22	0.94	0.00																	
SSA	0.31	0.69	0.99	0.90	0.00																
EXP	0.86	0.51	0.99	0.19	0.77	0.00															
YS	0.14	0.19	0.47	0.24	0.16	0.15	0.00														
BFZ	0.53	0.88	0.04	0.44	0.82	0.67	0.18	0.00													
MFZ	0.02	0.06	0.86	0.15	0.03	0.03	0.53	0.06	0.00												
GR	0.00	0.00	0.00	0.00	0.00	0.00	0.23	0.00	0.00	0.00											
SEA	0.80	0.01	0.45	0.86	0.90	0.84	0.29	0.95	0.42	0.00	0.00										
WAS	0.00	0.00	0.00	0.00	0.00	0.00	0.00	0.00	0.00	0.00	0.00	0.00									
ESRP	0.23	0.39	0.74	0.58	0.30	0.27	0.41	0.37	0.67	0.00	0.64	0.00	0.00								
NWSR	0.15	0.25	0.92	0.38	0.19	0.17	0.55	0.24	0.98	0.01	0.49	0.00	0.75	0.00							
CAS	0.09	0.18	0.88	0.30	0.13	0.12	0.55	0.18	0.99	0.00	0.45	0.00	0.71	0.02	0.00						
ESA	0.01	0.06	0.26	0.39	0.01	0.03	0.31	0.11	0.28	0.00	0.70	0.00	0.80	0.53	0.45	0.00					
SAN	0.12	0.27	0.67	0.49	0.18	0.16	0.38	0.26	0.59	0.00	0.63	0.00	0.99	0.71	0.66	0.75	0.00				
SAC	0.00	0.00	0.00	0.00	0.00	0.00	0.55	0.00	0.01	0.25	0.02	0.00	0.01	0.04	0.03	0.00	0.00	0.00			
SAB	0.13	0.31	0.47	0.59	0.19	0.17	0.33	0.31	0.03	0.00	0.70	0.00	0.86	0.59	0.53	0.94	0.84	1.00	0.00		
SAS	0.83	0.41	0.99	0.11	0.71	1.00	0.15	0.63	0.98	0.00	0.84	0.00	0.25	0.16	0.11	1.00	0.14	0.00	0.14	0.00	
WLB	0.01	0.03	0.91	0.13	0.01	0.01	0.45	0.04	0.78	0.00	0.20	0.00	0.80	0.87	0.83	0.30	0.73	1.00	0.52	0.01	0.00

Table 5: P-values for the 1999-2000 date cutoff. Values that are statistically significant at the 95% confidence interval are shown in red lettering and blue-backed rectangles. Sub-region initials shown in green rectangles.

Statistical Significance Tests

Two-tailed statistical significance tests were conducted, and analyzed using a 95% level of statistical significance, in order to ascertain the extent to which levels of CS predictability for certain sub-regions are different from others. Is the level of CS predictability of a certain sub-region significantly higher or lower than another? To address this question, each sub-region was compared to every other sub-region using the Post-Cat earthquakes in each of their respective catalogs. The hit percentages used in these calculations were the hit percentages for M3.5+ events, because the Post-Cats for that magnitude cutoff had sufficient numbers of events to make a statistical significance analysis meaningful.

From Tables 4 and 5 it can be seen that the 1999-2000 date cutoff produced a higher number of statistically significant differences in CS predictability between specific sub-regions than the 2007-2008 date cutoff. This might be due to the fact that the 1999-2000 date cutoff contains more Post-Cat earthquakes. For both date cutoffs, the Wasatch fault zone (WAS) had significantly lower levels of CS predictability than any other sub-region analyzed in this study.

In the 2007-2008 analysis (Table 4) we can see that the WHR does not show a significantly lower level of CS predictability than any of the other large sub-regions, and does not have a significantly lower level of CS predictability than either the ESA sub-region, representing the San Andreas fault, or the CAS and SEA sub-regions representing the subduction zone in this study. The only sub-region that was part of either the SAF or the Cascadia region that was significantly different than the WHR was the San Andreas North sub-region, where the level of CS predictability for the WHR was actually higher than the SAN.

The 1999-2000 date cutoff (Table 5) produced more statistically significant sub-region p-value combinations than the 2007-2008 analysis (Table 4), again, possibly due to the greater number of Post-Cat earthquakes in the catalogs. In this set of analyses, the WAS, as well as the Gorda Ridge (GR) and San Andreas central (SAC), showed significantly lower levels of CS predictability than almost every other sub-region (exceptions being the combination of the GR with SAC or YS sub-regions). The WHR region was shown to have a significantly lower level of CS predictability than the northern Juan de Fuca and southern Juan de Fuca sub-regions, as well as the southern San Andreas sub-region, and also significantly lower CS predictability than the SAC and SAS sub-regions. This would suggest that the WHR level of CS predictability is lower than the subduction zone and parts of the SAF analyzed in this study, which would confirm the third hypothesis of this study; that the WHR region would show the lowest level of CS predictability of the three tectonic regions.

Discussion

The Entire Western United States

The analyses for the entire WUS show where most of the seismicity in the study area is located. As one would expect from plate tectonic principles, the majority of the seismicity occurs along or near the plate boundaries, primarily in the northern and southern ends of the Cascadia region, and the southern half of the SAF.

This set of analyses can also show us where the majority of the larger (M5+) earthquakes take place. For the most part, M5+ events are confined to the same three areas listed above, but are more abundant in the Cascadia region. There are several that occurred along the SAF, mostly in the SSA sub-region, and a few scattered events in the WHR region.

For the entire WUS, the level of CS predictability was high. The 2007-2008 date cutoff produced a 96.6% hit rate for all M3.5+ events, and a 97.1% hit rate for M5+ events. The 1999-2000 date cutoff produced slightly lower percentages, 93.9% for M3.5+ earthquakes and 93.6% for M5+ earthquakes.

Why are both these values less than their 2007-2008 counterparts? The first answer to come to mind is that the difference might be random variation. The results of this study show that the earthquakes that came after 2007 tend to occur where the earthquakes between years 2000-2007 occurred. In contrast, prior to the year 2000 earthquakes had not occurred in those areas. This level of variation in earthquake occurrence is not surprising given the typical level of unpredictable variation in the time dependence of earthquakes (Shimazaki and Nakata, 1980; Anagnos, 1984). Spatial and temporal patterns could vary between the two date cutoffs analyzed in this study, and the earthquakes that appeared in the 2007-2008 analysis could very well just show the migration of seismicity within the regions over time.

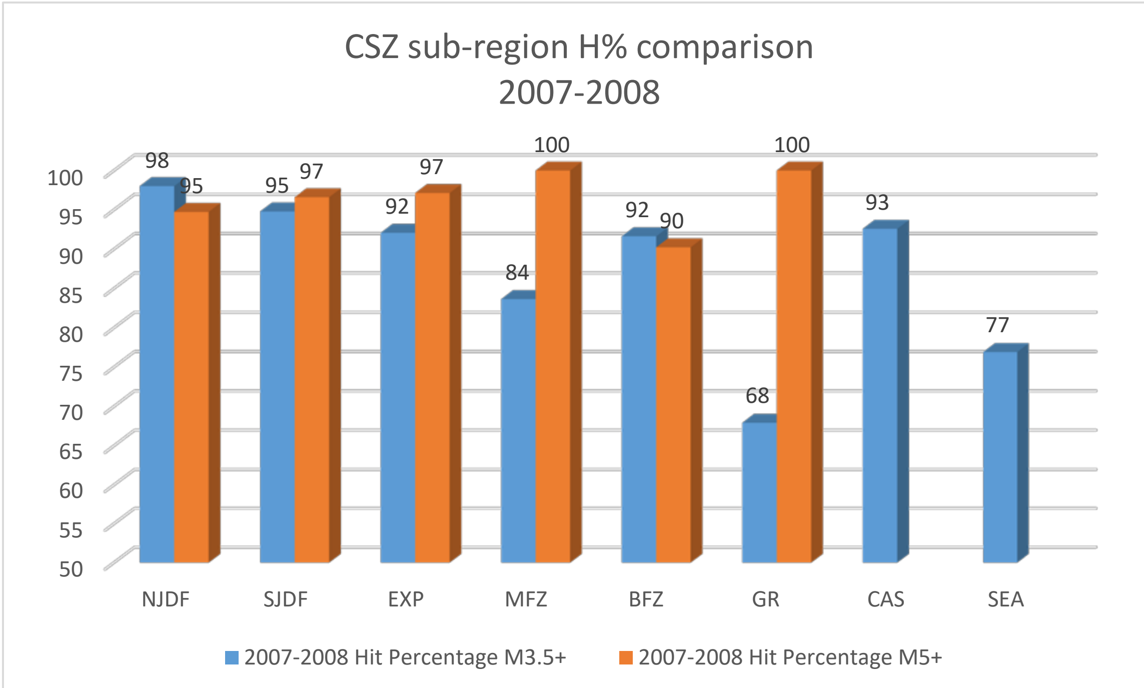

Figure 72: Hit percentages for M3.5+ and M5+ events for the sub-regions of the Cascadia region for the 2007-2008 date cutoff.

The results of this study show that for certain sub-regions, like the Gorda Ridge, the earthquakes that occurred after 2007 tended to occur where earthquakes occurred between the years 2000 and 2007, but that prior to 2000 earthquakes had not happened in those specific areas. An example of this can be found in Figure 39 (GR), looking at the southeast corners.

Varying the Post-Cat date range did not have much of an effect on the results for the WUS. Based on these CS results, it would appear that the earthquakes in the WUS were more “CS predictable” in the more recent years (2008-2014) analyzed here. However, the results for the WUS as a whole do not tell us which region, or sub-region of the WUS, has the highest level of CS predictability. It merely shows us that seismicity in the WUS does in general “delineate zones where future earthquakes are likely to occur.” (Kafka, 2002; Kafka and Levin, 2000).

In terms of the “Really Big One” along the CSZ - an M9 earthquake - my results for the recurrence intervals for the WUS are in good agreement with previous studies of Goldfinger et al. (2003). The recurrence interval I found for M9+ events is around 585-650 years (based on WUS and NJDF respectively). Goldfinger et al. (2003) found a 1-1 correlation between M9 events and offshore turbidites occurring every 655 years, which is within 10% of my result. Priest et al. (2014) found a recurrence interval of 530+ years; also within 10% of my result. Thus, the seismicity rate is seen to be consistent with the rate for very large earthquakes determined from offshore turbidites.

The Cascadia Region

The Cascadia region showed a wide range of results, some expected based on my hypotheses, some unexpected. Overall, the hit rates for both the northern Cascadia and southern Cascadia sub-regions are quite high. The CS hit percentages are a little higher for the NJDF than for the SJDF, but not significantly higher, as determined from the statistical significance tests (Tables 4 and 5). The majority of the earthquakes in the Cascadia region occurred on the plate boundaries, which is to be expected. What wasn’t expected was the range of hit percentages for the sub-regions since they are mostly on plate boundaries.

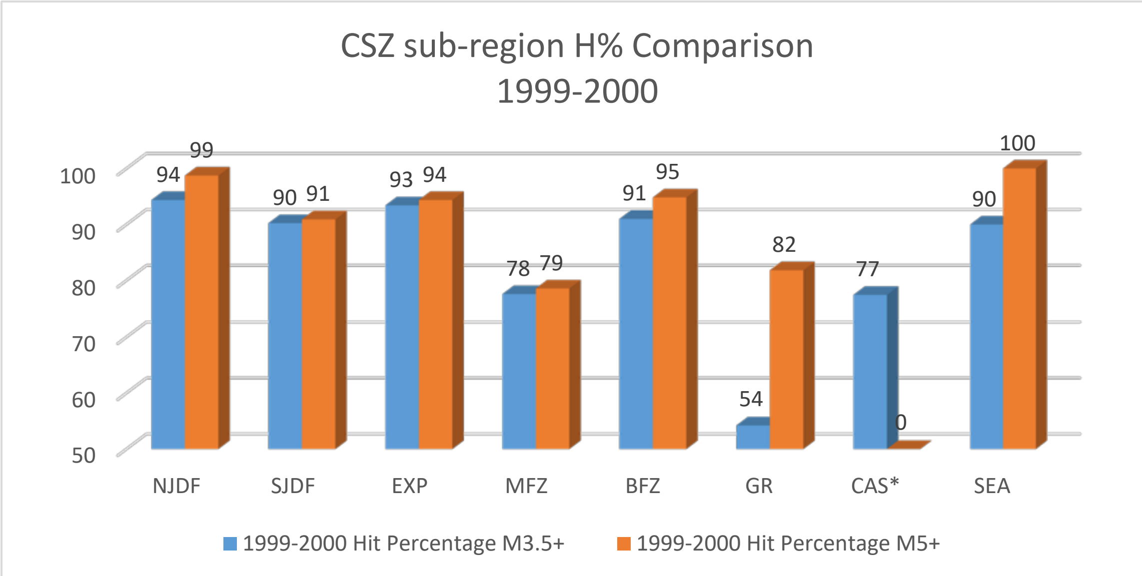

Figure 73: Hit percentages for M3.5+ and M5+ events for the sub-regions of the Cascadia region for the 1999-2000 date cutoff.

Going from the southern end of the Cascadia sub-regions to the north: the MFZ shows hit percentages of around 77.6-83.6% for all earthquakes M3.5+ (Figure 72, Figure 73). Next is the Gorda Ridge. Of all the sub-regions that were part of a major plate boundary this sub-region had the lowest hit percentages, even lower than some of the intraplate sub-regions, and lower than the WHR region overall (Figure 74). The 1999-2000 date cutoff results for the sub-regions are also shown in Figure 75, to better show how certain sub-regions CS results compare to others found by Kafka and his colleagues. What makes this ridge have such a low level of CS predictability? Looking at figure 39b, you can see that there is a length of the ridge that did not experience much seismicity before the year 2000. Many of the earthquakes that happened along this part of the ridge were not forecast successfully. This is likely what led to the low level of CS predictability for the Gorda Ridge for the 1999-2000 date cutoff.

The Blanco Fracture zone has hit percentages for both date ranges of about 90% (Figure 72, Figure 73). There was a slightly lower result for the 1999-2000 date cutoff. These results are around 10% higher than the MFZ, despite both being fracture zones. Why does one fracture zone show a higher level of CS predictability than the other?

Despite indicating where and when such differences are observed, CS can't answer this question as CS is, fundamentally, an empirical method, and it does not tell us *why* one ridge has a higher level of predictability than another. However, it might be that because of the relative motions between the plates bounded by each of the fracture zones, and because the motion on either side of the BFZ more closely resembles that of a classic strike-slip boundary, the BFZ has more focused seismicity than the MFZ. Also, the older, colder, more brittle crust along the BFZ could lead to more seismicity along this fracture zone. The seismicity would thus be highly localized and lead to higher levels of CS predictability.

The Juan de Fuca ridge connects the BFZ to the Sovanco fracture zone. In this study the Sovanco fracture zone is incorporated into the Explorer plate sub-region. Along the Juan de Fuca ridge there is almost no seismicity even though my catalog goes back over 200 years (space between areas 5 and 9 in Figure 19). This is the reason why the Sovanco fracture zone was not made into its own sub-region for this study. The only area with seismic activity along the Juan de Fuca ridge, disregarding the dozen or so Pre and Post-Cat earthquakes along the rest of the ridge, is at its northern end where it

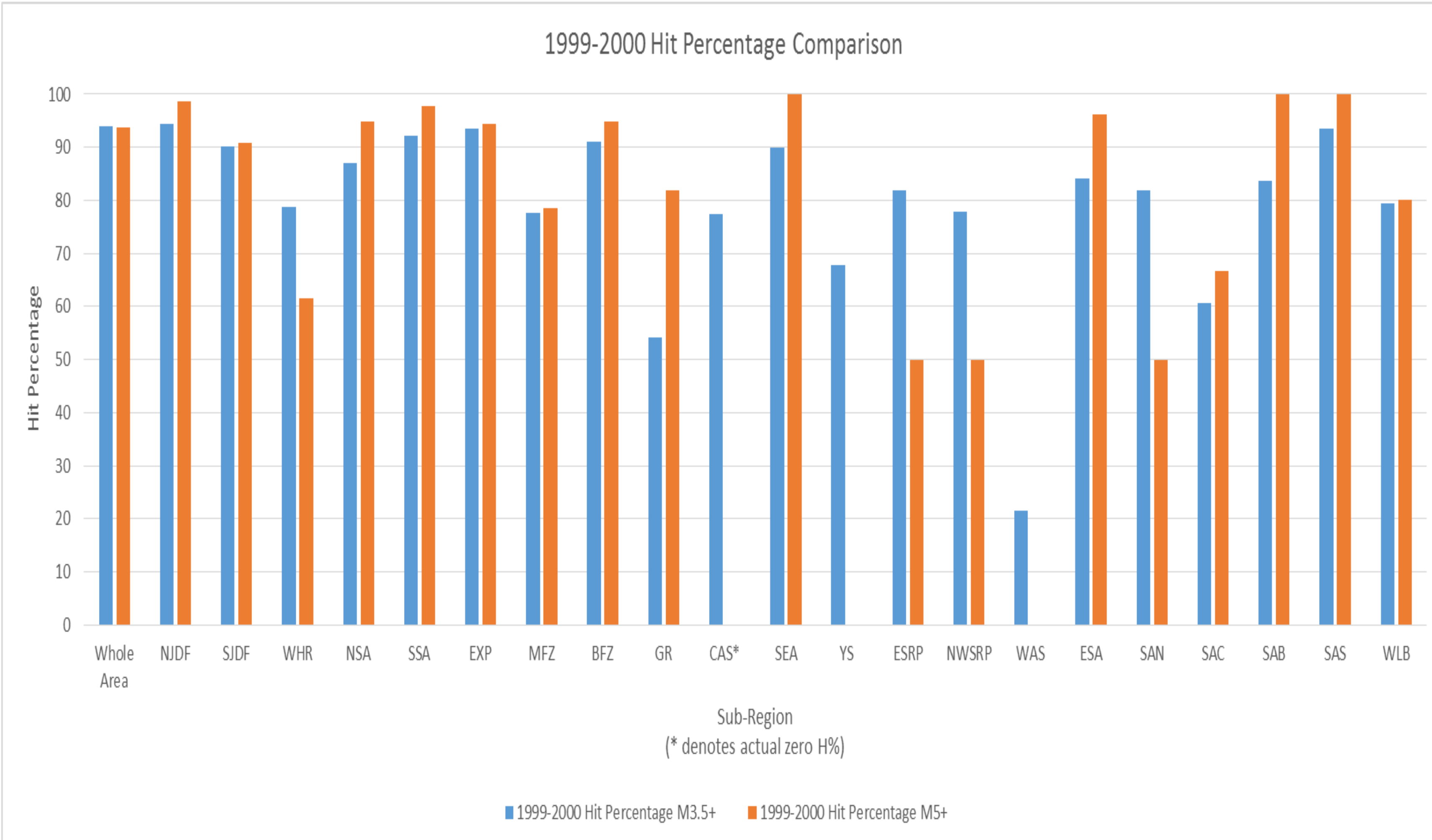

Figure 74: Hit percentages for all of the sub-regions for M3.5+ seismic events for the 1999-2000 date cutoff.

connects to the Sovanco fracture zone and the Nootka fault by way of a triple junction (Figure 32).

The Explorer plate sub-region is the northernmost of the Cascadia sub-regions. It includes ridge segments, transform faults, and part of the CSZ margin (Figure 32). This sub-region showed the highest rate of CS predictability of any Cascadia sub-region for M3.5+ events (Figure 72, Figure 73), most likely because of the highly localized areas of seismicity in this sub-region, and the high number of plate boundaries. Larger earthquakes (M5+) were forecasted quite well here, with 97.1% being hits in the 2007-2008 catalog, and 94.4% in the 1999-2000 catalog.

The most interesting thing about the Cascadia region is the variety of results we see along different types of plate boundaries in the region. The fracture zones differed in the percentage of hits by 10%. The ridges in the Cascadia region were either seismically quiet, or showed the lowest level of CS predictability of any sub-region situated on a plate boundary. Subducting slab earthquakes (sub-regions CAS and SEA) were of lower magnitude than the earthquakes along the ridges and fracture zones. Further, they showed a level of CS predictability higher than that of the GR, were statistically significantly higher in the 1999-2000 analyses, and were comparable to the fracture zone results. Breaking the Explorer plate sub-region down into smaller sub-regions based on the tectonic boundary would provide more insight as to whether or not ridges show a generally lower level of CS predictability than the fracture zones, and the subducting slab zones. These results demonstrate that there can be as much

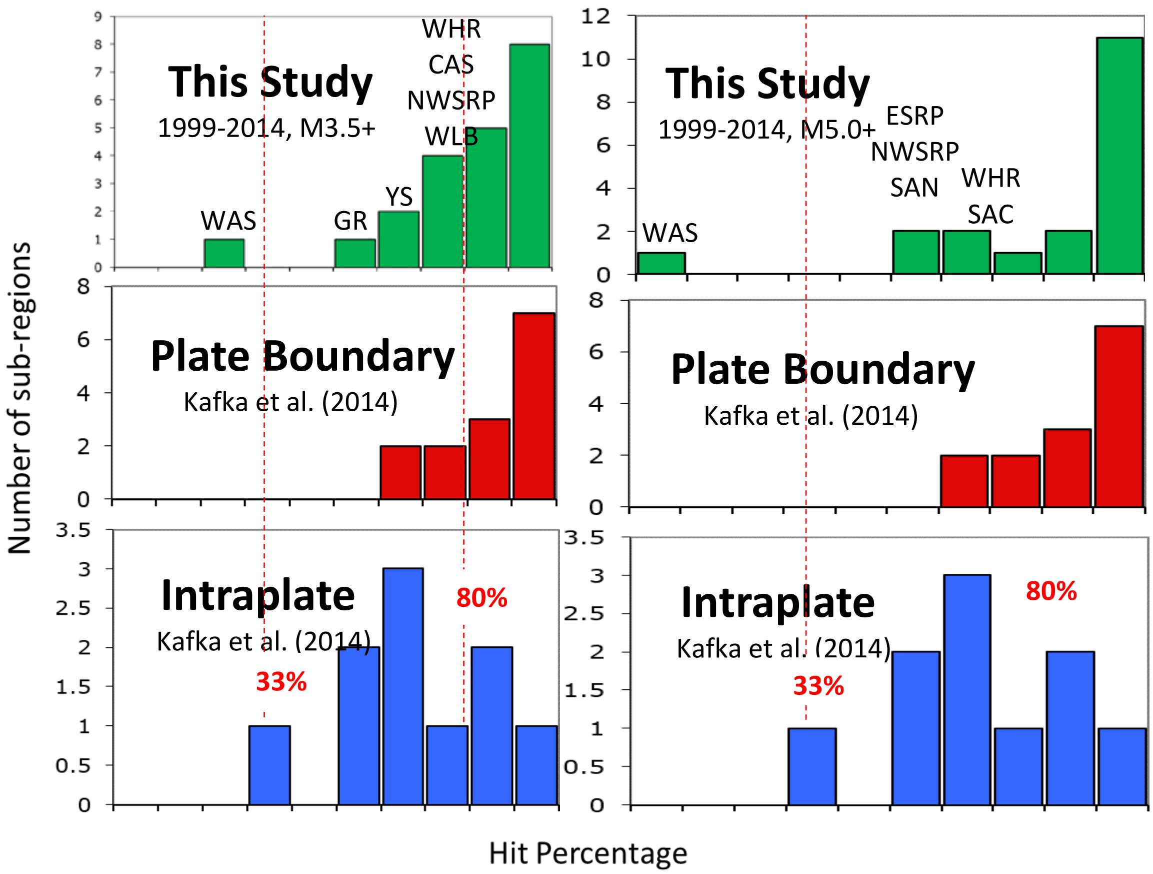

Figure 75: Histograms for the 1999-2000 date cutoff for M3.5+ (left) and M5+ (right) earthquakes, showing the number of sub-regions whose level of CS predictability fall within a given hit percentage range, such as the WAS sub-region falling within the 20-30% range for M3.5+ events. Results of this study are then compared to the results found in Kafka (2014) for plate boundary and intraplate regions around the world.

variation in CS predictability within plate boundary regions as there is between plate boundary and intraplate regions.

The southern Cascadia sub-region showed recurrence intervals that appeared to follow a Gutenberg-Richter slope of -0.85 to -0.90 rather than a slope of -1.0. M5 earthquakes occurred 7-8 times as often as M6 earthquakes in the SJDF sub-region during the time period within this study. The results I obtained for M8+ events were in agreement with a study by Priest et al. (2014), who found recurrence intervals for earthquakes rupturing certain portions of the Cascadia margin (Figure 10). I obtained a recurrence interval of 230 years, while Priest et al. (2014) found a recurrence interval of 200-240 years for rupture events at the southern end of the CSZ (Figure 10). Their study included all ruptures along the margin, 43 total events, over a 10,000 year period. So their recurrence interval is not only for M8+ events, but includes margin ruptures smaller than M8 as well. The specific magnitudes of the smaller events were not given by Priest et al. (2014). Removing the sub-M8 events left a recurrence interval along the margin of approximately 417 years. This would explain why we haven't seen a M8+ event since the supposed M9 earthquake of the year 1700. It is important to note that my analysis covers a much broader area than just the CSZ margin, so these results are only somewhat comparable to the findings of Priest et al. (2014).

The San Andreas Transform Region

The San Andreas Transform region, as defined here, is an area that includes not only the SAF, but the SAF's branch faults and the WLB. The inclusion of the area surrounding the SAF, to the west (ocean) and the east (Great Valley), may have led to exaggerated hit percentages for the region by artificially enlarging the Pre-Cat radius of the larger sub-regions. To counter this effect, when each of the smaller sub-regions for the SAF were created, they each included a polygon so as to include only earthquakes located inside each of the individual polygons, eliminating the extra space that could artificially pad the CS results. The polygons only include the SAF and its branch faults including the Hayward, North Creek, Calaveras, San Jacinto, and Elsinore faults, amongst others. By doing this, any earthquakes occurring in the Pacific Ocean, and earthquakes within the Great Valley of California were eliminated from the analyses. The area of each of the sub-regions was also reduced, therefore giving us a smaller Pre-Cat radius since the area covered by the Pre-Cat earthquakes remained at 33%, providing higher resolution results.

The SAF was divided into four segments based on fault geometry and the amount of creep occurring along certain portions of the fault as given by Wallace (1970) (Figure 14). Doing this allowed for individual results representing portions of the SAF, showing where there is a greater amount of seismicity, and more importantly, what sections of the SAF have a higher level of CS predictability. In one of the sub-regions (ESA) the SAF was not divided and was evaluated using CS from its northern to southern ends. This sub-region includes some major branch faults of the SAF including the Calaveras, Hayward, North Creek, Elsinore, and San Jacinto fault zones. The WLB was the final sub-region in the San Andreas Transform Region, and represents another area of strike-slip motion, but is different from the SAF in that it is a broader and discontinuous system of faults, and is farther away from the primary plate boundary than the SAF.

Combining the results of these analyses would lead to a comparison, and hopefully similar results, to those presented in the UCERF2 and UCERF3 earthquake analyses performed by the USGS for California. My results were similar to the results found in the UCERF models for California. My estimate of the rate for M5+ events is 5.6

events per year, UCERF2 had 5.8 per year, and UCERF3 has 8.3 per year. For M6.7+ earthquakes, like the 1994 Northridge, CA earthquake, which was a reference magnitude analyzed and discussed in the UCERF models, my results show an event of that magnitude happening once every 4.2 years, UCERF2 predicts these events to occur every 4.8 years, and UCERF3 suggests every 6.3 years. Thus my findings are in closer overall agreement with the UCERF2 findings than the newer UCERF3 findings.

	M5+ Events Per Year	M6.7+ Recurrence Interval (years)
This Study	5.6	4.2
UCERF2	5.8	4.8
UCERF3	8.0	6.3

Table 6: Summary of the comparisons between the findings of this study and the findings of UCERF2 and UCERF3 for M5+ and M6.7+ events along the San Andreas Fault.

In terms of recent earthquakes, between the years 2008-2014, the earthquake catalog used in this study shows there are 2-3 times more earthquakes in the southern half of the SAF than in the northern half. This is likely due to several reasons: 1) the WLB is included in the San Andreas region, and has a broader network of faults in the southern portion of the belt, 2) there are a greater amount of significant, long branch faults in the southern half of the San Andreas region, such as the San Jacinto and Elsinore fault systems (Figure 2; Field and Milner, 2008), 3) the southern half of the region contains the “Big Bend” which not only has transcurrent movement, but also has a significant compressive component leading to a greater number of earthquakes, and

4) the northern edge of Gulf of California rift zone is included in the southern half of the region.

The southern San Andreas sub-region ended up having a higher level of CS predictability than the northern San Andreas sub-region. The 2007-2008 date cutoff produced hit rates of 97.3% for the entire catalog and 96.8% for M5+ earthquakes. The 1999-2000 had a 92.1% hit rate for the entire catalog and 97.7% for M5+ events (Figure 74). Common to both sub-regions is that out of all the M5+ events for both sub-regions there was only a single event for each sub-region that was not forecasted successfully; 6 of 7 for the NSA and 18 of 19 for the SSA. Statistically, the two sub-regions are not

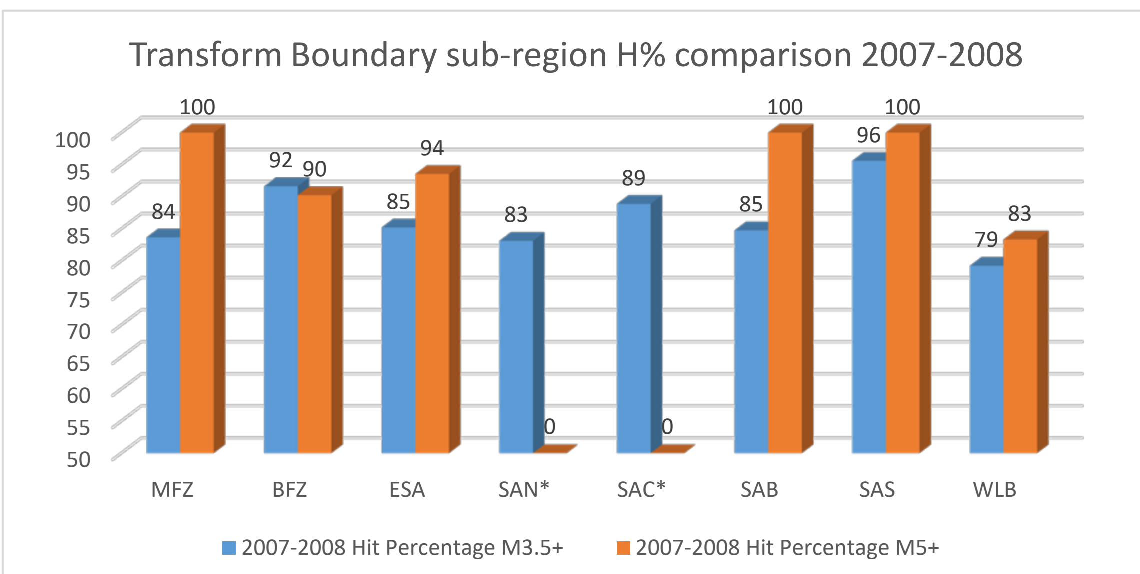

Figure 76: Hit percentage comparison for the smaller sub-regions that are part of a transform plate boundary, for the 2007-2008 date cutoff. Percentages for M3.5+ events shown in blue. Percentages for M5+ events shown in orange. Vertical scale exaggerated to show the subtle differences in hit percentages more clearly.

different, at least at the 95% level of significance (Tables 4 and 5), as their p-values were 0.89 and 0.90 for the 2007-2008 and the 1999-2000 analyses respectively.

Focusing on the SAF seismicity and eliminating the rest of California (Great Valley, Sierra-Nevadas, and part of the WLB) through the use of a polygon (Figure 50), the interpretation of the CS results is a little different. When considering the entire SAF there is only a success rate of 85.0% (1999-2000 analysis). For M5+ events this number increases to 93.6% and 96.1% for the 2007-2008 and 1999-2000 date cutoffs respectively. For both of the date ranges the same two Post-Cat earthquakes were not forecasted successfully.

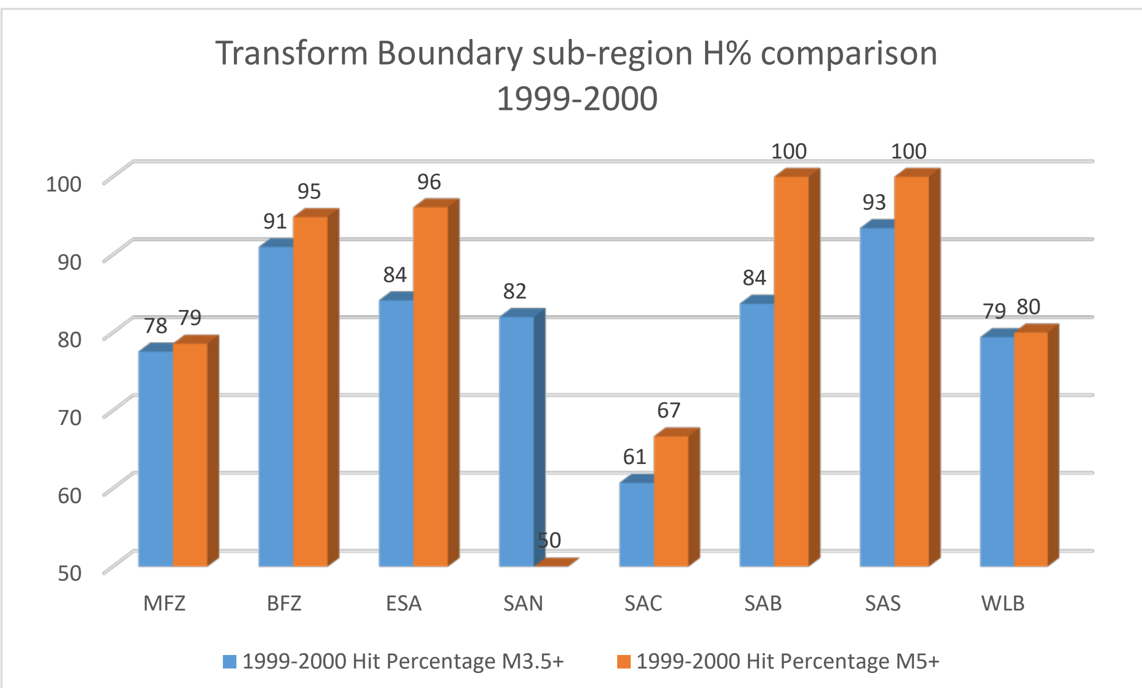

Figure 77: Hit percentage comparison for the smaller sub-regions that are part of a transform plate boundary, for the 1999-2000 date cutoff. Percentages for M3.5+ events shown in blue. Percentages for M5+ events shown in orange. Vertical scale exaggerated to show the subtle differences in hit percentages more clearly.

Breaking the SAF down further into four other sub-regions: the SAN, SAC, SAB, and SAS, provided insight into how CS predictability varies along the length of the SAF. The SAN, SAC, and SAB sub-regions all showed similar hit percentages for M3.5+ events for the 2007-2008 date cutoff (Figure 70). For M5+ events the hit percentages increased as we moved to the south. SAN was 0/1 and 1/2 for M5+ events for the 2007-2008 and 1999-2000 date cutoffs, respectively, the SAC was 0/1 and 4/6, and the SAB showed higher levels of CS predictability at 2/2 and 7/7. The SAB sub-region had a 100% success rate, but there were not that many earthquakes in that sub-region. Lastly, the SAS sub-region showed a very high level of CS predictability. Hit rates for the entire catalog were 95.6% and 93.4% for 2007-2008 and 1999-2000, respectively (Figure 76, Figure 77). What was more astonishing was the 100% success rate for the larger events of M5+. Both catalogs had a 100% success rate, with 27/27 and 36/36 hits.

Significance tests for the 2007-2008 date cutoff showed that, for the San Andreas regions, none of the levels of CS predictability were significantly different from one another. The tests for the 1999-2000 had a slightly different outcome. The level of CS predictability for the SAC sub-region was significantly lower than the SAN, SAB, and SAS sub-regions. The level of CS predictability for the SAN sub-region was also significantly lower than the level for the SAS sub-region. These analyses suggest that the two northernmost sub-regions of the SAF have significantly lower levels of CS predictability than the two southernmost sub-regions.

Another issue of concern regarding the SAF, specifically the area covered by the SAS sub-region, is the rate at which the larger events are occurring. There are 27 events in the 2008-2014 Post-Cat, and only 36 in the 2000-2014 Post-Cat. By doubling the Post-Cat date range, you would expect a doubling or near doubling of the number of

Sub-Region	M4+	M5+	M6+	Last EQ	Overdue	M7+	Last EQ	Overdue	M8+*	Overdue
Whole Area	0.03	0.14	0.8	2014	Yes	7.2	2010	No	70	Yes
NJDF	0.26	1.61	11.9	2014	No	90.0*	1946	No	650	
SJDF	0.13	0.64	4.0	2014	No	28.6	2005	No	230	Yes
WHR	0.20	1.02	7.2	2008	On Verge	42.5	1983	No	255	
NSA	0.08	0.45	2.6	2014	No	25.5	1954	Yes	255	No
SSA	0.10	0.64	4.0	2012	On Verge	25.5	2010	No	155	Yes
EXP	0.36	1.81	9.7	2012	No	50.0*	1929	Yes	250	
MFZ	0.49	2.44	9.5	2010	No* (but close)	63.8	1994	No	320	
BFZ	0.36	6.22	25.5	1942	Yes	102.0*	1872	Yes	410	
GR	0.72	4.04	20.2	2005	No	100.0*		Likely	500	
CAS	1.43	6.41	50.9	1942	Yes	400.0*	1872	No	3200	
SEA	3.77	10.20	42.6	2001	No	170.0*		Not Likely	680	
YS	2.12	9.69	63.7	1959	No	380.0*	1959	No	2280	
ESRP	0.81	5.09	32.1	1964	Yes	190.0*	1959	No	1150	
NWSRP	1.34	9.05	63.7	1983	No	445.0*	1983	No	4500	
WAS	2.55	7.19	63.7	1921	Yes	500.0*		Likely	4000	
ESA	0.05	0.26	1.5	2014	On Verge	12.8	2010	No	110	On verge* (7.9 fort Tejon in 1857, 1906 SF 7.8)
SAN	1.14	6.55	28.6	2014	No	128.0	1906	No* (but close)	575	
SAC	0.40	2.02	6.4	2004	Yes	128.0	1857	Yes* (6.9 in 1989)	1000	
SAB	0.26	1.61	8.1	1994	Yes	42.5	1992	No	210	
SAS	0.14	1.02	8.1	2010	No	84.5	2010	No	850	
WLB	0.14	0.67	5.6	1993	Yes	51.0	1954	Yes	500	

Table 7: List of recurrence intervals for M4+, M5+, M6+, M7+, and M8+ events for all sub-regions and for the entire WUS given in years. Columns in yellow represent the last earthquake of the magnitude range to the left of the yellow column (i.e. the first yellow column is the last year an M6+ event occurred in that sub-region), and whether or not that sub-region is overdue for that specific magnitude earthquake according to this study, and assuming that the characteristics of the past record of seismicity will be similar in the future. Blocks in red show the estimated recurrence interval for M8+ events in the ESA sub-region, and that the ESA sub-region, according to this study, is due for an M8+ event as of 2016, the year in which this thesis was written.

earthquakes. Either M5+ events in the SAS sub-region are becoming more frequent, or there had been a lull in activity in the years between 2000 and 2007. Alternatively, this could just be random variation. The answer to this might be found in future research by adding additional years to the Post-Cat date range and seeing how many events occur. If the M5+ earthquakes are becoming more frequent though, this might be a cause for concern for the people of southern California. An increase in activity could be the precursor to another, even larger, earthquake in the near future. It could, however, also mean that stress has been released along the SAF lowering the probability of a larger earthquake for the time-being. As pointed out in the recurrence interval analyses for the SAF in this study, there is approximately a 110 year recurrence interval for M8+ events along the SAF (Table 7). An increase in M5+ seismicity in recent years is consistent with the increase of M5+ event projections between UCERF2 (Field and Milner, 2008) and UCERF3 (Field, 2015) from 5.8 to 8.0 per year, respectively.

The WLB produced hit percentages similar to the SAN and SAC sub-regions, only around 80% success rates for the entire catalog. There were a number of M5+ events in the WLB, and for the most part they were forecasted successfully using the CS method. Five of six, and eight of ten were forecasted successfully for the 2007-2008 and 1999-2000 date cutoffs, respectively. Given the tectonic nature of the WLB - a network of left-stepping, although discontinuous, transform faults - a high level of CS predictability was expected. Perhaps due to the discontinuity of the left-stepping faults the level of CS predictability is lower than expected. The lower level of CS predictability could be caused by earthquakes moving from fault segment to fault segment as stress is released on one and moves to another.

The Western Intraplate Hinterland Region

The WHR region is unlike the other two regions analyzed here since it does not lie along a plate boundary. It is still an active seismic area, and an area of NW-SE directed extension. The Snake River Plain is a flat-lying area in the center of the WHR region. At the northern end of the Snake River Plain is Yellowstone, a sub-region in this study, and to its north and east, two other sub-regions - the NWSRP and ESRP. In the southeast corner of the region is the Wasatch Fault zone.

The WHR has the lowest hit percentages of any of the three regions, significantly so in the 1999-2000 analyses, at least in comparison to the NJDF and SJDF sub-regions (Table 5). Seismicity is concentrated in specific places (i.e. the four sub-regions listed

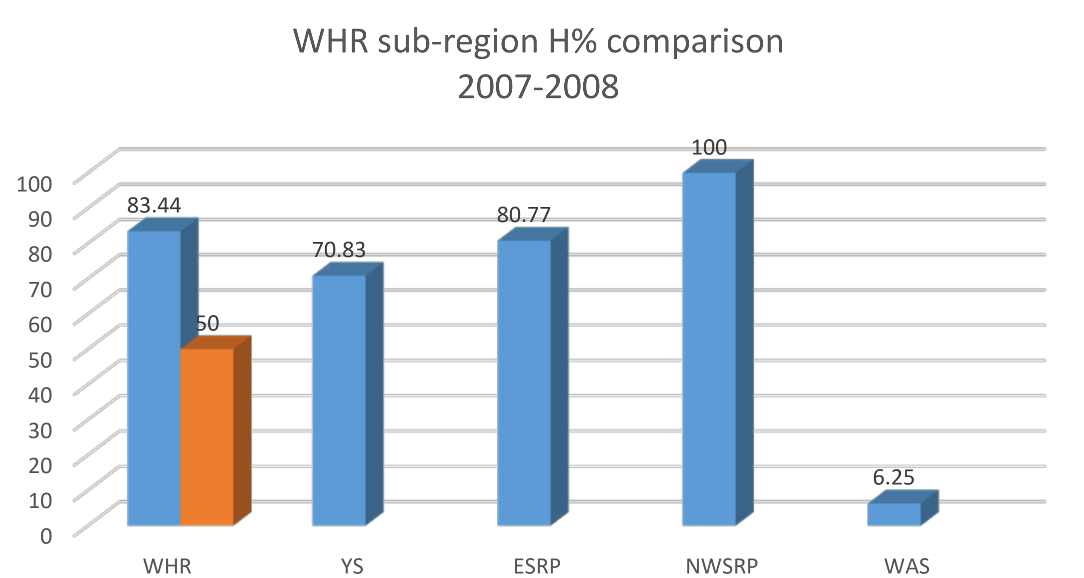

Figure 78: Hit percentage comparison of the Western intraplate hinterland region and the sub-regions within the WHR region for the 2007-2008 date cutoff. M3.5+ hit percentages shown in blue. M5+ percentages shown in orange.

above), and is quite scattered elsewhere. While we can see that these specific areas are where most of the seismicity takes place, there doesn't appear to be a systematic pattern, spatially, to the earthquakes that occur in those areas, at least from what is seen in this study.

There is localized extension on either side of the Snake River Plain. The ESRP and NWSRP sub-regions represent these extensional areas. The ESRP is a sub-region that includes the entire Yellowstone sub-region (Rectangles 1 and 3 in Figure 19). The ESRP wraps around the northern end of the Snake River Plain and shows a relatively high rate of CS predictability with a hit rate of 81.8% (Figure 78). Events within the ESRP sub-region are very limited in magnitude though. There are no M5+ events in the 2007-2008 catalog and only two in the 1999-2000 catalog.

The NWSRP is the other area of extension surrounding the Snake River Plain. This sub-region is a little peculiar in that there is a 100% hit rate in the 2007-2008 catalog

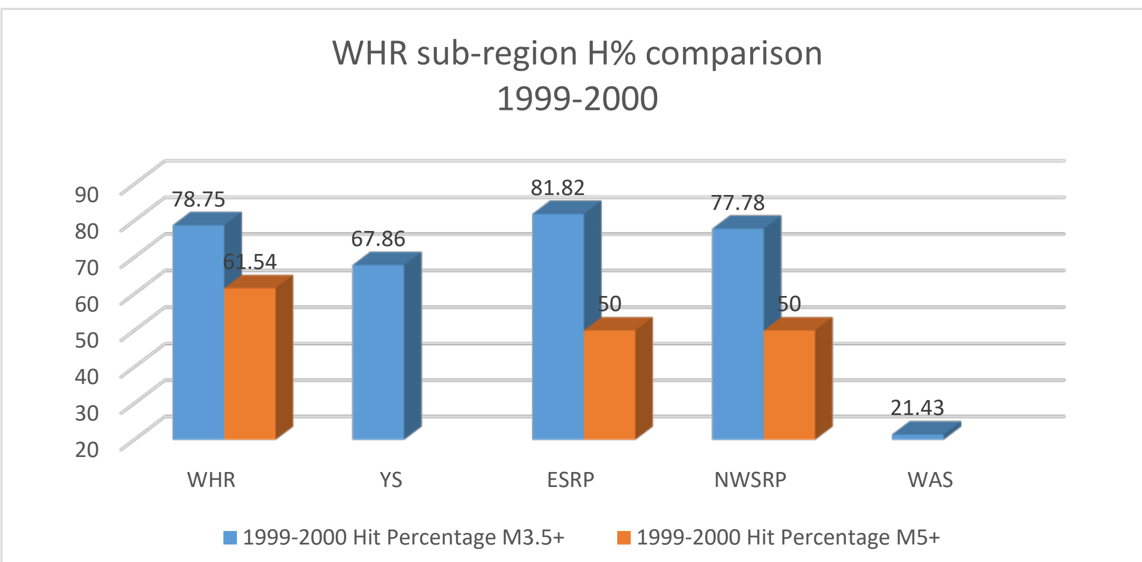

Figure 79: Hit percentage comparison of the Western intraplate hinterland region and the sub-regions within the WHR region for the 1999-2000 date cutoff. M3.5+ hit percentages shown in blue. M5+ percentages shown in orange.

(Figure 78). Being an "intraplate" environment, seismicity is expected to not be as spatially uniform as an area along a major plate boundary, and therefore not have a high level of CS predictability, but all of the events were forecasted successfully. There were only 14 events though. The 1999-2000 catalog showed results more in tune with what we would expect from WHR results. CS predictability was less than 80%, and decreased as the low-end magnitude increased (Figure 79). Dropping from 1000% to less than 80% was likely due to the additional Post-Cat earthquakes, and the different area covered by the Pre-Cat earthquakes as a result of changing the date cutoff.

The Yellowstone (YS) sub-region had very low hit percentages. The seismicity around Yellowstone is very limited in magnitude, with about 80% of the earthquakes in this catalog being less than M3.75. This makes it very difficult to make conclusions regarding CS predictability of earthquakes for this area.

Last, and actually least, is the Wasatch Fault zone (WAS). The WAS is perhaps the oddest outcome of this entire study. Although the area is an active, high-angle, normal fault zone, the seismicity here produced the lowest CS predictability results of any sub-region (Table 2; Figure 74). Only 1 out of 16 events in the 2007-2008 Post-Cat was successfully forecast, a mere 6.3% (Figure 78). This percentage is the lowest of any CS analyses for results found in this study or previous CS studies for any area (Figure 80) (e.g. Kafka et al., 2014; Kafka 2002, 2007; Kafka and Ebel, 2011; Kafka and Levin, 2000; Kafka and Walcott, 1999). Extending the Post-Cat back to the year 2000 did not produce CS predictability results that were much higher, with only 6 of 28 events forecasted

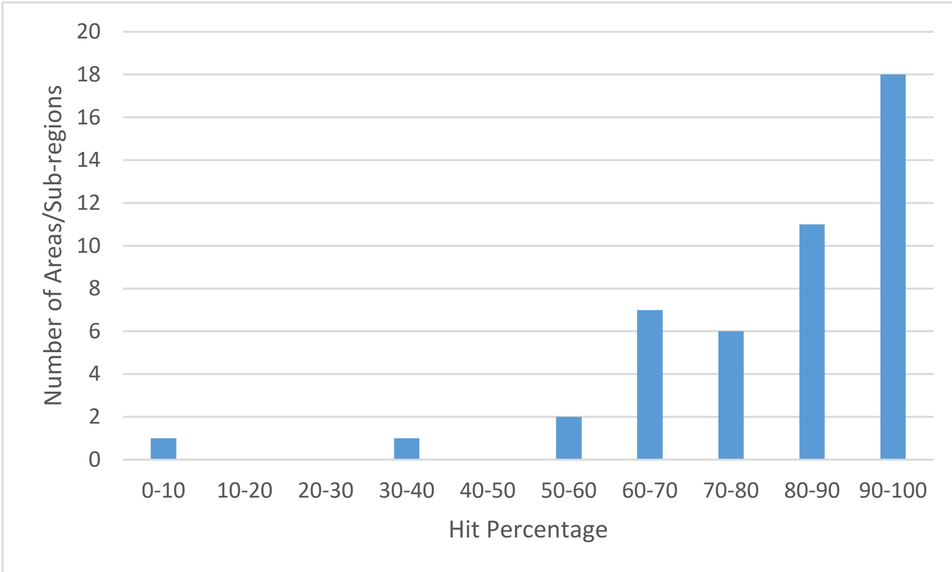

Figure 80: Number of previous study areas and sub-regions from this study whose CS results belong to a specific hit percentage range. All sub-region values shown here from this study were the 2007-2008 date cutoff values. The number of sub-regions from this study were added to the number of areas from figure 30 of this study, belonging to a specific hit percentage range. Both the intraplate and plate boundary values from figure 30 were used in this calculation. The single sub-region in the 0-10% range is the Wasatch Fault Zone analyzed in this study.

successfully, 21.4% (Figure 79). At just 21.4%, this is one of the lowest levels of CS predictability of all CS studies by Kafka and Colleagues, so far.

The WAS has not had any major earthquakes in historic times, and there has not been much seismicity recorded during the time interval of this catalog. The fact that there hasn't been a major event there in a long time could be the reason behind the low hit rate of this sub-region. It's possible that the larger events produce smaller foreshocks and aftershocks before and after the main event, and that since then there hasn't been a large earthquake in recent times, there isn't much seismicity overall. It is still odd that the hit percentages were this low considering it is a clearly delineated fault zone in terms of its surface expression.

Shorter Versus Longer Post-Cat Date Range

Changing the Post-Cat date range had a noticeable effect on the CS predictability results, and also affected the levels of statistical significance. For the most part the 2007-2008 date cutoff had higher levels of CS predictability than the 1999-2000 date cutoff. A possible explanation for this is that the longer Pre-Cat provided a better representation of the long-term pattern of seismicity.

There were, however, a few sub-regions, such as the BFZ and the Explorer plate that showed slightly higher hit percentages for the 1999-2000 cutoff, but most of the sub-regions, and the entire WUS showed a lower level of CS predictability for the 1999-2000 date cutoff. The San Andreas' smaller sub-regions showed very little change between the two Post-Cat sets. The WLB sub-region only changed by 0.2%, and with the exception of the SAC sub-region, the other sub-regions along the SAF only decreased by a small amount. From the 1999-2000 statistical significance analyses we saw that changing the Post-Cat lead to the SAC having a significantly lower level of CS predictability than the other SAF sub-regions except the SAB (Table 5), whereas for the 2007-2008 analyses the SAC was not significantly different than any of the San Andreas sub-regions (Table 4). The Gorda Ridge sub-region also had a significantly lower level of CS predictability than almost every other sub-region in the 1999-2000 analyses (Table 5), whereas it didn't in the 2007-2008 analyses (Table 4).

For M5+ events the result isn't quite as clear. For the WUS there is an overall decrease in the level of CS predictability from the 2007-2008 cutoff to the 1999-2000 cutoff (Figure 74). However, the changes vary by sub-region. The NJDF increases, the SJDF decreases, and the NSA and SSA hit percentages increase slightly. The WHR hit percentage increases. Most of the Cascadia sub-regions decrease with the exception of the BFZ. There are several sub-regions that do not have any M5+ events for the 2007-2008 Post-Cat, so it's difficult to draw a conclusion from those sub-regions. The SAS shows a 100% success rate for both the Post-Cat date ranges (Table 2, Table 3).

Tectonic Implications behind the CS Results

The results found in this study show that sub-regions that include a transform boundary generally show the highest levels of CS predictability (Table 2, Table 3). The BFZ and MFZ along with the SAB and the SAS all have considerably high levels of CS predictability. The SAN and SAC sub-regions show lower levels of CS predictability. They may have shown lower levels of CS predictability because they are experiencing a higher level of creep than their southern San Andreas counterparts (Zoback et al., 1987; Williams et al., 2005), or may even be locked (Schwartz and Coppersmith, 1984; Wallace, 1970).

The Walker Lane Belt shows the lowest levels of CS predictability of any sub-region that I consider a transform boundary with the exception of the 1999-2000 SAC sub-region and is only 1% greater than the 1999-2000 MFZ sub-region. This could be due to the WLB's extensional deformation component. None of the other transform boundary sub-regions are characterized by such a large component of extensional deformation.

The Cascade (CAS) and Seattle (SEA) sub-regions - sub-regions that represent subduction zone earthquakes - show results that are similar to the results of Western Intraplate Hinterland sub-regions (with the exception of the Wasatch fault zone) and with the WHR region overall. Excluding the WAS, the subduction zone results are barely higher than the WHR sub-region results.

The type of faulting within each of the sub-regions appears to play a big part in the level of that sub-regions CS predictability. The sub-regions that contain transform boundaries generally show the highest levels of CS predictability. The sub-regions that are representative of compressive deformation (particularly subduction zones) are generally second in terms of CS predictability. The sub-regions that are part of areas of extension in the WUS show the lowest levels of CS predictability; the lowest of which is the Gorda Ridge sub-region which is the one sub-region representative of solely a mid-ocean ridge segment. Essentially, the high-angle faulting of the San-Andreas shows greater CS predictability than the low-angle faulting and broad areas of extension present in the subduction and WHR sub-regions. The only outlier to this pattern is the WAS sub-region.

Relationship to Seismic Hazard Analysis

Having hit percentages that are so close to one another for the Cascadia and SAF sub-regions, and seeing the region with the higher hit percentage change between the two date cutoffs means that, in terms of CS predictability, the two regions show similar characteristics. This is good for use in earthquake hazard analyses, like that of the UCERF models, because we can use data from a broader range of areas to analyze the hazard in a specific area and to forecast the level of CS predictability we might expect in a certain area. However, since the hit percentages are so close, it also means that there doesn't seem to be any *significant* difference between CS predictability in significantly different tectonic regions, such as subduction zones versus transform zones. Geologically and geophysically this is not very satisfying since differences would be expected due to different tectonic settings. Analyzing transform, mid-ocean ridge, and subduction zones separately, which was only done to a small extent in this study, could help bring out more subtle differences of this phenomenon.

Based on the recurrence interval results found in this study (Table 7) there is a clear seismic hazard in the WUS. The northern half of the San Andreas (NSA), the Explorer Plate (EXP), the Blanco Fracture zone (BFZ), the Walker Lane Belt (WLB), and likely the Wasatch Fault zone (WAS) are all overdue for M7+ earthquakes (Table 7). The results presented here show that the NSA sub-region is 36 years overdue. The EXP sub-region is 37 years overdue; The BFZ is 44 years overdue; the WLB is 9 years overdue; and although the Wasatch fault zone does not have any M7+ events during the time interval of this study, the sub-region is overdue for M6+ events and may also be overdue for a M7+ earthquake.

More importantly, the San Andreas Fault as a whole (ESA) and the southern Cascadia (SJDF) sub-regions are overdue for an M8+ earthquake (Table 7). The last earthquake of close to M8+ along the SAF was the M7.8 San Francisco earthquake of 1906. The results of this study show a recurrence interval for 110 years for M8+ events along the San Andreas Fault. Thus, as of 2016 the SAF is due for an M8+ event according to the findings presented here. Since an event of M8+ did not happen by the end of the year 2016, the SAF, according to the results presented here, is overdue for a M8+ earthquake. The recurrence interval found here for M8+ earthquakes in the SJDF sub-region is 230 years, and there haven't been any M8+ events in this sub-region during the 255 year catalog used in this study. This does not mean that the Cascadia subduction zone is necessarily overdue for a M8+ margin rupture, but it does mean that it is likely overdue for a smaller margin rupture. As stated previously, the recurrence interval found for M8+ margin ruptures along the CSZ was found to be 417 years.

The findings of this study suggest that the WUS is at high risk for at least an M7+ event in the near future. Whether that earthquake occurs along the SAF, the CSZ, or further inland remains to be seen, as earthquakes are not yet able to be predicted, however, the findings presented here should be taken into account when calculating and presenting seismic hazards across the WUS.

CONCLUSIONS

The hit percentages for the Cascadia and SAF larger sub-regions were quite similar, and not particularly indicative of one region or the other having the higher level of CS predictability. The statistical significance tests did not show any of these larger sub-regions to be significantly different in the 2007-2008 analyses, but the WHR region did have significantly lower levels of CS predictability in the 1999-2000 analyses when compared to the two larger Cascadia sub-regions. There was a statistically significant difference between the northern Juan de Fuca sub-region (NJDF) and the entire San Andreas sub-region (ESA) as well (Tables 4 and 5). The level of CS predictability for the ESA sub-region was significantly lower than the level of CS predictability for the NJDF sub-region for both of the date cutoffs in this study.

The Cascadia region had the highest level of predictability of any region, in particular the northern half of the Cascadia region. The SAF region followed behind Cascadia, and the WHR showed the lowest levels of CS predictability (Table 2, Table 3). These results support my previously stated hypothesis that the Cascadia region would show the highest levels of CS predictability of any region, at least for the 1999-2000 date cutoff.

Breaking down the regions into smaller sub-regions, primarily based upon tectonic boundaries (Cascadia), and fault geometries as well as level of creep (SAF), and averaging the hit percentages for all of the sub-regions in a particular region yielded an 85.4% hit rate for the Cascadia sub-regions, and 86.1% for the SAF sub-regions. The average hit percentage for the WHR sub-regions was 64.5% including the WAS, and 83.9% without the WAS (Figure 81). So even the results from the WHR sub-regions are only slightly less than those of the Cascadia and SAF sub-regions. The averages for the 1999-2000 date cutoff were 81.4% for the Cascadia region, 80.6 for the SAF, and 62.2/75.8% for the WHR with and without the WAS respectively (Figure 81). The 1999-2000 results help distinguish the difference between the WHR region and the other regions, but only add to the uncertainty between the Cascadia region and SAF regions since the region with the higher hit percentage switches.

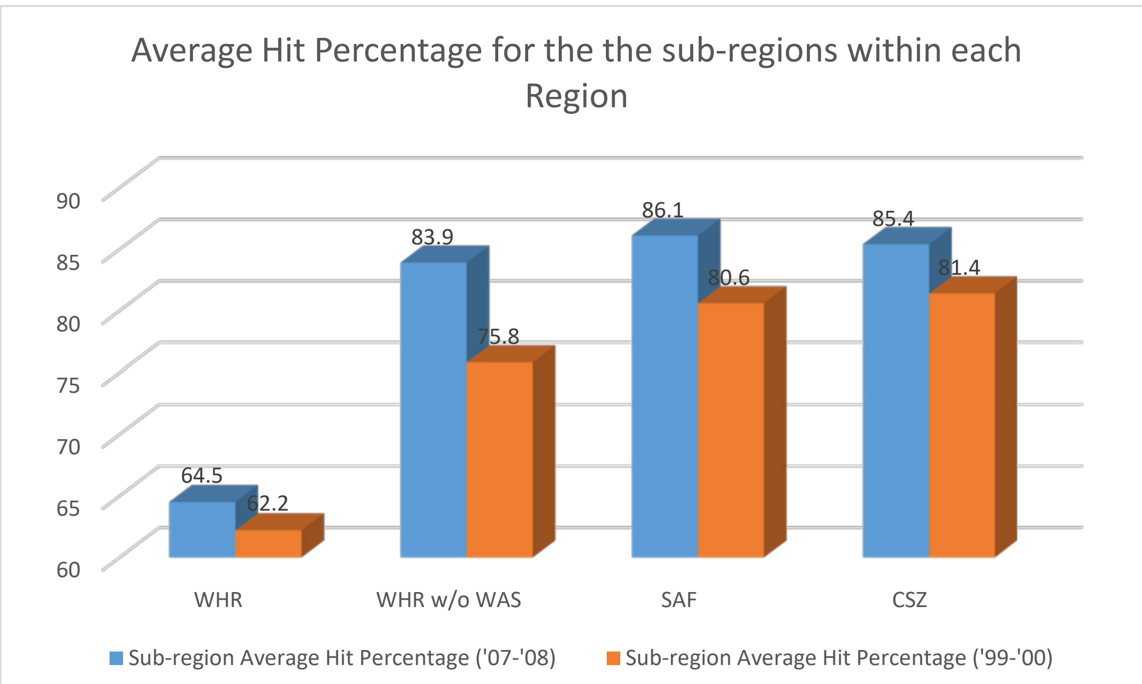

Figure 81: Averaged hit percentages of each of the regions combined sub-regions, including the Western intraplate hinterland region with and without the Wasatch fault Zone hit percentage factored in. Vertical exaggeration to show the subtle differences in hit percentages between the regions.

In terms of CS predictability for higher magnitude events, M5+, the Cascadia region had a 94.4% hit rate, the SAF had 96.8% success, and the WHR had a 61.5% success rate. These results are from the 1999-2000 date cutoff so as to include more

M5+ events as opposed to the 2007-2008 cutoff. Thus, the SAF has a higher level of CS predictability when speaking of higher magnitude earthquakes, although, as it turns out, not statistically significantly higher.

The sub-regions with the highest levels of CS predictability were the Explorer plate sub-region and the SAS sub-region (Figure 74). The Explorer plate had a 97.0% hit rate for the 2007-2008 date cutoff for M5+ events. The SAS shows the highest levels of CS predictability, with about a 94% success rate overall, and 100% success rates for both the 2007-2008 and 1999-2000 date cutoffs for M5+ events (Table 2 and Table 3 respectively). This is important for seismic hazard analysis because it suggests that, in this sub-region, earthquakes of M5+ are very likely to happen where previous earthquakes have happened.

A conclusion can be drawn about which type of plate boundary has the highest level of CS predictability. The transform boundaries within this study show the highest results for CS predictability. The subduction regions show the next highest level of CS predictability. Lastly, sub-regions of diffuse extension and mid-ocean ridges showed the lowest levels of CS predictability. Both the Gorda Ridge and the WHR are areas of high heat flow. That high heat flow may be leading to lower seismicity levels and lower production of large earthquakes because of the inability of the area to build up stress. Despite being an active, high-angle, normal fault zone and not technically an intraplate zone, the WAS had the lowest percentage of hits, which is consistent with the idea found here that tectonic zones with primarily extensional deformation have a lower level of CS predictability than their plate boundary zone counterparts. This study also shows that because of the more scattered/less spatially focused areas of seismicity there is a lower level of CS predictability (Kafka and Walcott, 1998; Kafka 2002, 2007; Kafka et al., 2014). More work on this should be done to investigate these issues further. By adding more sub-regions to the study that are specifically subduction zone sub-regions or mid-ocean ridge segments we can gain more insight into the CS differences between subduction zones, transforms, and ridges.

One hypothesis stated at the beginning of this thesis is that, of the larger regions, the region expected to have the highest level of CS predictability would be the Cascadia region, and that the sub-region with the highest level of CS predictability would be a sub-region along the SAF. Both of these hypotheses are supported by the results of this study.

In future research on this topic, it is likely that extending the Post-Cat date range a second time or a third time would give us a more complete picture to compare to what I have found in this study. Doing a third, or even a fourth date range, in which the Post-Cat range was extended further back in time, would provide more "long-term" results about CS predictability in the WUS through time. There is, however, always going to be a trade-off regarding where the Pre-Cat/Post-Cat boundary is set. If it is set earlier, then the Post-Cat provides a better statistical basis for estimating the level of CS predictability. But, if it is set later, the longer Pre-Cat provides a better representation of the long-term pattern of seismicity.

Breaking the Explorer plate sub-region down further by type of plate boundary may provide better results. Analyzing the Juan de Fuca ridge, instead of leaving it out of the study due to its low level of seismicity, would also be a good idea. Finding out which type of plate boundary has the highest and lowest level of CS predictability may prove more useful than attempting to find differences for specific tectonic regions. The results of this study, as well as of other CS studies, show that while there seems to be some “signal” of CS predictability being dependent on tectonic region, that signal is, in most cases, subtle. As seen above, this can be considered both good news and bad news: Good news, because it means we can apply CS predictability studies widely across different regions, but bad news because it, counterintuitively, suggests that tectonic understanding of a region does not necessarily yield an answer to the question of how predictable past versus future patterns of earthquakes are in that region.

References

Anagnos, T., & Kiremidjian, A. S. (1984). Stochastic time-predictable model for earthquake occurrences. *Bulletin of the Seismological Society of America*, *74*(6), 2593-2611.

Bakun, W. H., & Lindh, A. G. (1985). The Parkfield, California, earthquake prediction experiment. *Science*, *229*(4714), 619-624.

Bennett, R. A., Wernicke, B. P., Niemi, N. A., Friedrich, A. M., & Davis, J. L. (2003). Contemporary strain rates in the northern basin and range province from GPS data. *Tectonics*, *22*(2).

Brocher, T. M., Boatwright, J., Lienkaemper, J. J., Prentice, C. S., Schwartz, D. P., & Bundock, H. (2008). The Hayward Fault-Is It Due for a Repeat of the Powerful 1868 Earthquake? (No. 2008-3019). *US Geological Survey.*

Calvert, A. J., et al. (2006). Local thickening of the Cascadia fore arc crust and the origin of seismic reflectors in the uppermost mantle. *Tectonophysics*, Volume 420, Issues 1–2, 175-188

Chambless, H., and Kafka, A. L. (2014). Class II wastewater injection and its correlation to reservoir-induced seismicity in the United States, Senior Thesis. Boston College.

Cinella, J.R., & A.L. Kafka (2012). Cellular Seismology Investigation of the Caribbean Plate, Eastern Section Meeting, Seismological Society of America, Virginia Polytechnic Institute and State University, Blacksburg, VA, October 29, 2012

Chen, C., Zhao, D., & Wu, S. (2015). Tomographic imaging of the Cascadia subduction zone: Constraints on the Juan de Fuca slab. *Tectonophysics*, Volumes 647–648, 73-88

DeMets, C., Gordon, R. G., Argus, D. F., & Stein, S. (1990). Current plate motions. *Geophysical journal international*, *101*(2), 425-478.

Dickinson, W. R., & Snyder, W. S. (1979). Geometry of triple junctions related to San Andreas transform. *Journal of Geophysical Research: Solid Earth*, *84*(B2), 561-572.

Earthquake facts & earthquake fantasy: Fact of fiction (2015, May 28). Retrieved from http://earthquake.usgs.gov/learn/topics/megaqk_facts_fantasy.php

Earthquake hazards program: 2008 NSHMP Catalogs: WUS catalog #3 (2008). USGS. Retrieved from http://earthquake.usgs.gov/hazards/products/conterminous/2008/catalogs/

Field, D.H., Jackson, D.D., & Dolan, J.F. (1999),A Mutually Consistent Seismic-hazard Source Model for Southern California, Bull. Seismol. Soc. Am.89, 559–578.

Field, E. H., & Milner, K. R. (2008). Forecasting California's earthquakes: What can we expect in the next 30 years? (No. 2008-3027). *US Geological Survey*.

Field, E. H. (2015). UCERF3: A new earthquake forecast for California's complex fault system (No. 2015-3009). *US Geological Survey*.

Goldfinger, C., Nelson, C. H., & Johnson, J. E. (2003). Holocene earthquake records from the Cascadia subduction zone and northern San Andreas Fault based on precise dating of offshore turbidites. *Annual Review of Earth and Planetary Sciences*, *31*(1), 555-577.

Griscom, A., & Jachens, R. C. (1989). Tectonic history of the north portion of the San Andreas Fault system, California, inferred from gravity and magnetic anomalies. *Journal of Geophysical Research: Solid Earth (1978–2012)*, *94*(B3), 3089-3099.

Gutscher, M. A., Klaeschen, D., Flueh, E., & Malavieille, J. (2001). Non-Coulomb wedges, wrong-way thrusting, and natural hazards in Cascadia. *Geology*, *29*(5), 379-382.

Hammond, W. C., & Thatcher, W. (2004). Contemporary tectonic deformation of the basin and range province, western United States: 10 years of observation with the Global Positioning System. *Journal of Geophysical Research: Solid Earth (1978–2012)*, *109*(B8).

Holliday, J. R., Chen, C. C., Tiampo, K. F., Rundle, J. B., Turcotte, D. L., & Donnellan, A. (2007). A RELM earthquake forecast based on pattern informatics. *Seismological Research Letters*, *78*(1), 87-93.

Holliday, J. R., Rundle, J. B., Tiampo, K. F., Klein, W., & Donnellan, A. (2006). Systematic procedural and sensitivity analysis of the pattern informatics method for forecasting large (M> 5) earthquake events in southern California. *Pure and Applied Geophysics*, *163*(11-12), 2433-2454.

Hyndman, R. D. (2013), Downdip landward limit of Cascadia great earthquake rupture, J. Geophys. Res. Solid Earth, 118, 5530–5549, doi:10.1002/jgrb.50390.

Hyndman, R. D., & Wang, K. (1993). Thermal constraints on the zone of major thrust earthquake failure: The Cascadia subduction zone. *Journal of Geophysical Research: Solid Earth (1978–2012)*, *98*(B2), 2039-2060.

Hyndman, R. D., & Wang, K. (1995). The rupture zone of Cascadia great earthquakes from current deformation and the thermal regime. Journal of Geophysical Research, v. 100, p 22133-22154

Kafka, A. L. (2002). Statistical analysis of the hypothesis that seismicity delineates areas where future large earthquakes are likely to occur in the central and eastern United States. *Seismological Research Letters*, *73*(6), 992-1003.

Kafka, A. L. (2007). Does past seismicity delineate zones where future large earthquakes are likely to occur in intraplate environments?. *Geological Society of America Special Papers*, *425*, 35-48.

Kafka, A. L., & Ebel, J. E. (2007). Exaggerated claims about earthquake prediction. *EOS*, Transactions of the American Geophysical Union, 88(1), 1,6.

Kafka, A. L., & Ebel, J. E. (2011). Proximity to past earthquakes as a least-astonishing hypothesis for forecasting locations of future earthquakes. *Bulletin of the Seismological Society of America*, *101*(4), 1618-1629.

Kafka, A. L., & Levin, S. Z. (2000). Does the spatial distribution of smaller earthquakes delineate areas where larger earthquakes are likely to occur?. *Bulletin of the Seismological Society of America*, *90*(3), 724-738.

Kafka, A. L., & Walcott, J. R. (1998). How Well Does the Spatial Distribution of Smaller Earthquakes Forecast the Locations of Larger Earthquakes in the Northeastern United States?.*Seismological Research Letters*, *69*(5), 428-440.

Kafka, A. L, A.J. Kotowski, O. Ayandele, and A. Ferenczi (2014). Cellular Seismology: Is Past Seismicity a Good Basis for Seismic Source Characterization of the Central and Eastern U.S.?, *Eastern Section Meeting, Seismological Society of America*, College of Charleston, Charleston, SC, November 2-4, 2014.

Kijko, A. (2004). Estimation of the maximum earthquake magnitude, m max. *Pure and Applied Geophysics*, *161*(8), 1655-1681.

Lerner, K.L., & Lerner, B.L., (2003). Basin and Range Topography. World of Earth Science.

McCaffrey, R., & Goldfinger, C. (1995). Fore arc deformation and great subduction earthquakes: implications for Cascadia offshore earthquake potential. *Science*, *267*(5199), 856-859.

McCrory, P.A., Blair, J.L., Waldhauser, F., & Oppenheimer, D.H. (2012), Juan de Fuca slab geometry and its relation to Wadati-Benioff zone seismicity, *Journal of Geophysical Research*, 117, B09306

Mount, V. S., & Suppe, J. (1987). State of stress near the San Andreas Fault: Implications for wrench tectonics. *Geology*, *15*(12), 1143-1146.

Nicholson, C., Sorlien, C. C., Atwater, T., Crowell, J. C., & Luyendyk, B. P. (1994). Microplate capture, rotation of the western Transverse Ranges, and initiation of the San Andreas transform as a low-angle fault system. *Geology*, *22*(6), 491-495.

Parsons, T., Thompson, G. A., & Smith, R. P. (1998). More than one way to stretch: a tectonic model for extension along the plume track of the Yellowstone hotspot and adjacent basin and range province. *Tectonics*, *17*(2), 221-234.

Parsons, T. (2006). The basin and range province. *Developments in Geotectonics*, *25*, 277-XV.

Piana Agostinetti, N., & Miller, M. S. (2014). The fate of the down-going oceanic plate: Insight from the northern Cascadia subduction zone. *Earth and Planetary Science Letters*, Volume 408, 237-251

Plate motion calculator. (2015). Retrieved from https://www.unavco.org/software/geodetic-utilities/plate-motion-calculator/plate-motion-calculator.html

Priest, G. R., Zhang, Y., Witter, R. C., Wang, K., Goldfinger, C., & Stimely, L. (2014). Tsunami impact to Washington and northern Oregon from segment ruptures on the southern Cascadia subduction zone. *Natural hazards*, *72*(2), 849-870.

Roeloffs, E., & Langbein, J. (1994). The earthquake prediction experiment at Parkfield, California. *Reviews of Geophysics*, *32*(3), 315-336

Rogers, G., & Dragert, H. (2003). Episodic tremor and slip on the Cascadia subduction zone: The chatter of silent slip. *Science*, *300*(5627), 1942-1943.

Romanyuk, T. V., Blakely, R., & Mooney, W. D. (1998). The Cascadia subduction zone: Two contrasting models of lithospheric structure. *Physics and Chemistry of the Earth*, Volume 23, Issue 3, 297-301.

Rundle, J. B., Tiampo, K. F., & Klein, W. (2007). Pattern informatics and cellular seismology: A comparison of methods. Eos, Transactions American Geophysical Union, Volume 88, Issue 24, 254-254.

Schulz, K. (2015). The really big one. *Annals of Seismology*, June 20, 2015, 1-14

Schulz, S. S., & Wallace, R. E. (1989). The San Andreas Fault. *US Department of the Interior*, *Geological Survey*.

Schwartz, D. P., & Coppersmith, K. J. (1984). Fault behavior and characteristic earthquakes: Examples from the Wasatch and San Andreas Fault zones. *Journal of Geophysical Research: Solid Earth (1978–2012)*, *89*(B7), 5681-5698.

Shimazaki, K., & Nakata, T. (1980). Time-predictable recurrence model for large earthquakes. *Geophysical Research Letters*, *7*(4), 279-282.

Sornette, D., & Sornette, A. (1999). General theory of the modified Gutenberg-Richter law for large seismic moments. *Bulletin of the Seismological Society of America*, *89*(4), 1121-1130.

Steele, Bill. (2013). The Last Cascadia Great Earthquake and Tsunami; 313 Years and Ticking. Pacific Northwest Seismic Network.

Teyssier, C., Tikoff, B., & Markley, M. (1995). Oblique plate motion and continental tectonics. *Geology*, *23*(5), 447-450.

The Cascade episode: Evolution of the Pacific Northwest. (2016). Retrieved from http://www.burkemuseum.org/geo_history_wa/Cascade%20Episode.htm

Tiampo, K. F., Rundle, J. B., McGinnis, S. A., & Klein, W. (2002). Pattern dynamics and forecast methods in seismically active regions. In *Earthquake Processes: Physical Modelling, Numerical Simulation and Data Analysis Part II* (pp. 2429-2467). Birkhäuser Basel.

Wallace, R. E. (1970). Earthquake recurrence intervals on the San Andreas fault. *Geological Society of America Bulletin*, *81*(10), 2875-2890.

Wang, K. (2000). Stress–strain 'paradox', plate coupling, and fore arc seismicity at the Cascadia and Nankai subduction zones. *Tectonophysics*, *319*(4), 321-338.

Wells, D. L., & Coppersmith, K. J. (1994). New empirical relationships among magnitude, rupture length, rupture width, rupture area, and surface displacement. *Bulletin of the seismological Society of America*, *84*(4), 974-1002.

Wells, R. E., Weaver, C. S., & Blakely, R. J. (1998). Fore-arc migration in Cascadia and its neo-tectonic significance. *Geology*, *26*(8), 759-762.

Wesnousky, S. G. (2005). The San Andreas and Walker Lane fault systems, western North America: Transpression, transtension, cumulative slip and the structural evolution of a major transform plate boundary. *Journal of Structural Geology*, *27*(8), 1505-1512.

Williams, T. B., Kelsey, H. M., & Freymueller, J. T. (2005). GPS-derived strain in northwestern California: Termination of the San Andreas Fault system and convergence of the Sierra Nevada-Great Valley block contribute to southern Cascadia fore-arc contraction. *Tectonophysics*, Volume 413, Issues 3–4, 171-184

Wyss, M. (1979). Estimating maximum expectable magnitude of earthquakes from fault dimensions. *Geology*, *7*(7), 336-340.

Zoback, M. D., Zoback, M. L., Mount, V. S., Suppe, J., Eaton, J. P., Healy, J. H., ... & Wong, I. G. (1987). New evidence on the state of stress of the San Andreas Fault system. *Science*, *238*(4830), 1105-1111.